STRUCTURAL SYSTEMS

RESEARCH PROJECT

Report No.
SSRP–04/14
Final

SEISMIC RESPONSE OF SACRIFICIAL EXTERIOR SHEAR KEYS IN BRIDGE ABUTMENTS

by

AZADEH BOZORGZADEH

SAMI HANNA MEGALLY

SCOTT ASHFORD

JOSÉ I. RESTREPO

Final Report Submitted to the California Department of Transportation (Caltrans) Under Contract No. 59A0337

October 2007

Department of Structural Engineering
University of California, San Diego
La Jolla, California 92093-0085

University of California, San Diego
Department of Structural Engineering
Structural Systems Research Project

Report No. SSRP–04/14
Final

SEISMIC RESPONSE OF SACRIFICIAL EXTERIOR SHEAR KEYS IN BRIDGE ABUTMENTS

by

Azadeh Bozorgzadeh
Graduate Student Researcher

Sami Hanna Megally
Graduate Student Researcher

Scott A. Ashford
Professor of Structural Engineering

José I. Restrepo
Professor of Structural Engineering

Final Report Submitted to the California Department of Transportation
(Caltrans) Under Contract No. 59A0337

Department of Structural Engineering
University of California, San Diego
La Jolla, California 92093-0085
October 2007

Technical Report Documentation Page

1. Report No.	2. Government Accession No.	3. Recipient's Catalog No.
4. Title and Subtitle Seismic Response of Sacrificial Exterior Shear Keys in Bridge Abutments		5. Report Date April 2005 6. Performing Organization Code
7. Author(s) Azadeh Bozorgzadeh, Sami Hanna Megally, José I. Restrepo, Scott A. Ashford		8. Performing Organization Report No. UCSD / SSRP-04/14
9. Performing Organization Name and Address Department of Structural Engineering School of Engineering University of California, San Diego La Jolla, California 92093-0085		10. Work Unit No. (TRAIS) 11. Contract or Grant No. 59A0337
12. Sponsoring Agency Name and Address California Department of Transportation Division of Engineering Services 1801 30th St., West Building MS-9 Sacramento, California 95807		13. Type of Report and Period Covered Final Report – July 2002 / May 2003 14. Sponsoring Agency Code

15. Supplementary Notes

Prepared in cooperation with the State of California Department of Transportation.

16. Abstract

Seismic response and capacity evaluation of sacrificial exterior shear keys are the main objectives of this work. Shear keys are used in bridge abutments to provide transverse support for the superstructure. However, it has been recognized that to protect abutment piles from severe damage under transverse forces, shear keys must be designed as a locking mechanism that limits the magnitude of the transverse force that can be transmitted into the abutment. In philosophical terms, a shear key could transversely be designed as a sacrificial element to limit transverse inertial forces in the abutment walls and supporting piles. If shear keys are designed as sacrificial elements within a capacity design framework, their overstrength must be accurately determined to ensure other elements can be designed to remain elastic.

An experimental program to study the seismic behavior of shear keys was carried out at University of California, San Diego. These specimens were built at a 40% scale of the exterior shear keys of a prototype abutment. The design philosophy was to force a shear sliding failure at the interface of the shear key-abutment stem wall to control damage to the abutment walls and the piles under transverse seismic force. This report presents recommendations for design and construction details of sacrificial exterior shear keys based on test results

Several factors were considered in this experimental program such as including construction joints between the abutment stem wall and the shear key, different amount and configuration of the vertical reinforcement crossing the abutment stem wall-shear key interface, and different amounts and configuration of the horizontal reinforcement in the stem wall. A total of five specimens were built and tested at UCSD; each specimen included two exterior shear key test units. Experimental results of specimens 4 and 5 are given in this report.

17. Key Words	18. Distribution Statement
Abutments, sacrificial, shear keys, experimental test, seismic	No restrictions

19. Security Classification (of this report)	20. Security Classification (of this page)	21. No. of Pages	22. Price
Unclassified	Unclassified	82	

Form DOT F 1700.7 (8-72) Reproduction of completed page authorized

DISCLAIMER

The contents of this report reflect the views of the authors who are responsible for the facts and accuracy of the data presented herein. The contents do not necessarily reflect the official views or policies of the California Department of Transportation or the Federal Highway Administration. This report does not constitute a standard, specification or regulation.

ACKNOWLEDGEMENTS

This study was made possible by funding from the California Department of Transportation under contract No. 59A0337.

As in any other research program there are several people that made this work possible. We would like to thank Dr. Charles Sikorsky from Caltrans for his technical participation during the design and testing phases of this research program.

The experiments presented in this report were tested at the Charles Lee Powell Laboratory of the University of California-San Diego (UCSD). A number of technical personnel at UCSD assisted in the experimental investigation. Among them Mr. Lawrence Berman and Dr. Christopher Latham deserve special mention for their contribution in construction and testing of the shear key units. Thanks are also due to Mr. Charles Stearns and Alex Sherman for their invaluable assistance.

LIST OF SYMBOLS

A_{vf} = area of vertical reinforcement crossing the shear key-abutment stem wall;

A_{sh} = area of horizontal tie reinforcement in the abutment stem wall;

a = distance from the location of the applied force to the surface of the stem wall;

b = distance between the top surface of the stem wall and center line of the lowest horizontal tie reinforcement;

d = length of shear key-stem wall interface;

d_b = diameter of reinforcement bar;

f'_c = specified concrete compressive strength;

f_{su} = ultimate tensile strength of steel;

f_y = yield strength of steel;

$\bar{f}_y$ = mean value of yield strength of steel;

h = height of the abutment stem wall;

l_{dh} = development length of reinforcing steel;

v_u = ultimate shear strength (V_u / bd);

V = applied lateral force;

$V_{u,t}$ = shear force capacity observed in the tests;

$V_{n,Calt}$ = shear force capacity calculated from caltrans equation;

V_n = calculated shear force capacity using Eq.(8);

V_o = overstrength shear key capacity;

V_u = ultimate shear force capacity;

α = angle of kinking of shear key vertical bars with respect to the vertical axis;

$\bar{\alpha}$ = mean value of angle of kinking of shear key vertical bars with respect to the vertical axis;

β = angle of inclined face of shear key with respect to the vertical axis;

ϕ = strength reduction factor;

ϕ_o = overstrength factor;

μ_f = kinematic coefficient of friction for concrete;

$\bar{\mu}_f$ = mean value of kinematic coefficient of friction for concrete;

μ = static coefficient of friction for concrete

TABLE OF CONTENTS

DISCLAIMER ii
ACKNOWLEDGEMENTS iii
LIST OF SYMBOLS iv
TABLE OF CONTENTS v
LIST OF FIGURES vii
LIST OF TABLES x
ABSTRACT xi
1 INTRODUCTION 1
2 SCOPE 1
3 SUMMARY OF RESEARCH WORK 2
3.1 MODES OF FAILURE 2
3.1.1 UNITS 4A AND 4B 2
3.1.2 UNITS 5A AND 5B 2
4 RECOMMENDATIONS FOR CONSTRUCTIONS 4
4.1 Discussion of Experimental Results 4
5 EVALUATION OF THE CAPACITY OF EXTERIOR SHEAR KEYS 6
6 RECOMMENDATIONS FOR FUTURE RESEARCH 11
7 APPENDIX A-1 12
8 APPENDIX A-2 18
9 APPENDIX A-3 25
9.1 Analytical Studey of Sacrificial Shear Keys 25
10 APPENDIX A-4 29
10.1 Evaluation of the Capacity of the Test Series IV 29
10.1.1 Strut-and-Tie Mechanism and Hysteretic Model: 29
10.1.2 Horizontal Reinforcement Strain Profiles 34
10.1.3 Vertical Reinforcement Strain Profiles 42
10.1.4 Shear friction capacity model proposed by Mattock 45

10.1.5 Capacity Evaluation of Exterior Shear Key with Shear Friction Capacity Model Proposed by Walraven *et al*. (1987) 46
10.1.6 Capacity Evaluation of Exterior Shear Key with Caltrans Sliding Shear Friction Model 47
10.2 Evaluation of the Capacity of the Test Series V 48
10.2.1 Strut-and-Tie Model: 48
10.2.2 Horizontal Reinforcement Strain Profiles 50
10.2.3 Vertical Reinforcement Strain Profiles 65
10.2.4 Shear friction capacity model proposed by Mattock 68
10.2.5 Capacity Evaluation of Exterior Shear Key with Shear Friction Capacity Model Proposed by Walraven *et al*. (1987) 69
11 Appendix A-5 71
11.1 Geometry and Reinforcement Details of Test Series IV 71
Reinforcement Layout 71
11.2 Geometry and Reinforcement Details of Test Series V 73
11.3 Instrumentation 76
12 REFERENCES 82

LIST OF FIGURES

Figure 3-1 Test Observations 3

Figure 4-1 Schematic of Reinforcement Configuration with Hanger Bars 6

Figure 5-1 Mechanistic Model of Exterior Shear Key 8
Figure 5-2 Frequency Distribution of V / A_{sv} Obtained from a Monte-Carlo Simulation. 9

Figure A1- 1 Elevation View of the Reinforcement Layout 14
Figure A1- 2- Observation at First Yield of Hanger Bars of Test Unit 4-A 15
Figure A1- 3- Observation at the End of Test Unit 4-A 15
Figure A1- 4- Observation at First Yield of Hanger Bars of Test Unit 4-B 16
Figure A1- 5- Observation at the End of Test Unit 4-B 16
Figure A1- 6- Exterior Shear Keys Test Units 4-A and 4-B: Load vs. Displacement at top of shear key 17

Figure A1- 1 Elevation View of the Reinforcement Layout 14
Figure A1- 2- Observation at First Yield of Hanger Bars of Test Unit 4-A 15
Figure A1- 3- Observation at the End of Test Unit 4-A 15
Figure A1- 4- Observation at First Yield of Hanger Bars of Test Unit 4-B 16
Figure A1- 5- Observation at the End of Test Unit 4-B 16
Figure A1- 6- Exterior Shear Keys Test Units 4-A and 4-B: Load vs. Displacement at top of shear key 17

Figure A2- 1- Elevation View of the Reinforcement Layout 20
Figure A2- 2- Observation at Peak Load of Test Unit 5-A 21
Figure A2- 3- Observation at 0.6 in. Displ. of Test Unit 5-A 21
Figure A2- 4- Observation at 103 kips lateral Load with 1.0 in. Displ.of Shear Key in Test Unit 5-A 22
Figure A2- 5- Observation of Specimen at Failure 22
Figure A2- 6- Observation of Specimen at Failure After Removing the Keys 22
Figure A2- 7-Observation at Peak Load of Test Unit 5 23
Figure A2- 8- Observation at 1.6 in. Displ. of Test Unit 5 23
Figure A2- 9- Observation at 44 kips lateral Load with 2.0 in. Displ.of Shear Key in Test Unit 5 23
Figure A2-10- Exterior Shear Keys Test Units 5-A and 5-B: Load vs. Displacement at top of shear key 24

Figure A3- 1- Strut-and-Tie Model for Shear Key 25
Figure A3- 2- A Fractured Vertical Bar in Unit 5B, Removed from Inside of Concrete 26

Figure A4- 1- Schematic of Strut-and-Tie Model for Exterior Shear Key 30
Figure A4- 2- Hysteresis Model for Exterior Shear Key 32
Figure A4- 3- Horizontal Strain Profiles, Layer x, Line 1, Unit 4A 34

Figure A4- 4- Horizontal Strain Profiles, Layer x, Line 2, Unit 4A 35
Figure A4- 5- Horizontal Strain Profiles, Layer x, Line 3, Unit 4A 35
Figure A4- 6- Horizontal Strain Profiles, Layer x, Line 4, Unit 4A 35
Figure A4- 7- Horizontal Strain Profiles, Layer y, Line 1, Unit 4A 36
Figure A4- 8- Horizontal Strain Profiles, Layer y, Line 2, Unit 4A 36
Figure A4- 9- Horizontal Strain Profiles, Layer y, Line 3 Unit 4A 37
Figure A4- 10- Horizontal Strain Profiles, Layer y, Line 4, Unit 4A 37
Figure A4- 11- Horizontal Strain Profiles, Layer x, Line 1, Unit 4B 38
Figure A4- 12- Horizontal Strain Profiles, Layer x, Line 2, Unit 4B 38
Figure A4- 13- Horizontal Strain Profiles, Layer x, Line 3, Unit 4B 39
Figure A4- 14- Horizontal Strain Profiles, Layer x, Line 4, Unit 4B 39
Figure A4- 15- Horizontal Strain Profiles, Layer y, Line 1, Unit 4B 40
Figure A4- 16- Horizontal Strain Profiles, Layer y, Line 2, Unit 4B 40
Figure A4- 17- Horizontal Strain Profiles, Layer y, Line 3, Unit 4B 41
Figure A4- 18- Horizontal Strain Profiles, Layer y, Line 4, Unit 4B 41
Figure A4- 19- Vertical Strain Profiles, Layer x, Line 1, Unit 4A 42
Figure A4- 20- Vertical Strain Profiles, Layer x, Line 2, Unit 4A 42
Figure A4- 21- Vertical Strain Profiles, Layer y, Line 1, Unit 4A 43
Figure A4- 22- Vertical Strain Profiles, Layer y, Line 2, Unit 4A 43
Figure A4- 23- Vertical Strain Profiles, Layer x, Line 1, Unit 4B 44
Figure A4- 24- Vertical Strain Profiles, Layer x, Line 2, Unit 4B 44
Figure A4- 25- Vertical Strain Profiles, Layer y, Line 1, Unit 4B 45
Figure A4- 26- Vertical Strain Profiles, Layer y, Line 2, Unit 4B 45
Figure A4- 27- Strut-and-Tie Model for Exterior Shear Key Unit 5A 49
Figure A4- 28- Strut-and-Tie Model for Exterior Shear Key Unit 5B 49
Figure A4- 29- Horizontal Strain Profiles, Layer 1, Line 1, Unit 5A 51
Figure A4- 30- Horizontal Strain Profiles, Layer 1, Line 2, Unit 5A 51
Figure A4- 31- Horizontal Strain Profiles, Layer 1, Line 3, Unit 5A 52
Figure A4- 32- Horizontal Strain Profiles, Layer 1, Line 4, Unit 5A 52
Figure A4- 33- Horizontal Strain Profiles, Layer 1, Line 5, Unit 5A 53
Figure A4- 34- Horizontal Strain Profiles, Layer 1, Line 6, Unit 5A 53
Figure A4- 35- Horizontal Strain Profiles, Layer 1, Line 7, Unit 5A 54
Figure A4- 36- Horizontal Strain Profiles, Layer 2, Line 1, Unit 5A 54
Figure A4- 37- Horizontal Strain Profiles, Layer 2, Line 2, Unit 5A 55
Figure A4- 38- Horizontal Strain Profiles, Layer 2, Line 3, Unit 5A 55
Figure A4- 39- Horizontal Strain Profiles, Layer 2, Line 4, Unit 5A 56
Figure A4- 40- Horizontal Strain Profiles, Layer 2, Line 5, Unit 5A 56
Figure A4- 41- Horizontal Strain Profiles, Layer 2, Line 6, Unit 5A 57
Figure A4- 42- Horizontal Strain Profiles, Layer 2, Line 7, Unit 5A 57
Figure A4- 43- Horizontal Strain Profiles, Layer 1, Line 1, Unit 5B 58
Figure A4- 44- Horizontal Strain Profiles, Layer 1, Line 2, Unit 5B 58
Figure A4- 45- Horizontal Strain Profiles, Layer 1, Line 3, Unit 5B 59
Figure A4- 46- Horizontal Strain Profiles, Layer 1, Line 4, Unit 5B 59
Figure A4- 47- Horizontal Strain Profiles, Layer 1, Line 5, Unit 5B 60
Figure A4- 48- Horizontal Strain Profiles, Layer 1, Line 6, Unit 5B 60
Figure A4- 49- Horizontal Strain Profiles, Layer 1, Line 7, Unit 5B 61

Figure A4- 50- Horizontal Strain Profiles, Layer 2, Line 1, Unit 5B 61
Figure A4- 51- Horizontal Strain Profiles, Layer 2, Line 2, Unit 5B 62
Figure A4- 52- Horizontal Strain Profiles, Layer 2, Line 3, Unit 5B 62
Figure A4- 53- Horizontal Strain Profiles, Layer 2, Line 4, Unit 5B 63
Figure A4- 54- Horizontal Strain Profiles, Layer 2, Line 5, Unit 5B 63
Figure A4- 55- Horizontal Strain Profiles, Layer 2, Line 6, Unit 5B 64
Figure A4- 56- Horizontal Strain Profiles, Layer 2, Line 7, Unit 5B 64
Figure A4- 57- Vertical Strain Profiles, Layer 1, Unit 5A 65
Figure A4- 58- Vertical Strain Profiles, Layer 2, Unit 5A 65
Figure A4- 59- Vertical Strain Profiles, Layer 3, Unit 5A 66
Figure A4- 60- Vertical Strain Profiles, Layer 4, Unit 5A 66
Figure A4- 61- Vertical Strain Profiles, Layer 1, Unit 5B..... 67
Figure A4- 62- Vertical Strain Profiles, Layer 2, Unit 5B..... 67
Figure A4- 63- Vertical Strain Profiles, Layer 3, Unit 5B..... 68
Figure A4- 64- Vertical Strain Profiles, Layer 4, Unit 5B..... 68

Figure A5- 1- Elevation View of the Reinforcement Layout-Test Series IV 72
Figure A5- 2- Reinforcement Layout (Section A-A)-Test Series IV 72
Figure A5- 3- Reinforcement Layout (Section B-B)-Test Series IV 73
Figure A5- 4- Elevation View of the Reinforcement Layout-Test Series V 74
Figure A5- 5- Reinforcement Layout (Section C-C)-Test Series V 74
Figure A5- 6- Reinforcement Layout (Section A-A)-Test Series V..... 75
Figure A5- 7- Reinforcement Layout (Section B-B)-Test Series V 75
Figure A5- 8- Labels of Displacement Transducers- Test Series IV..... 76
Figure A5- 9- Labels of Displacement Transducers- Test Series V 76
Figure A5- 10- Labels of Strain Gages on U Shape Vertical Bars, in Diagonal Direction- Test Series IV..... 77
Figure A5- 11- Labels of Strain Gages on U Shape Vertical Bars, in Horizontal direction- Test Series IV..... 78
Figure A5- 12- Labels of Strain Gages on Horizontal Hanger Bars- Test Series IV..... 78
Figure A5- 13- Location of Strain Gages on Horizontal and Vertical Bars- Test Series IV 79
Figure A5- 14- Labels of Strain Gages on Vertical Shear Key Reinforcement- Test Series V.... 80
Figure A5- 15- Labels of Strain Gages on Horizontal Headed Bars- Test Series V 80
Figure A5- 16- Location of Strain Gages on Horizontal and Vertical Bars- Test Series V 81

LIST OF TABLES

Table 5-1 Summary of Statistic Analysis for Variables μ_f, α, and $f_{su}/\ \overline{f}_y$..... 8

Table A1- 1: Experimental and Calculated Maximum Load Carrying Capacities of Shear Key (Units 4-A and 4-B) 17

Table A2- 1: Experimental and Calculated Maximum Load Carrying Capacities of Shear Key (Units 5-A and 5-B) 24

Table A4- 1: Calculated the Steel Contribution to the Capacity of Exterior Shear Key Test Units 4A and 4B 31
Table A4- 2: Calculated Capacity of Exterior Shear Key Test Units 4A and 4B..... 31
Table A4- 3: Calculated Load andDisplacement of Test Series IV at Each Damage Level 33
Table A4- 4: Capacity Evaluation of Exterior Shear key Test Units 4A and 4B with Mattock Equation..... 46
Table A4- 5: Capacity Evaluation of Exterior Shear key Test Units 4A and 4B with Walraven *et al*. (1987)'s Equations..... 47
Table A4- 6: Capacity Evaluation of Exterior Shear key Test Units 4A and 4B with Caltrans Sliding Shear Friction Equation..... 48
Table A4- 7: Calculated Load andDisplacement of Test Series V at Each Damage Level..... 50
Table A4- 8: Capacity Evaluation of Exterior Shear key Test Units 5A and 5B with Mattock Equation 69
Table A4- 9: Capacity Evaluation of Exterior Shear key Test Units 5A and 5B with Walraven *et al*. (1987)'s Equations..... 70

ABSTRACT

Seismic response and capacity evaluation of sacrificial exterior shear keys are the main objectives of this work. Shear keys are used in bridge abutments to provide transverse support for the superstructure. However, it has been recognized that to protect abutment piles from severe damage under transverse forces, shear keys must be designed as a locking mechanism that limits the magnitude of the transverse force that can be transmitted into the abutment. In philosophical terms, a shear key could transversely be designed as a sacrificial element to limit transverse inertial forces in the abutment walls and supporting piles. If shear keys are designed as sacrificial elements within a capacity design framework, their overstrength must be accurately determined to ensure other elements can be designed to remain elastic.

An experimental program to study the seismic behavior of shear keys was carried out at University of California, San Diego. These specimens were built at a 40% scale of the exterior shear keys of a prototype abutment. The design philosophy was to force a shear sliding failure at the interface of the shear key-abutment stem wall to control damage to the abutment walls and the piles under transverse seismic force. This report presents recommendations for design and construction details of sacrificial exterior shear keys based on test results

Several factors were considered in this experimental program such as including construction joints between the abutment stem wall and the shear key, different amount and configuration of the vertical reinforcement crossing the abutment stem wall-shear key interface, and different amounts and configuration of the horizontal reinforcement in the stem wall. A total of six specimens were built and tested at UCSD; each specimen included two exterior shear key test units. Experimental results of specimens 4 and 5 are given in report.

1 INTRODUCTION

Seismic response and capacity evaluation of sacrificial exterior shear keys are the main objectives of this work. Shear keys are used in bridge abutments to provide transverse support for the superstructure. However, it has been recognized that to protect abutment piles from severe damage under transverse forces, shear keys must be designed as a locking mechanism that limits the magnitude of the transverse force that can be transmitted into the abutment. In philosophical terms, a shear key could transversely be designed as a sacrificial element to limit transverse inertial forces in the abutment walls and supporting piles. If shear keys are designed as sacrificial elements within a capacity design framework, their overstrength must be accurately determined to ensure other elements can be designed to remain elastic.

Damage to abutments under a major seismic event is admissible provided that any abutment damage is repairable and there is no damage to the piles (ACI, 2005).. Therefore, transfer of seismic forces to the abutments is controlled by design of sacrificial shear keys such that the capacity of the shear keys does not exceed the smaller of 30% of the dead load vertical reaction at the abutment or 75% of the total shear capacity of the piles plus one of the wing walls (Caltrans, 1993a)..

2 SCOPE

An experimental program to study the seismic behavior of shear keys was carried out at University of California, San Diego. These specimens were built at a 40% scale of the exterior shear keys of a prototype abutment. The design philosophy was to force a shear sliding failure at the interface of the shear key-abutment stem wall to control damage to the abutment walls and the piles under transverse seismic force. This report presents recommendations for design and construction details of sacrificial exterior shear keys based on test results

Several factors were considered in this experimental program such as including construction joints between the abutment stem wall and the shear key, different amount and configuration of the vertical reinforcement crossing the abutment stem wall-shear key interface, and different amounts and configuration of the horizontal reinforcement in the stem wall. A total of five specimens were built and tested at UCSD; each specimen included two exterior shear key test

units. Experimental results of specimens 4 and 5 are given in Appendices A-1 and A-2, respectively.

3 SUMMARY OF RESEARCH WORK

Construction details and experimental results of Test Units 4A, 4B, 5A, and 5B are described in Appendices A-1 and A-2. Test Units 4A and 4B represented the standard shear key design. Caltrans provided the design and construction details for Test Units 4A and 4B. Design of Test Units 5A and 5B was proposed by UCSD. Design of Units 5A and 5B developed based on strut-and-tie modeling.

3.1 MODES OF FAILURE

3.1.1 UNITS 4A AND 4B

A large diagonal crack developed in the stem wall for both test units. Thus, failure occurred in the stem wall rather than at the interface of the shear key-abutment stem wall as intended. No shear sliding was observed at the interface of the shear key-stem wall during these tests [Appendix A-1]. Figure 3-1a shows Test Unit 4A after failure.

3.1.2 UNITS 5A AND 5B

A horizontal shear sliding at the interface of the shear key-abutment stem wall developed in Test Units 5A and 5B. Capacity of the shear key of Unit 5B was very close to that initially estimated. Few hair line cracks developed in the stem wall during the test, but the width of these hair line cracks was very small throughout the test [Appendix A-2]. Figure 3-1b shows Test Unit 5B after failure.

(a) Failure mode of Test Unit 4A.

(b) Failure mode of Test Unit 5B

Figure 3-1 Test Observations

4 RECOMMENDATIONS FOR CONSTRUCTIONS

4.1 Discussion of Experimental Results

Based on the results of the experimental work performed at the University of California, San Diego, several recommendations are proposed in this section for construction details of sacrificial exterior shear keys.

- A smooth construction joint should be considered at the interface of the shear key-abutment stem wall, to effectively create a weaker plane at the shear key-abutment stem wall interface. Similarly, the smooth construction joint should exist between the shear key and the abutment back wall for the same reason. The abutment stem and back walls should be constructed first followed by smooth finishing of all surfaces.
- A bond breaker film should be applied on the abutment stem wall and back wall at the location of their interface with the shear keys. The purpose of bond breaker is to prevent any chemical bond between concretes of shear keys and abutments at the interface of the shear key-stem or back wall. Form oil could be used as a bond breaker. Other alternatives include use of available commercial products (used for Test Unit 5B). Another option could be the use of a mix of soap and talc, as used in precast segmental practice to break the bond between the match cast segments.
- Shear key vertical reinforcement should be lumped in a single group and be placed as close as possible to center of the shear key. These vertical reinforcing bars should be the only ones that connect the shear key to the abutment stem wall. Temperature and shrinkage reinforcement should be provided as standard design in the shear key and abutment wall. However, temperature and shrinkage reinforcement should not cross the shear key-abutment wall interface. No reinforcement should be used to connect the shear key to the abutment back wall.
- Horizontal reinforcement, required to carry the tension force in the stem wall arising from the force transmitted by the shear key, can be headed bars or standard hanger bars. These reinforcement should be placed in the stem wall as close as possible to the shear key. If headed bars are provided, the bars should be as long as possible; minimum concrete

cover should be maintained at the ends of the headed bars. If hanger bars are used, minimum length should be provided from the intersection of the lowest layer of the hanger bars and the shear key vertical reinforcement. Figure 4.1 shows a schematic of reinforcement configuration for hanger bars.

In order to be conservative the coefficient of friction, μ, is assumed to be equal to 0.6, which is the static coefficient of friction for concrete placed against hardened concrete surface not intentionally roughened (ACI, 2005). Hence the angle θ is equal to 31° (μ = tan θ) .

The basic development length of standard hooks (hanger bars) in tension is given by Crisafulli *et al*., 2002:

$$l_{dh} = \frac{1200\, d_b}{\sqrt{f'_c}} \tag{1}$$

Where d_b (in.) is the bar diameter and f'_c (psi) is the compressive strength of concrete. The basic development length should be multiplied by the appropriate correction factors to account for specified yield strength different than 60 ksi, concrete cover, presence of ties or stirrups around the bars, excess reinforcement, light weight aggregate concrete and epoxy coating of reinforcement (Crisafulli *et al*., 2002). Thus, for hanger bars:

$$L_{\min} = \tan\theta(a+b) + l_{dh} \tag{2}$$

$$L_{\min} = 0.6(a+b) + l_{dh} \tag{3}$$

Where "a" is the distance from the location of the applied force to the surface of the wall and "b" is the distance between the top surface of the stem wall to centroid of the lowest horizontal reinforcement layer. For headed bars L_{min} is equal to:

$$L_{\min} = 0.6(a+b) + c \tag{4}$$

Where "c" is recommended as 3 in (76 mm). L_{min} should be satisfied for the lowest layer of horizontal hanger bars or headed bars so that these reinforcing bars would be effective in transferring the tensile force.

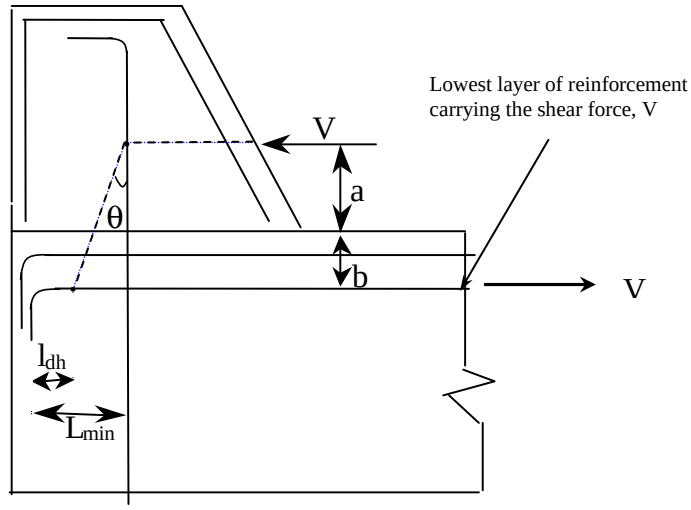

Figure 4-1 Schematic of Reinforcement Configuration with Hanger Bars

- The horizontal reinforcement should be concentrated close to top surface of the stem wall. If they are distributed along the height of the wall, the lower layers will not be effective in carrying any tension force. On the other hand L_{min} is a function of the location of the lowest layer of hanger bars or headed bars, indicating of the need to place the hanger bars close to top surface of the abutment stem wall.

5 EVALUATION OF THE CAPACITY OF EXTERIOR SHEAR KEYS

The capacity evaluation of exterior shear keys can be performed using Strut-and-Tie models. As reference the Strut-and-Tie model for shear keys at the failure is discussed in Appendix A-3. A mechanism model was developed for shear key 5B because this shear key performed as a sacrificial element with sliding shear failure at the expected load. Figure 5.1 shows the model of an exterior shear key, which is based on that proposed by Crisafulli *et al*., 2002. The nominal capacity of shear key is given by:

$$V_n = \frac{\mu_f \cos\alpha + \sin\alpha}{1 - \mu_f \tan\beta} A_{vf} f_{su} \tag{5}$$

where α is an angle of kinking of the vertical bars with respect to the vertical axis; β is an angle of inclined face of shear key with respect to the vertical axis (see Fig. 5.1); μ_f is a kinematic coefficient of friction of concrete; and f_{su} is an ultimate tensile strength of the vertical reinforcement. Due to the kinematics of the sliding shear key, the vertical bars which connect the shear key to the stem wall must kink. Experimental tests indicate the average kink angle, α, to be 37° at failure (Fig. A3-2). By back-calculating the tensile force of vertical reinforcement and kink angle, α, from displacement data (measured during the test in unit 5B) and substituting in Eq. (5), the value of μ_f for concrete with smooth finishing was determined to be 0.36. A smooth construction joint should be considered at the interface of the shear key-abutment stem wall, to effectively create a weaker plane at the shear key-abutment stem wall interface and enable occurrence of sliding shear failure at the interface. In shear key 5B, the ultimate tensile strength of the vertical reinforcement (#4 bars) was 103.9 ksi (710 MPa) and the total area of vertical bars crossing the shear key-abutment stem wall was 0.8 in^2 (516.1) mm^2. The angle of inclined face of the shear key, β, in all shear key units was equal to 16.3°. By substituting values of these variables in Eq. (5), the nominal shear force capacity of unit 5B is equal to 82.5 kips (364 kN), which is 8% greater than the shear force measured in the experiment for shear key 5B.

Capacity design to protect abutment system requires evaluation of over-strength capacity, V_o. Over-strength evaluation can be obtained from Eq. (5) by considering for uncertainty

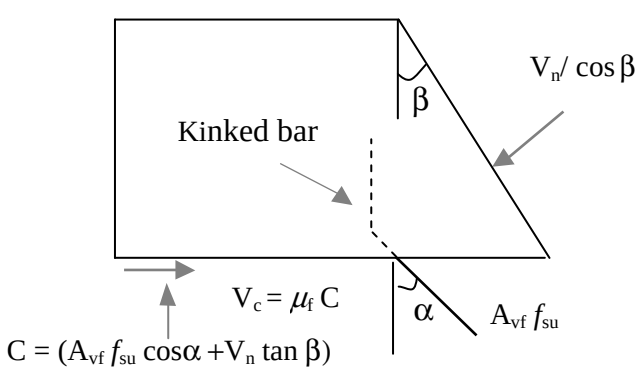

Figure 5-1 Mechanistic Model of Exterior Shear Key

and variability on the independent variables, using a Monte-Carlo simulation. Independent variables in Eq. (5) are α, the angle of kinked vertical bars with respect to vertical axis, μ_f, the kinematic coefficient of friction for concrete with smooth finishing, and f_{su}, the ultimate tensile strength of the vertical reinforcement. The independent variables are assumed to follow a truncated normal distribution as described in Table 5.1. Since there is only limited available test data for variables μ_f and α, the mean, upper, and lower values for these variables are assumed based on the limited test data. However, there are some available test data for yield strength of steel, f_y, that have been done at University of California, San Diego. Based on these data, it is assumed that the mean value for yield strength of steel (Grade 60), $\bar{f}_y$, is equal to 64.8 ksi.

Figure 5.2 shows the frequency distribution of (V_n / A_{vf}) as evaluated by using Eq. (5) for a number of randomly generated values of the independent variables. This distribution can be assumed as normally distributed with a mean value (V_n / A_{vf}) = 95.95 ksi and a standard deviation equal to 7.214 ksi:

Table 5-1 Summary of Statistic Analysis for Variables μ_f, α, and $f_{su}/\bar{f}_y$

Variable	Mean	COV*	Extreme Value	
			Upper	Lower
(1)	(2)	(3)	(4)	(5)
μ_f	0.36	6.8%	0.40	0.32
α	37°	4.9%	40°	34°
$f_{su}/\bar{f}_y$	1.55	5.9%	1.70	1.40

Coefficient of

* COV= Variation

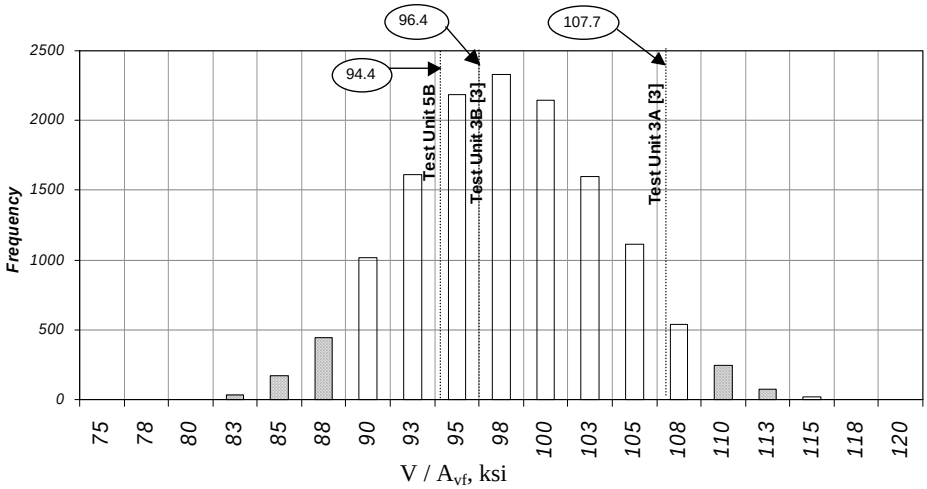

Figure 5-2 Frequency Distribution of V / A_{sv} Obtained from a Monte-Carlo Simulation.

$$V_o = \phi_o \overline{V_n} = \frac{\phi_o \left(\overline{\mu}_f \cos \overline{\alpha} + \sin \overline{\alpha}\right) A_{vf} \left(\dfrac{\bar{f}_{su}}{\bar{f}_y}\right) \bar{f}_y}{1 - \overline{\mu}_f \tan \beta} \tag{6}$$

For 95% confidence, the value of ϕ_o is equal to 1.13. By substituting values for $\overline{\mu_f}$, $\overline{\alpha}$, $\left(\dfrac{\bar{f}_{su}}{\bar{f}_y}\right)$ (from Table 5.1) and β:

$$V_o = \frac{(1.13)\left((0.36)\cos 37^\circ + \sin 37^\circ\right) A_{vf}\,(1.55)\,\bar{f}_y}{(1-(0.36)\tan 16.3^\circ)} \tag{7}$$

The ratio of mean value for yield strength of Grade 60 reinforcement to the specified yield strength results in:

$$\frac{\bar{f}_y}{f_y} = 1.08 \tag{8}$$

Where f_y is the specified yield strength (f_y = 60 ksi for Grade 60 steel). Hence, by substituting Eq. (8) into Eq. (7) and rounding up gives the following for design purposes:

$$V_o = 1.88 A_{vf}\, f_y \tag{9}$$

However, the capacity of a shear key should not exceed the smaller of 30% of the dead load vertical reaction at the abutment, W_a, or 75% of the total shear capacity of the piles, V_{piles}, plus one of the wing walls, $V_{wingwall}$, (Caltrans, 1993a). Therefore:

$$V_o \leq \min(0.3W_a, 0.75V_{piles} + V_{wingwall}) \tag{10}$$

By substituting Eq. (9) into Eq. (10) and solving for A_{vf}:

$$A_{vf} \leq \frac{\min(0.3W_a, 0.75V_{piles} + V_{wingwall})}{1.88 f_y} \tag{11}$$

The horizontal tie reinforcement in the stem wall below the shear key must be designed to carry the overstrength force, V_o, elastically. Thus, the area of reinforcement, A_{sh}, required in this region is equal to:

$$A_{sh} = \frac{1}{\phi}\frac{V_o}{f_y} \tag{12}$$

where ϕ, the strength reduction factor, is equal to 1.0, if capacity design has been used (Mattlock, 1974). Eq. (9) and Eq. (12) are the proposed design equations to determine the required amounts of shear key vertical reinforcement and horizontal tie reinforcement in the stem wall, respectively.

6 RECOMMENDATIONS FOR FUTURE RESEARCH

As mentioned above, Eq. (9) is recommended for design of sacrificial exterior shear keys with a smooth construction joint at the interface of the shear key-abutment stem wall. Future research would be recommended to:

1. Investigate the effect of the size and amount of vertical reinforcement on the capacity of shear keys.
2. Investigate the effect of changing the location of vertical reinforcement on capacity.
3. Use of standard hanger bars instead of headed bars with sufficient development length as reinforcement in the abutment stem wall.
4. Define the variation of the coefficient of friction, μ_f, for different types of construction joints.

7 APPENDIX A-1

Caltrans Contract No. 59A0337

Seismic Response of Sacrificial Exterior Shear Keys
in Bridge Abutments

Summary of the Experimental Results:
Test Units 4-A and 4-B

by

Azadeh Bozorgzadeh

Graduate Student Researcher

of

Department of Structural Engineering

University of California, San Diego

August 21, 2002

This report presents the results of the tests of two shear key Units 4-A and 4-B. These tests were held on August 21, 2002, at the University of California, San Diego (UCSD). Units 1-A to 3-B were tested earlier at UCSD under Caltrans Contract 59A0051 (Research report No. SSRP-2001/23).

Caltrans provided the main part of these specimens' design. Based on that design, eight #4 hanger bars were used horizontally close to the top surface of the abutment stem wall. In Test Unit 4-A, the shear key was built monolithically with the abutment stem wall. In Test Unit 4-B, there was a rough construction joint between the shear key and the wall. Figure A1-1 shows the schematic of the specimen.

In Test Unit 4-A, the first crack occurred at the lateral load of 100 kips, which was initiated at the interface between the shear key inclined face and the stem wall. The crack was inclined to the support (toe of the wall). The first yield occurred in one of the hanger bars at the load of 191 kips. The maximum load carrying capacity of the Unit 4-A was 329.3 kips. The first crack was the major crack during the test. The width of the major crack was around 0.4 in. at the maximum load carrying capacity. Figures A1-2 and A1-3 show the Test Unit 4-A at the first yield of the hanger bars and end of the test, respectively.

In Test Unit 4-B, the first crack occurred at the lateral load of 88 kips, which was initiated at the interface between the shear key inclined face and the stem wall. The crack was inclined to the support (toe of the wall). The first yield occurred in one of the hanger bars at the load of 147 kips. The maximum load carrying capacity of the Unit 4-B was 298.7 kips. The first crack was the major crack during the test. The width of the major crack was around 0.625 in. at the maximum load carrying capacity. Figures A1-4 and A1-5 show the Test Unit 4-B at the first yield of the hanger bars and end of the test, respectively.

Table A1-1 shows the experimental and calculated maximum load carrying capacities of the shear keys. In these calculations, f'_c was the strength of the concrete on date-of-test. A comparison of the values in columns 3 and 4 shows that the current Caltrans shear friction model severely underestimates the capacity of the shear keys. Column 5 represents the calculated maximum load carrying capacity of shear keys based on the Strut-and-Tie analogous model (Eqs.

5.2 to 5.4 in UCSD Research Report No. SSRP-2001/23 submitted to Caltrans on May 2002). Columns 6 and 7 show the ratio of the experimental and calculated maximum capacity of the shear keys based on the Caltrans model (shear friction) and Strut-and-Tie analogous model, respectively.

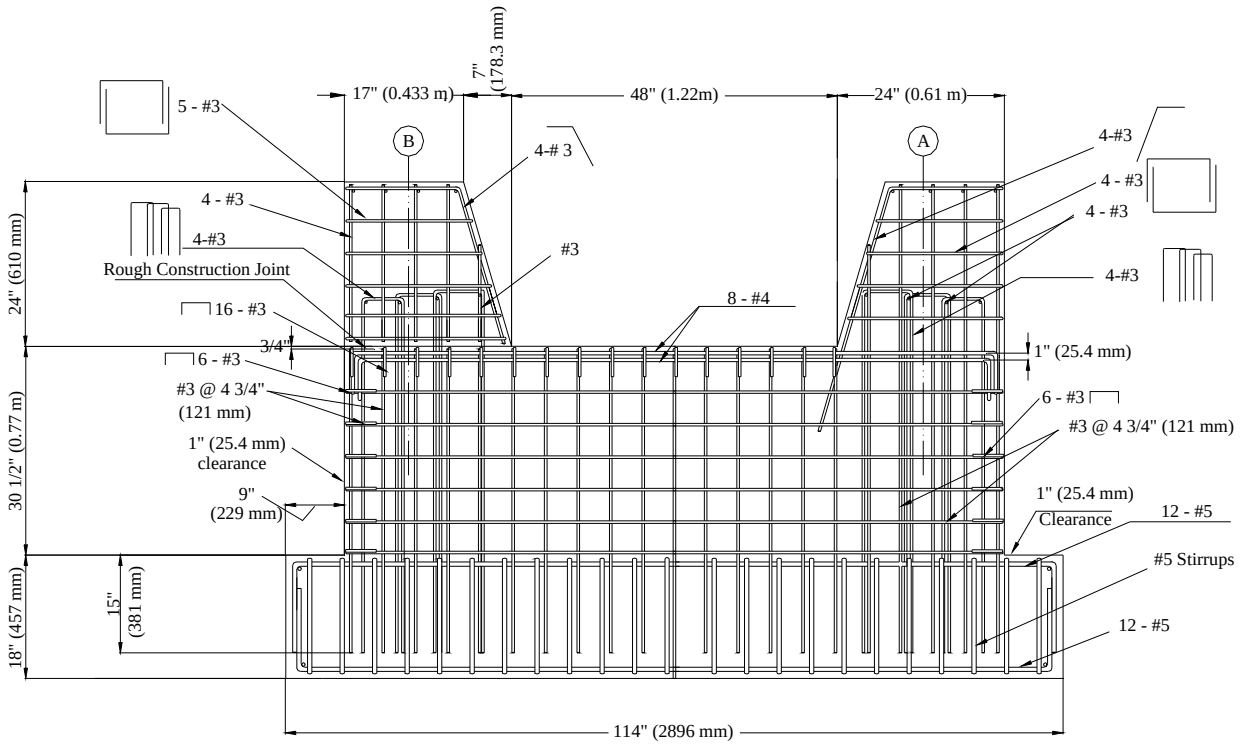

Figure A1- 1- Elevation View of the Reinforcement Layout

Figure A1- 2- Observation at First Yield of Hanger Bars of Test Unit 4-A

Figure A1- 3- Observation at the End of Test Unit 4-A

Figure A1- 4- Observation at First Yield of Hanger Bars of Test Unit 4-B

Figure A1- 5- Observation at the End of Test Unit 4-B

Results of this experiment indicate that the maximum load carrying capacity can be estimated using the Strut-and-Tie analogous model.

Table A1- 1: Experimental and Calculated Maximum Load Carrying Capacities of Shear Key (Units 4-A and 4-B)

TEST UNIT	f'_c psi (Mpa)	$V_{u,t}$ Kips (kN)	$V_{n,Calt}$ Kips (kN)	$V_{n,\ Strut\text{-}and\text{-}Tie}$ kips (kN)	$\frac{V_{n,Calt}}{V_{u,t}}$	$\frac{V_{n,\ Strut\text{-}and\text{-}Tie}}{V_{u,tt}}$
4-A	5780 (39.8)	329.3 (1464.8)	222.5 (989.7)	316 (1405.6)	0.68	0.96
4-B	5780 (39.8)	298.7 (1328.7)	160 (711.7)	297 (1321.1)	0.54	0.99

Figure A1-6 shows the Load vs. Displacement at top of the shear key Units 4-A and 4-B in one graph. Test Unit 4-B (with construction joint) has less capacity than that in Unit 4-A.

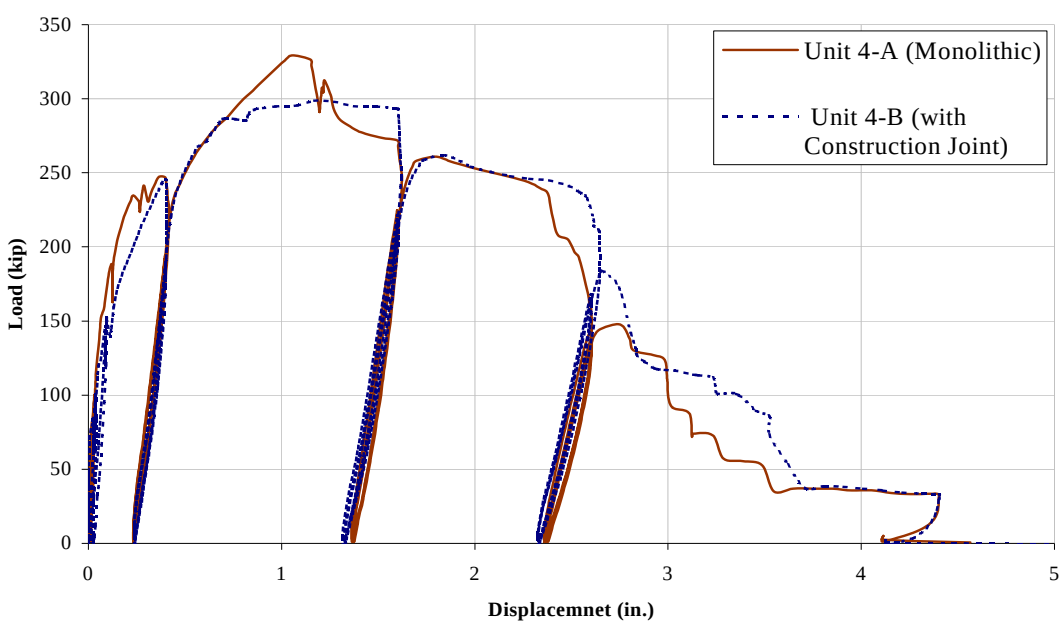

Figure A1- 6- Exterior Shear Keys Test Units 4-A and 4-B: Load vs. Displacement at top of shear key

8 APPENDIX A-2

Caltrans Contract No. 59A0337

Seismic Response of Sacrificial Exterior Shear Keys
in Bridge Abutments

Summary of the Experimental Results:
Test Units 5-A and 5-B

by
Graduate Student Researcher
of
Department of Structural Engineering
University of California, San Diego

December 20, 2002

This report presents the results of the tests of two shear key Units 5-A and 5-B. These tests were held on December 16, 2002, at the University of California, San Diego (UCSD). Units 1-A to 4-B were tested earlier at UCSD under Caltrans Contract 59A0051.

The design model and analysis of shear key units 5A and 5B were submitted to Caltrans previously. Based on strut-and-tie model, fourteen #4 headed bars were used horizontally close to the top surface of the abutment stem wall. In Test Unit 5-A, the foam was used at interface of the shear key and the wall. An 8x8 hole was provided at center of the foam. There was a rough construction joint between the shear key and the wall at the location of the hole and a smooth construction joint between the foam and the wall. All shear key vertical reinforcing bars are lumped at one location close to the side of the hole that is closer to the inclined face of the shear key. In Test Unit 5-B, there was a smooth construction joint between the shear key and the wall. A bond breaker is applied at interface to create a weak plane of failure. All shear key vertical reinforcing bars are lumped at one location near the centerline of the shear key. Figure A2-1 shows the schematic of the specimen.

In Test Unit 5-A, the first hair crack at surface of the wall occurred at the lateral load of 80 kips, which was initiated at the interface close to location of vertical bars. The crack was inclined to the support (toe of the wall). Several inclined hair cracks occurred during the test but the width of all cracks did not exceed 0.01 in. The maximum load carrying capacity of the Unit 5-A was 165.0 kips. The main slippage at interface occurred after the unit 5-A reached to the maximum load carrying capacity. Figures A2-2 and A2-3 show the Test Unit 5-A at the peak load and 0.6 in. displacement, respectively. Figure A2-4 shows the slippage of the test unit 5-A at 1.0 in. displacement and 103 kips load. The mode failure was shear failure at interface of the shear key and the stem wall. No damage was observed on the stem wall. Figure A2-5 and A2-6 show the specimen after failure with and without shear keys.

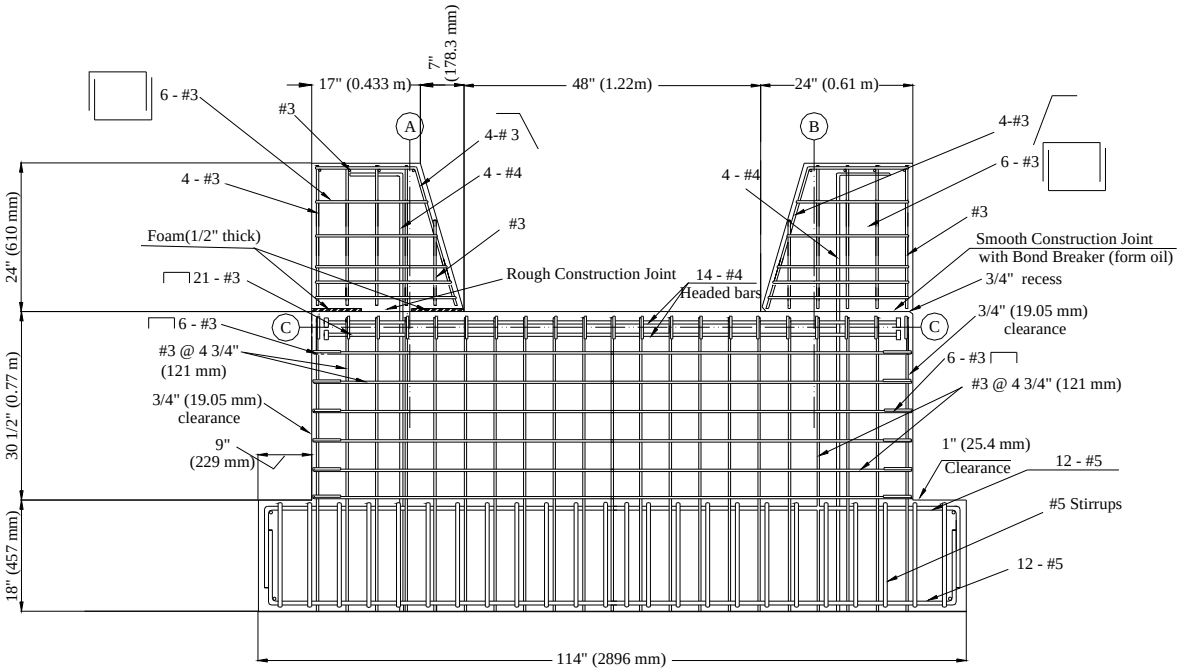

Figure A2- 1- Elevation View of the Reinforcement Layout

In Test Unit 5-B, the first hair crack occurred at the lateral load of 10 kips, which was the horizontal crack at the interface between the shear key and the stem wall. Few inclined hair cracks occurred during the test on the stem wall close to interface but the width of all cracks didn't exceed 0.01 in. The length of these hair cracks was shorter than those in test unit 5-A. The slippage between the shear key and the wall started at the load of 30 kips. The maximum load carrying capacity of the Unit 5-B was 75.5 kips which was very close to what was predicted. Figures A2-7 and A2-8 show the Test Unit 5-B at the peak load and 1.6 in. displacement, respectively. Figure A2-9 shows the slippage of the test unit 5-B at 2.0 in. displacement and 44 kips load. The mode failure was shear failure at interface of the shear key and the stem wall. No damage was observed on the stem wall. Figure 5 and 6 shows the specimen after failure with and without shear keys.

Table A2-1 shows the experimental and calculated maximum load carrying capacities of the shear keys. In these calculations, f'_c was the strength of the concrete on date-of-test. A comparison of the values in columns 3 and 4 shows that the current Caltrans shear friction model underestimates the capacity of the shear keys. In test unit 5-A the capacity was twice as what was

estimated. It is believed that the high strength was achieved due to cohesion of concrete at rough construction joint. More investigation and data analysis is required for more details. Column 5 shows the ratio of the experimental and calculated maximum capacity of the shear keys based on the Caltrans model (shear friction).

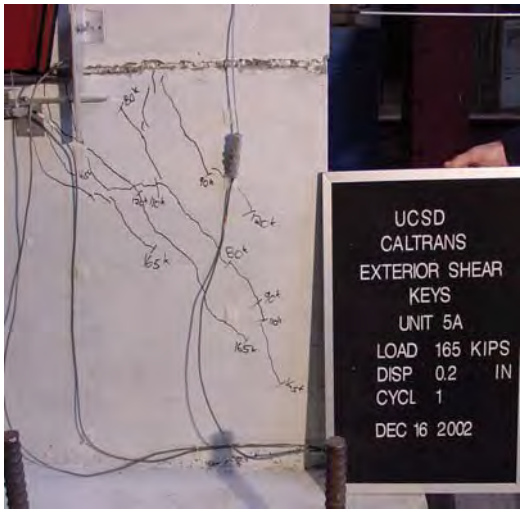

Figure A2- 2- Observation at Peak Load of Test Unit 5-A

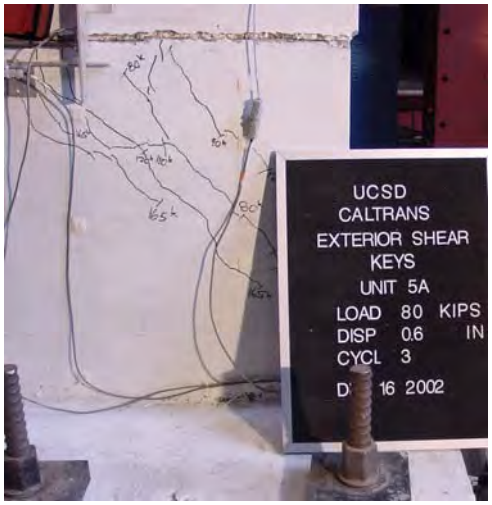

Figure A2- 3- Observation at 0.6 in. Displ. of Test Unit 5-A

Figure A2- 4- Observation at 103 kips lateral Load with 1.0 in. Displ. of Shear Key in Test Unit 5-A

Figure A2- 5- Observation of Specimen at Failure

Figure A2- 6- Observation of Specimen at Failure After Removing the Keys

Figure A2- 7-Observation at Peak Load of Test Unit 5 -B

Figure A2- 8- Observation at 1.6 in. Displ. of Test Unit 5 -B

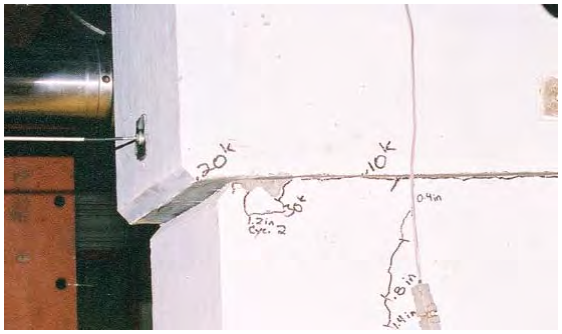

Figure A2- 9- Observation at 44 kips lateral Load with 2.0 in. Displ.of Shear Key in Test Unit 5-B

Results of this experiment indicate that the maximum load carrying capacity can be estimated using the Strut-and-Tie analogous model for exterior shear keys with smooth construction joint.

Table A2- 1: Experimental and Calculated Maximum Load Carrying Capacities of Shear Key (Units 5-A and 5-B)

TEST UNIT	f'_c psi (Mpa)	$V_{u,t}$ Kips (kN)	$V_{n,Calt}$ Kips (kN)	$\frac{V_{n,Calt}}{V_{u,t}}$
5-A	4900 (33.8)	165.5 (736.2)	50.4 (224.1)	0.3
5-B	4900 (33.8)	75.5 (335.8)	30.24 (134.5)	0.4

Figure A2-10 shows the Load vs. Displacement at top of the shear key Units 5-A and 5-B in one graph. Test Unit 5-B (with smooth construction joint) has less capacity than that in Unit 5-A.

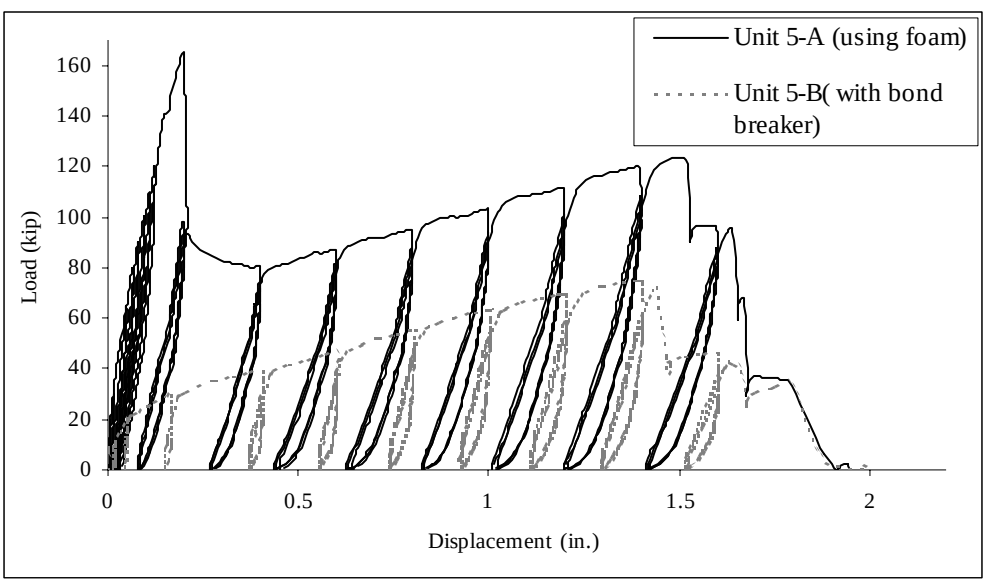

Figure A2-10- Exterior Shear Keys Test Units 5-A and 5-B: Load vs. Displacement at top of shear key

9 APPENDIX A-3

9.1 Analytical Study of Sacrificial Shear Keys

In order to estimate the capacity of shear keys, a Strut-and-Tie model is developed. The model takes into account the deformed shape of the shear key. Figure A3-1 shows the strut-and-tie

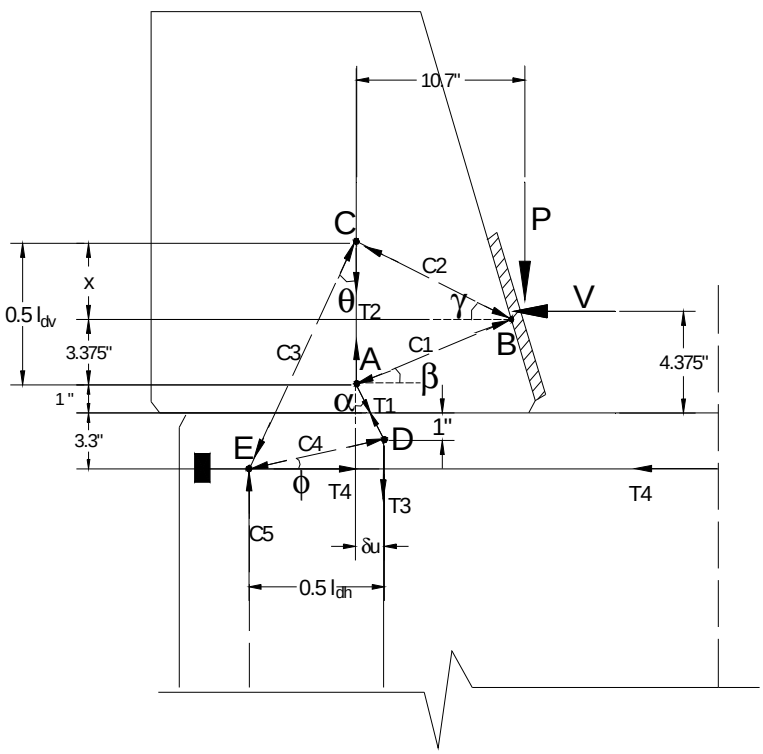

Figure A3- 1- Strut-and-Tie Model for Shear Key

model. In order to measure the angle of kinked vertical bars, fractured vertical bars were removed from inside shear key and stem wall. Figure A3-2 shows one of the kinked vertical bars after putting together the two fractured pieces. The forces in struts and ties are found as described below. The ultimate force in the shear key vertical reinforcement, T_1, is calculated by:

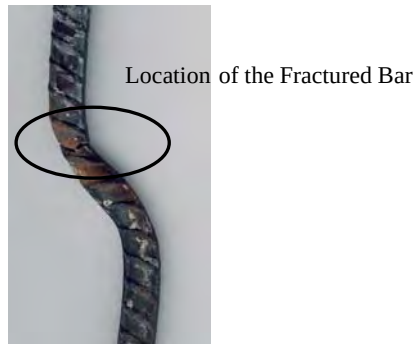

Figure A3- 2- A Fractured Vertical Bar in Unit 5B, Removed from Inside of Concrete

$$T_1 = A_{vf}\, f_{su} \qquad \text{(A-1)}$$

Where A_{sv} is the amount of the vertical reinforcement connecting the shear key to the abutment stem wall and f_{su} is the ultimate tensile strength of the vertical reinforcement. For Test Unit 5B, A_{vf}=0.8 in^2, and f_{su}=103.9 ksi (measured). Thus,

$$T_1 = (0.8)(103.9) = 82.472 \text{ kips}$$

The experimental shear key capacity of Unit 5B, V [see Fig. A3-1] was 75.5 kips and the angle of deformed reinforcement with respect to vertical axis was measured as $\alpha = 37^\circ$.

The development length of reinforcing bars is given by the following equation [5]:

$$l_d = \frac{0.025 d_b f_y}{\sqrt{f_c'}} \quad \text{(lb and in. units)} \qquad \text{(A-2)}$$

Where d_b is the bar diameter; f_y is the yield strength and f'_c is the concrete compressive strength. For Unit 5B, d_b=0.5 in (No. 4 bars); f'_c (abutment stem wall) = 4930 psi; f'_c (shear key) = 4870 psi; f_y (vertical bars) = 62.97 ksi and f_y (tension tie reinforcement) = 66.02 ksi. Thus, the development length of vertical reinforcement, l_{dv}, is given by:

$$l_{dv} = \frac{(0.025)(0.5)(62970)}{\sqrt{4870}} = 11.28''$$

$$\frac{l_{dv}}{2} = 5.64''$$

Similarly, the development length of the tension tie reinforcement (headed bars), l_{dh}, is given by:

$$l_{dh} = \frac{(0.025)(0.5)(66020)}{\sqrt{4930}} = 11.75''$$

$$\frac{l_{dh}}{2} = 5.88''$$

Thus,

$$0.5 l_{dh} - \delta u = 5.88 - 1.4 = 4.48''$$

Where δ_u is the measured displacement at failure (δ_u = 1.4 in. for Unit 5B). From geometries, the angles between struts and ties can be determines as follows:

$$\gamma = \tan^{-1}\left(\frac{5.64 - 3.375}{10.7}\right) = 11.95^\circ$$

$$\beta = \tan^{-1}\left(\frac{3.375}{10.7}\right) = 17.5^\circ$$

$$\theta = \tan^{-1}\left(\frac{4.48}{3.3 + 1 + 3.375 + 2.265}\right) = 24.26^\circ$$

$$\phi = \tan^{-1}\left(\frac{3.3 - 1}{5.88}\right) = 21.36^\circ$$

In order to find the force in each individual strut and tie, it is needed to solve the force equilibrium equations at each node as follows:

At node “A”:

$$\sum H = 0 \Rightarrow C_1 \cos\beta = T_1 \sin\alpha$$

$$C_1 = 49.6 \text{ kips}$$

At node “B”:

$$\sum H = 0 \Rightarrow V = C_1 \cos\beta + C_2 \cos\gamma$$

$$75.5 = (49.6)\cos 17.5^\circ + C_2 \cos 11.95^\circ$$

$$C_2 = 28.8 \quad \text{kips}$$

$$\sum V = 0 \Rightarrow P = C_1 \sin\beta - C_2 \sin\gamma$$

$$P = (49.6)\sin 17.5^\circ - (28.8)\sin 11.95^\circ$$

$$P = 8.95 \quad \text{kips}$$

At node "C":

$$\sum H = 0 \Rightarrow C_3 \sin\theta = C_2 \cos\gamma$$

$$C_3 = 68.57 \quad \text{kips}$$

At node "D":

$$\sum H = 0 \Rightarrow C_4 \cos\phi = T_1 \sin\alpha$$

$$C_4 = 50.79 \quad \text{kips}$$

At node "E":

$$\sum V = 0 \Rightarrow C_5 = C_3 \cos\theta + C_4 \sin\phi$$

$$C_5 = 81.01 \quad \text{kips}$$

$$\sum H = 0 \Rightarrow T_4 = C_4 \cos\phi + C_3 \sin\theta$$

$$T_4 = V = 75.5 \quad \text{kips}$$

$$\varepsilon_s = \frac{75.5}{((14)(0.2)(29000))} = 929.8\mu s$$

The maximum measured strain in the tension reinforcement was 974 μs, which agrees with the strain value calculated above. This indicates that the Strut-and-Tie model shown in figure (A3-1) is reasonable.

10 APPENDIX A-4

10.1 Evaluation of the Capacity of the Test Series IV

Capacity estimation of exterior shear keys series IV was evaluated using three different existing models.

10.1.1 Strut-and-Tie Mechanism and Hysteretic Model:

The strut-and-tie mechanism and hysteretic model presented in report SSRP 2001/23 (Megally *et al.,* 2001) was used to evaluate the capacity of shear keys unit 4A and 4B. The hysteric model is composed of two components, which represent the concrete behavior and steel behavior. The steel reinforcement is assumed as a tension tie where concrete is acting as compressive struts. Figure A4-1illustrates the schematic of the strut-and-tie behavior of shear key under lateral load. The diagonal concrete struts and steel reinforcement ties which are the horizontal and vertical bar in the abutment stem wall are shown clearly. A diagonal crack develops in the abutment stem wall below the shear key by applying lateral load. The load is transferred from the shear key to the footing by the diagonal strut as shown in Figure A4-1. The capacity of Test Units 4A and 4B was calculated using equilibrium of the shear key along this diagonal crack. Therefore, based on this model the capacity of the shear key is equal to:

$$V_N = V_C + V_S \qquad \textbf{(A4. 1)}$$

where V_C and V_S are the concrete and reinforcing steel contribution to the strength of the shear key respectively. V_C, the concrete contribution can be calculated by:

$$V_C = \begin{cases} 2.4\sqrt{f_c^{'}}\, b\ h & (psi) \\ 0.2\sqrt{f_c^{'}}\, b\ h & (MPa) \end{cases} \qquad \textbf{(A4. 2)}$$

where h is height of the abutment stem wall; b is width of the abutment stem wall and f_c' is the concrete compressive strength. By substituting h = 30.5 in (775 mm); b = 16.75 in. (425 mm) and f_c' = 5,780 psi (34.5 MPa), the contribution of the concrete is equal to:

$$V_C = 93.2 \text{ Kips (414.6 KN)}$$

The reinforcing steel contribution to the capacity of the shear key, V_S , is obtained by taking summation of moments about point A. All reinforcing bars intersecting the crack are assumed to yield. Thus the contribution of steel V_S is calculated as follows:

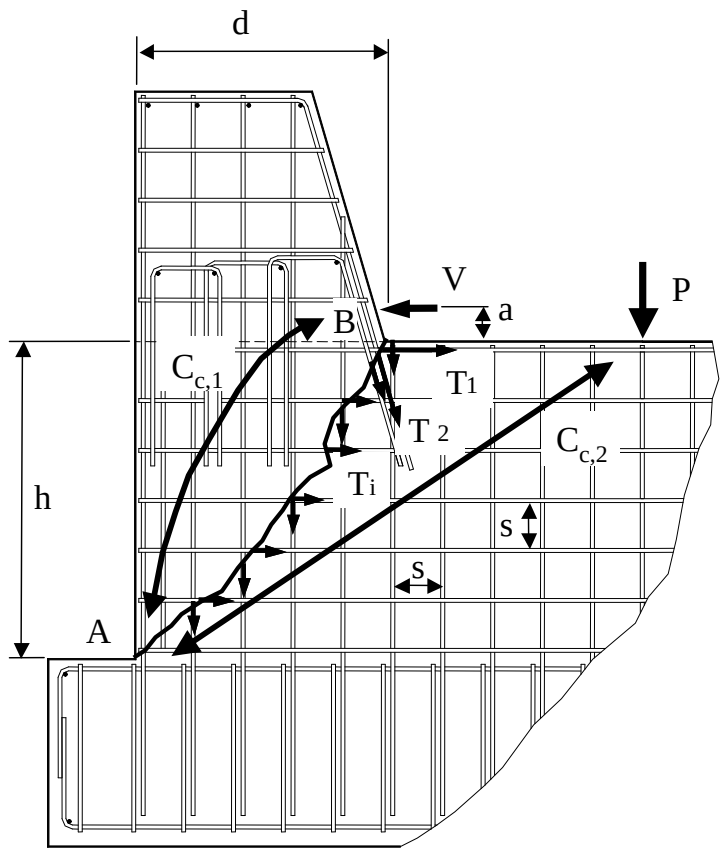

Figure A4- 1- Schematic of Strut-and-Tie Model for Exterior Shear Key, After Megally *et al*., 2001

$$V_S = \left[A_{vf}\, f_y \frac{d}{2} + A_{s,1} f_{y,1} h + A_{s,2} f_{y,2} d + n_h\ A_{s,s}\ f_{y,s} \frac{h^2}{2\,s} + n_v\ A_{s,s}\ f_{y,s} \frac{d^2}{2\,s} \right] \left(\frac{1}{h+a} \right) \quad \textbf{(A4.3)}$$

where A_{vf} is the total vertical reinforcement which connect the shear key to the stem wall and cross the crack, $A_{s,1}$ is the total area of steel of hanger bars; $A_{s,2}$ is the total area of steel along T_2 (see Figure A4-1). In general horizontal and vertical side reinforcement are same in amount and $A_{s,s}$ is the cross sectional area of the side reinforcement (Megally *et al*., 2001). For the test units 4A and 4B of this experimental program, a = 4 in. (102 mm) and s = 4.75 in. (121 mm). Table A4- 1 shows the calculated V_S , given by Eq.(A4.3) for Test Units 4A and 4B. Total Shear key capacity, given by Eq. (A4. 1), which is based on the proposed model in report SSRP 2001/23, is calculated and presented in Table A4- 2. The idealized load-displacement envelope, which

describes the behavior of exterior shear key under lateral load in terms of five damage level, is presented in Figure A4- 2. Damage level I is characterized by onset of cracking at the shear-key abutment stem wall interface.

Test Series	Test Unit	Vertical Steel Area Crossing Interface of Shear Key & Wall		Steel Areas for Strut-and-Tie Model		Cross Sectional Area of the Side Reinforcement		V_S Steel Contribution to Shear Key Capacity kips (KN) Eq. (1.4)
		No. of Bars	A_{vf} in^2. (mm^2)	$A_{s,1}$ in^2. (mm^2)	$A_{s,2}$ in^2. (mm^2)	Bar Size	$A_{s,s}$ in^2. (mm^2)	
IV	4A	24#3	2.64 (1,703)	1.6 (1,032)	0.44 (284)	#3	0.11 (71)	222.5 (989.7)
	4B	24#3	2.64 (1,703)	1.6 (1,032)	-------	#3	0.11 (71)	203.8 (906.5)

Table A4- 1: Calculated the Steel Contribution to the Capacity of Exterior Shear Key Test Units 4A and 4B

Test Series	Test Unit	Vc Concrete Contribution to Shear Key Capacity kips (KN) Eq. (A4. 2)	V_S Steel Contribution to Shear Key Capacity kips (KN) Eq. (A4.3)	V_N Shear Key Capacity kips (KN) Eq. (A4. 1)
IV	4A	93.2 (414.6)	222.5 (989.7)	315.7 (1404.3)
	4B	93.2 (414.6)	203.8 (906.5)	297 (1321.1)

Table A4- 2: Calculated Capacity of Exterior Shear Key Test Units 4A and 4B

The required shear force to cause crack in shear key is given by:

$$V_{cr} = \frac{7.5\sqrt{f_c^{'}}bd}{3k + \sqrt{9k^2 + 4}} \qquad \textbf{(A4. 5)}$$

where $a = kd$, is the distance from the top of the stem wall to center of application of the laeral load, V. The shear key top displacement at damage level I is:

$$\Delta_I = \Delta_{II}\frac{V_{cr}}{V_y} \qquad \textbf{(A4. 6)}$$

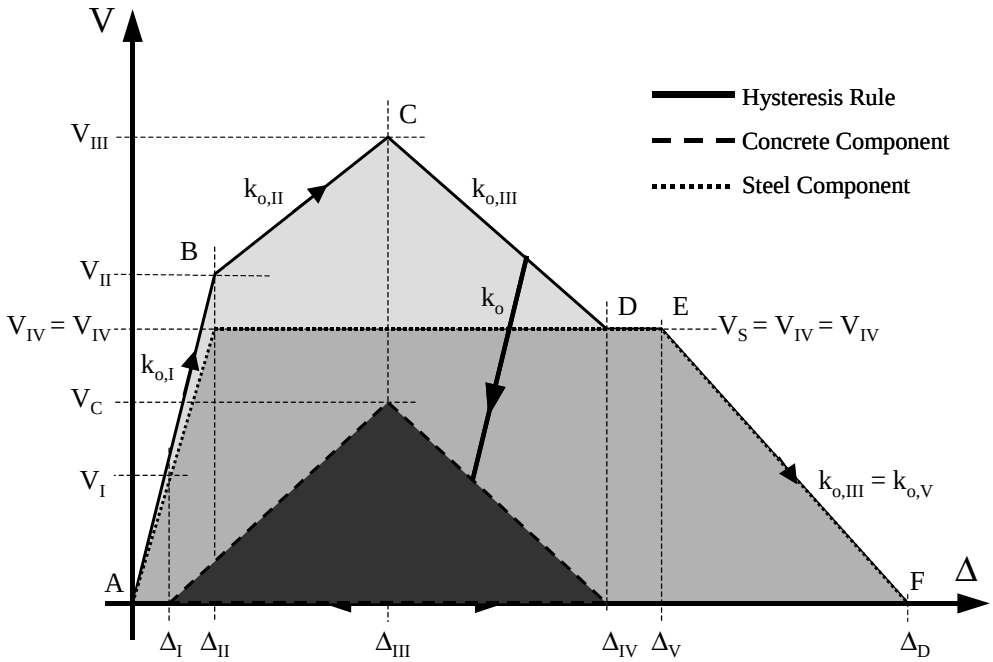

Figure A4- 2- Hysteresis Model for Exterior Shear Key, After Megally *et al*., 2001

which Δ_{II} and V_y is the shear key to displacement and shear force at level II, respectively. Level II represent to onset of yielding of the shear key reinforcement. The shear force at level II is computed by:

$$V_{II} = V_S + V_C \frac{\Delta_{II}}{\Delta_{III}} \qquad \textbf{(A4. 7)}$$

where V_C which is given by Eq (A4. 2), is the concrete component to the shear resisting mechanism. Δ_{II} and Δ_{III} are the shear keys top displacement at level II and III. The displacement at top of the shear key at Level II is calculated by:

$$\Delta_{II} = \sqrt{2}\varepsilon_y (L_d + L_a) \frac{(h+d)}{\sqrt{h^2 + d^2}} \qquad \textbf{(A4. 8)}$$

where L_d is the reinforcement development length given by:

$$L_d = \frac{d_b f_y}{25\sqrt{f_c^{'}}} \qquad [psi, in] \qquad \textbf{(A4. 9)}$$

where d_b is the bar diameter and L_a in Eq. (A4. 8) is the cracked region and based on the test observations this value is about the width of the stem wall, *b*. Level III is corresponding to the

peak load. Increase in width of the diagonal crack results in decreasing the contribution of concrete to the shear key capacity. At this level the peak load is calculated by Eq (A4. 1), and the displacement at top of the key is computed by:

$$\Delta_{III} = \sqrt{2}\varepsilon_y (L_d + L_a)\frac{(h+d)}{s} \qquad \textbf{(A4. 10)}$$

where s is the reinforcement spacing in the stem wall. At the level III it is assumed that all the rebars crossing the crack zone have been yielded. At the damage level IV the shear key capacity is equal to the steel contribution to the resisting mechanism and concrete contribution is small enough to be neglected. Thus, the capacity of the shear key is $V_{IV} = V_S$. It is assumed that the degradation of the concrete contribution to the shear resisting mechanism occurs likely at a steel strain of 0.005. Therefore, the displacement at this level is calculated by:

$$\Delta_{IV} = \sqrt{2}\varepsilon_{0.005} (L_d + L_a)\frac{(h+d)}{s} \qquad \textbf{(A4. 11)}$$

Finally, level V represents fracture of reinforcement crossing the cracking zone. The capacity of the shear key does not change from damage level IV since the shear key capacity is equal to just steel contribution. Investigation on test results show that the steel strain at onset of fracture is equal to approximately to 0.007. Thus, the displacement at top the shear key is computed by:

$$\Delta_{V} = \sqrt{2}\varepsilon_{0.007} (L_d + L_a)\frac{(h+d)}{s} \qquad \textbf{(A4. 12)}$$

	Test Unit 4A		Test Units 4B	
	Load kips(KN)	Displacement in.(mm)	Load kips(KN)	Displacement in.(mm)
LEVEL I	89.40(397.7)	0.060(1.52)	71.55(318.3)	0.052(1.32)
LEVEL II	233.8(1,040)	0.157(3.99)	215.1(956.8)	0.157(3.99)
LEVEL III	315.7(1,404.3)	1.30(33.02)	297(1,321.1)	1.30(33.02)
LEVEL IV	222.5(989.7)	2.66(67.56)	203.8(906.5)	2.66(67.56)
LEVEL V	222.5(989.7)	3.72(94.49)	203.8(906.5)	3.72(94.49)

Table A4- 3: Calculated Load and Displacement of Test Series IV at Each Damage Level

Table A4- 3 shows the calculated load and displacement at each level for Test series IV.

10.1.2 Horizontal Reinforcement Strain Profiles

Figures A4-3 to A4-18 show the horizontal profiles of strains in the two layers of horizontal reinforcement (hanger bars) nearest to the top surface of the abutment stem wall in Unit 4A and Unit 4B. The high strain after level 3 shows the agreement with the crack pattern in test 4A and 4B, which indicates significant diagonal cracking in the abutment stem wall started from the toe of the shear key.

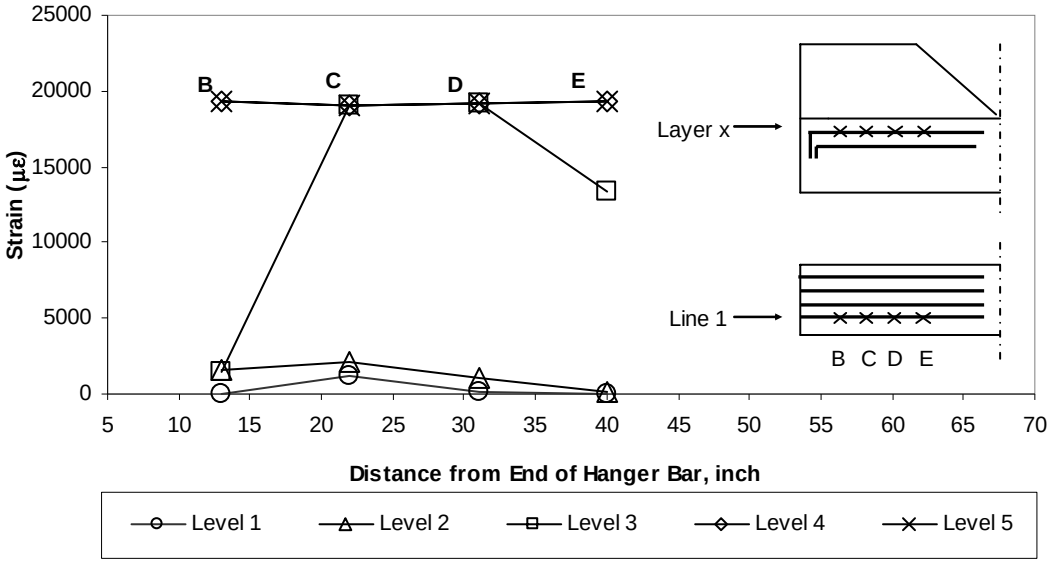

Figure A4- 3- Horizontal Strain Profiles, Layer x, Line 1, Unit 4A

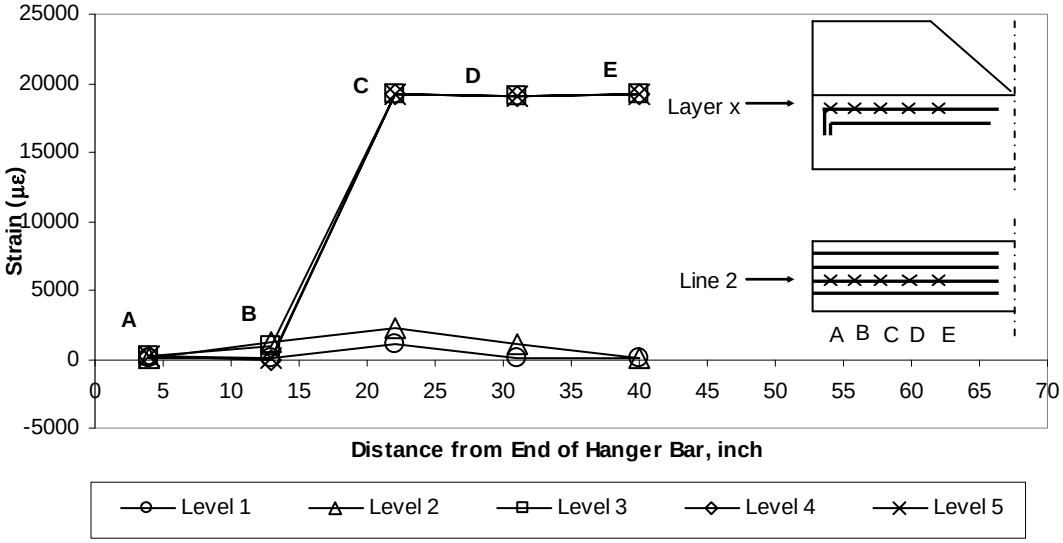

Figure A4- 4- Horizontal Strain Profiles, Layer x, Line 2, Unit 4A

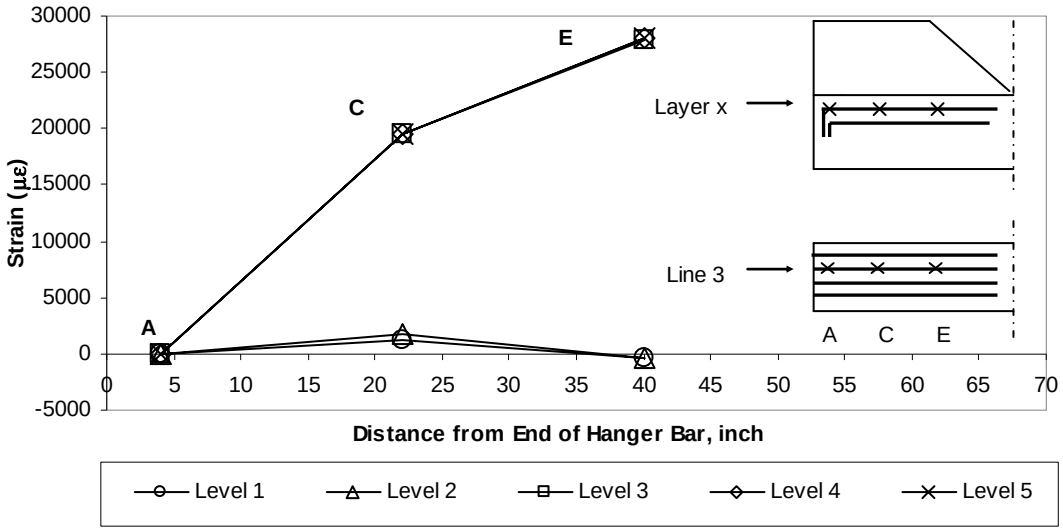

Figure A4- 5- Horizontal Strain Profiles, Layer x, Line 3, Unit 4A

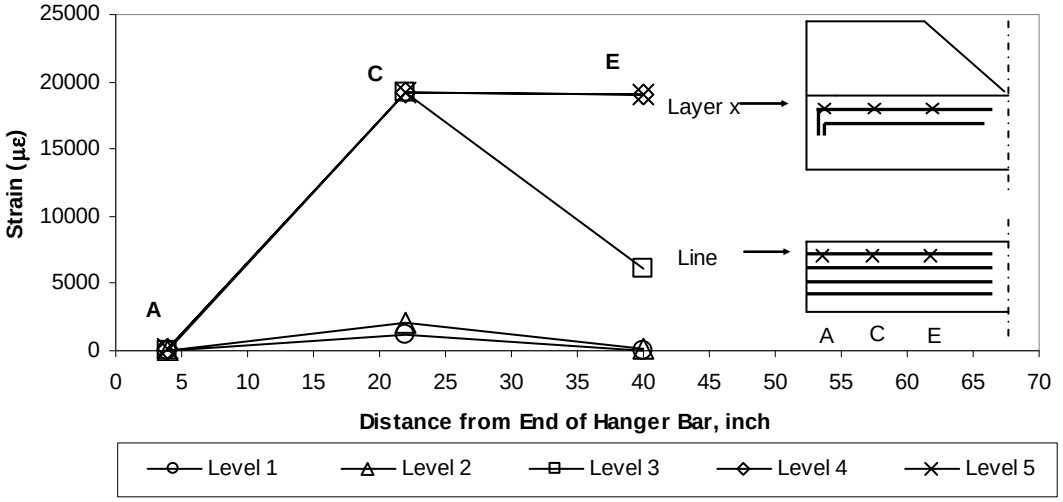

Figure A4- 6- Horizontal Strain Profiles, Layer x, Line 4, Unit 4A

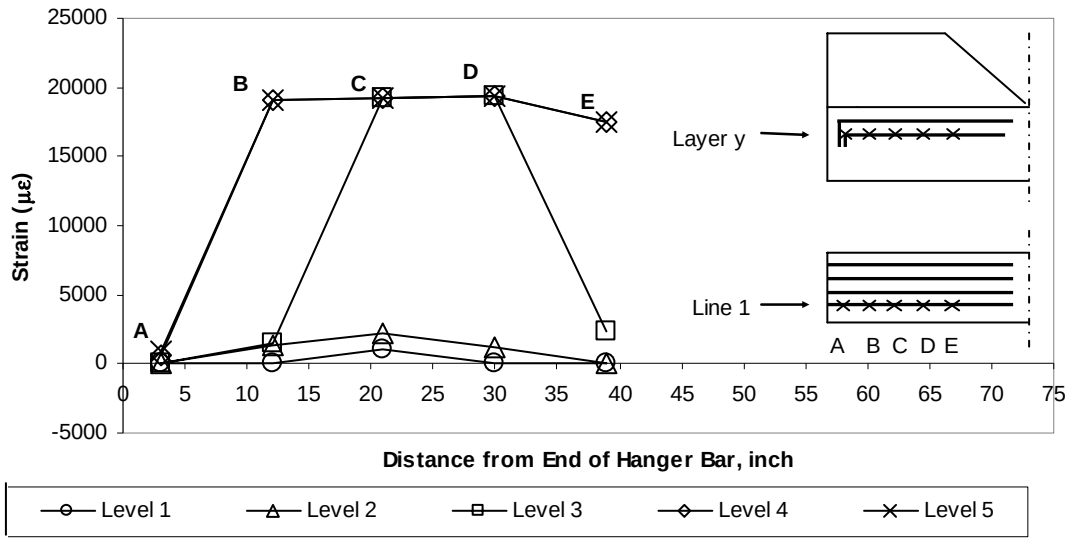

Figure A4- 7- Horizontal Strain Profiles, Layer y, Line 1, Unit 4A

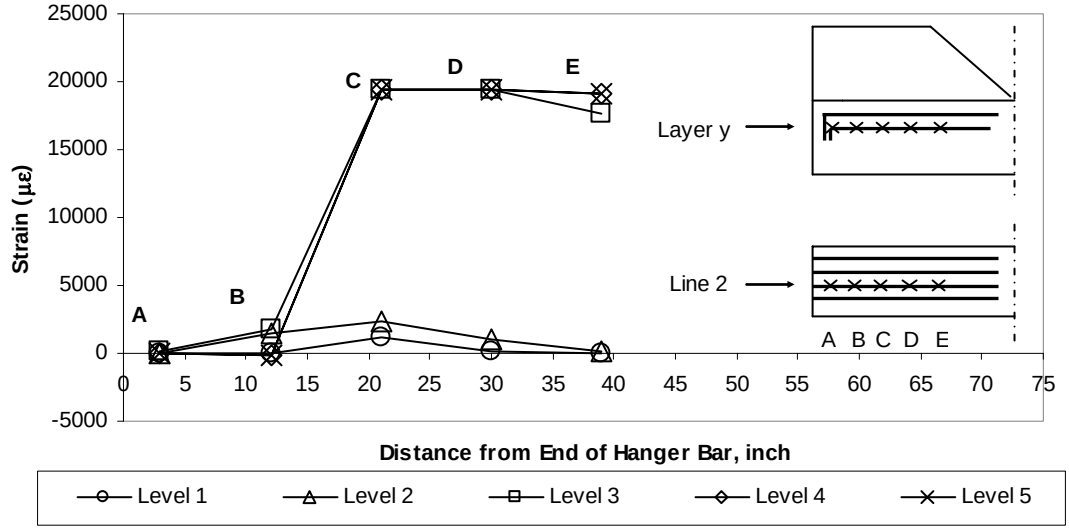

Figure A4- 8- Horizontal Strain Profiles, Layer y, Line 2, Unit 4A

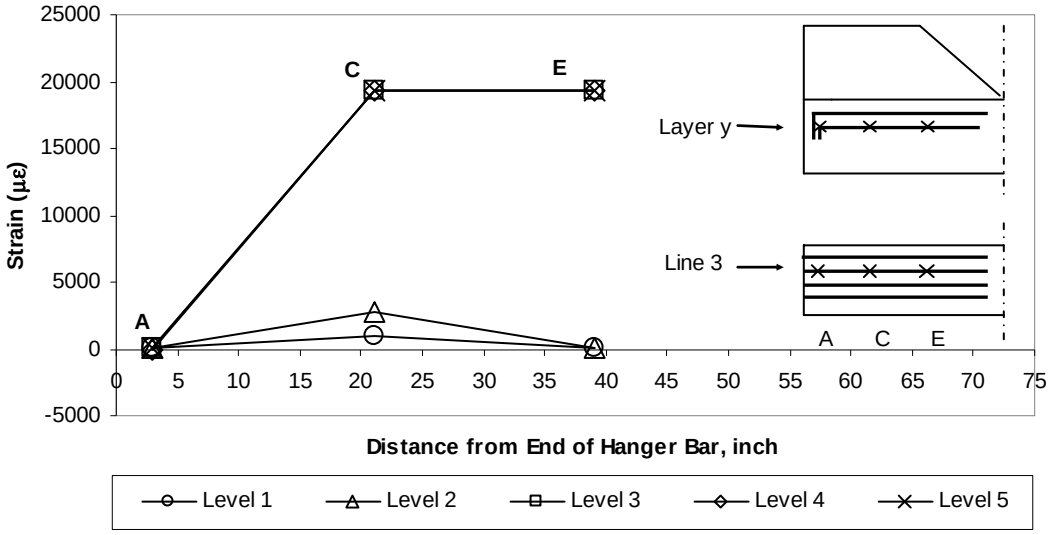

Figure A4- 9- Horizontal Strain Profiles, Layer y, Line 3 Unit 4A

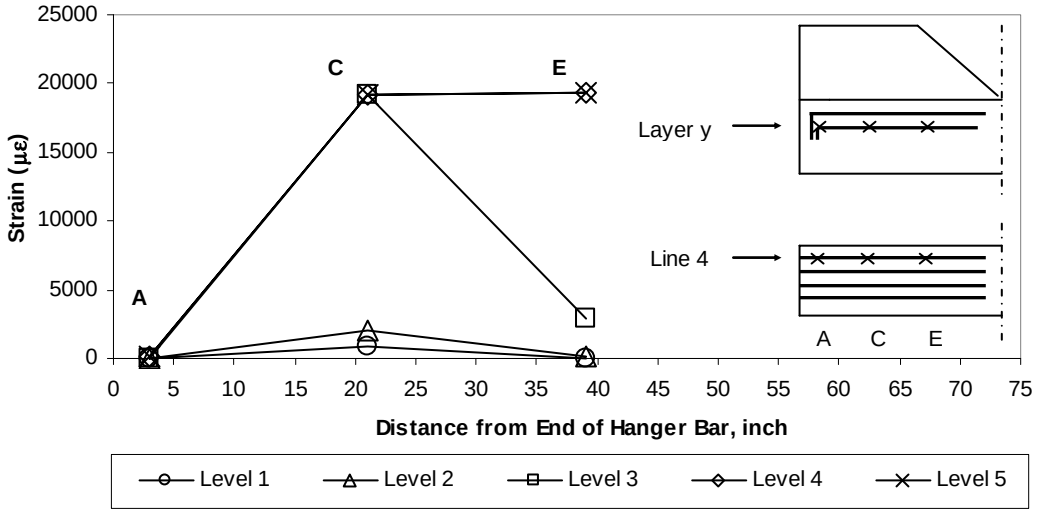

Figure A4- 10- Horizontal Strain Profiles, Layer y, Line 4, Unit 4A

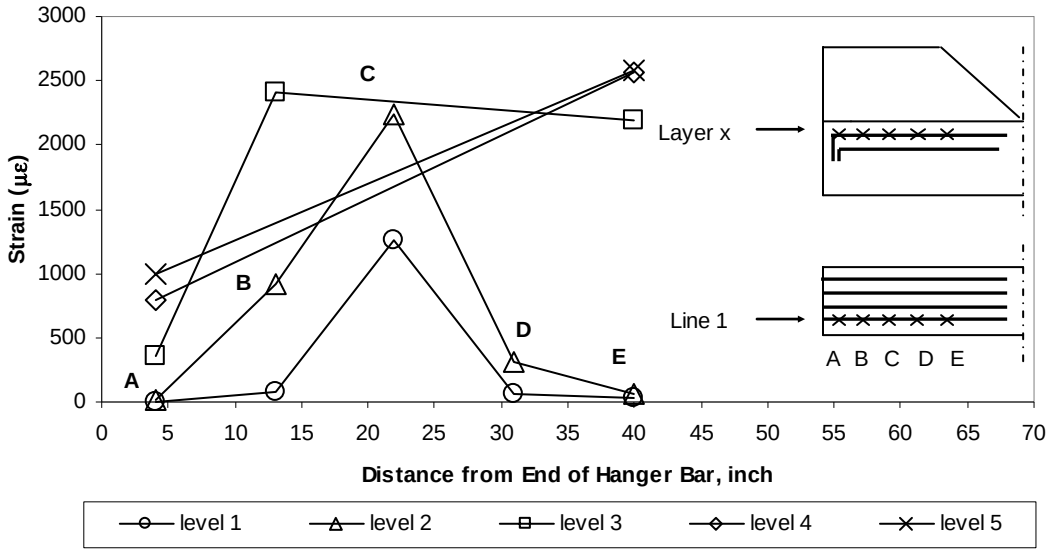

Figure A4- 11- Horizontal Strain Profiles, Layer x, Line 1, Unit 4B

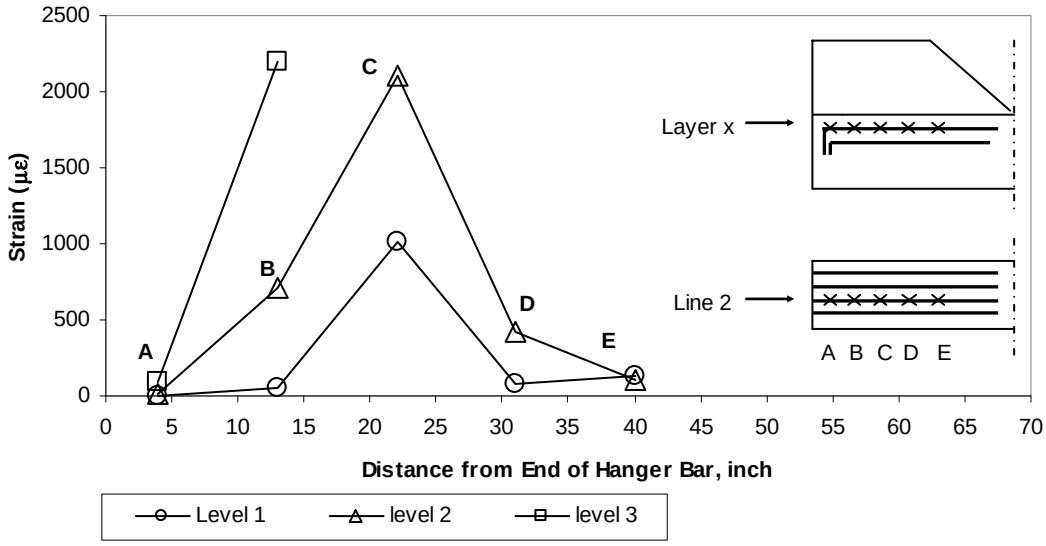

Figure A4- 12- Horizontal Strain Profiles, Layer x, Line 2, Unit 4B

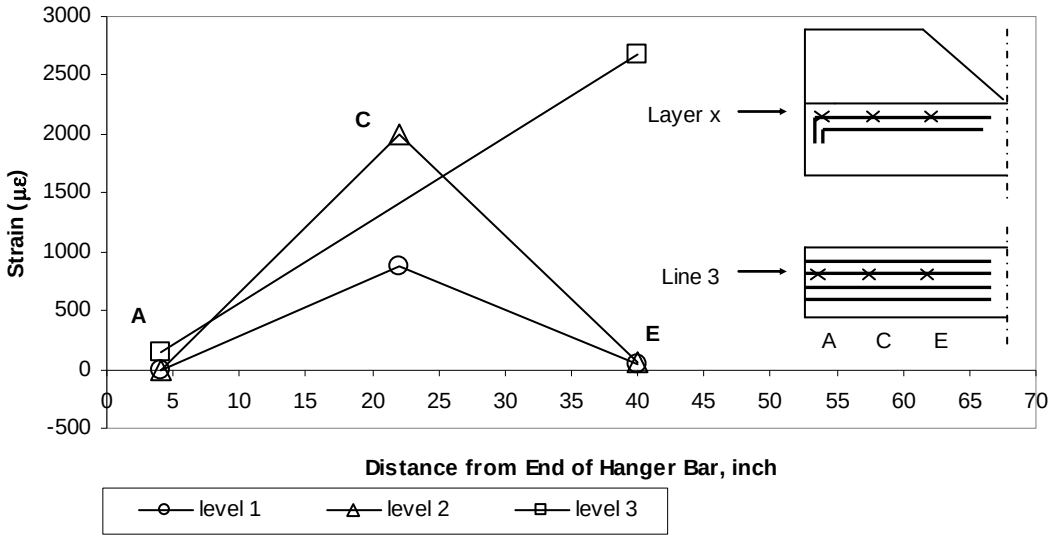

Figure A4- 13- Horizontal Strain Profiles, Layer x, Line 3, Unit 4B

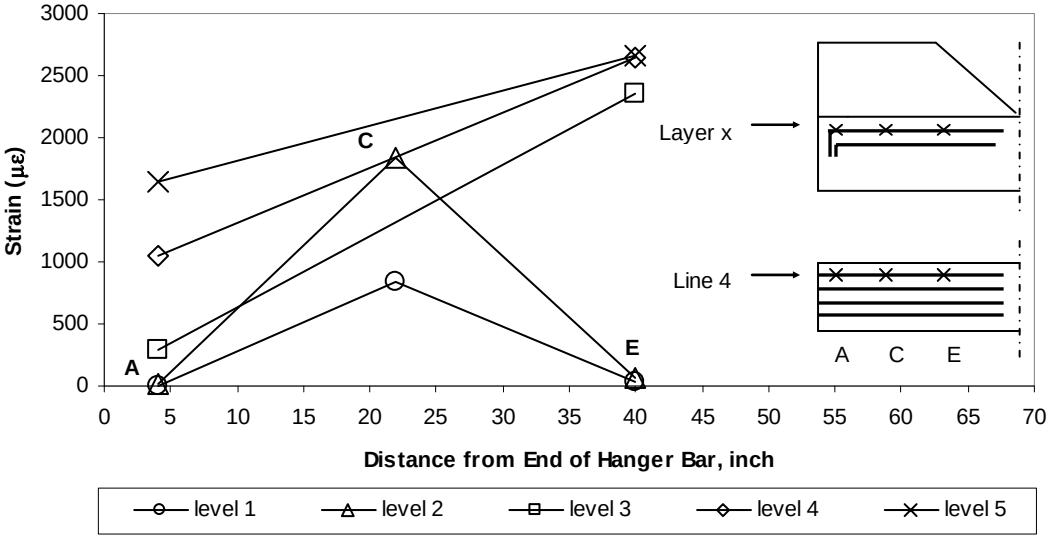

Figure A4- 14- Horizontal Strain Profiles, Layer x, Line 4, Unit 4B

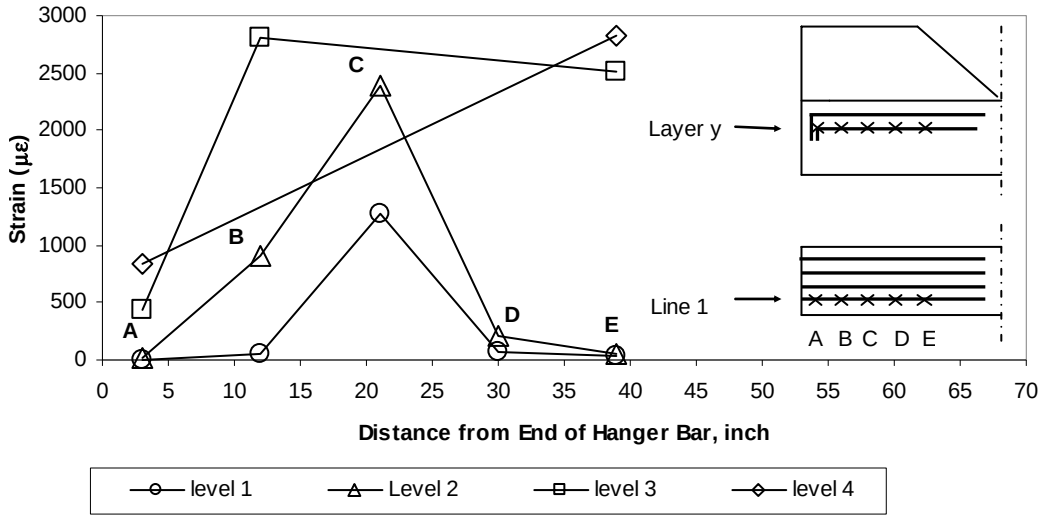

Figure A4- 15- Horizontal Strain Profiles, Layer y, Line 1, Unit 4B

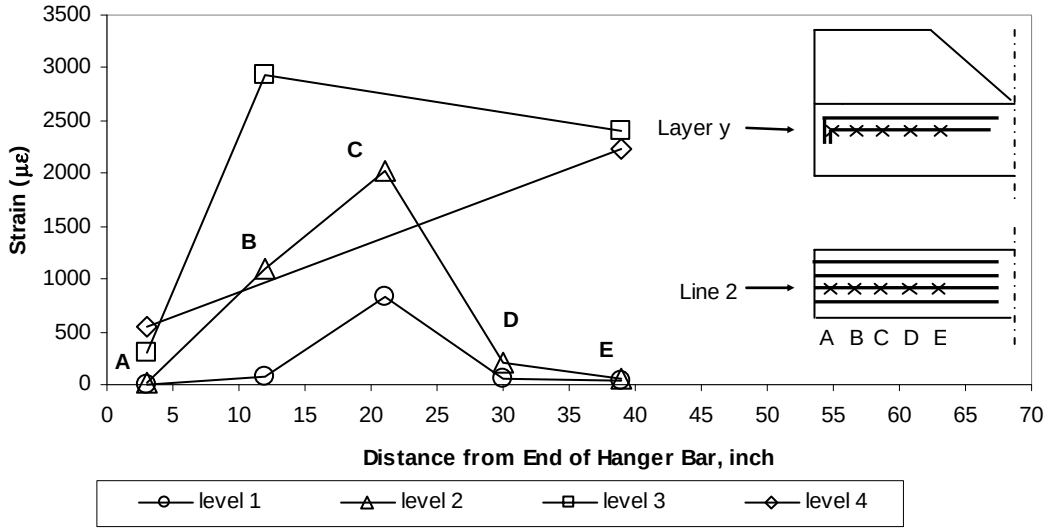

Figure A4- 16- Horizontal Strain Profiles, Layer y, Line 2, Unit 4B

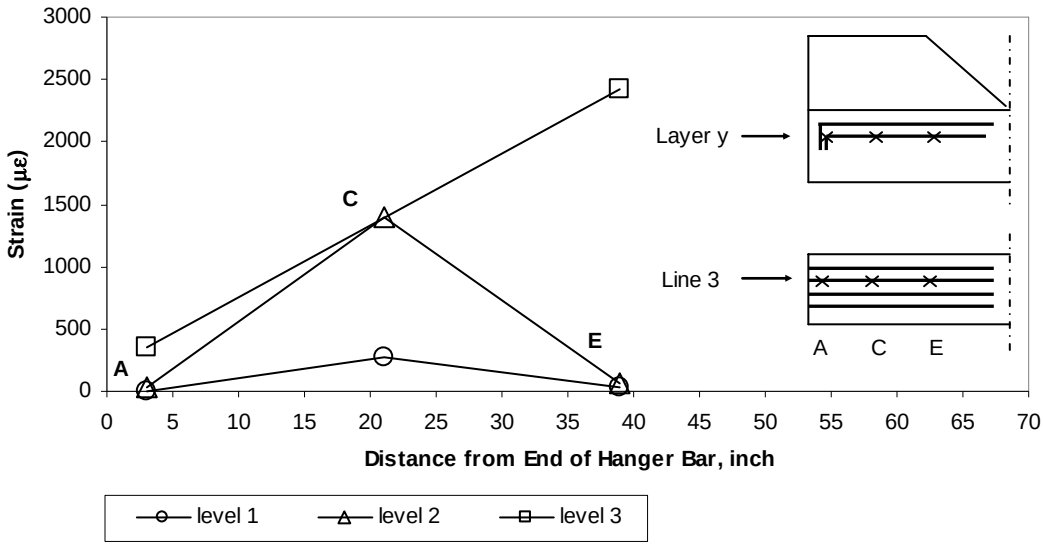

Figure A4- 17- Horizontal Strain Profiles, Layer y, Line 3, Unit 4B

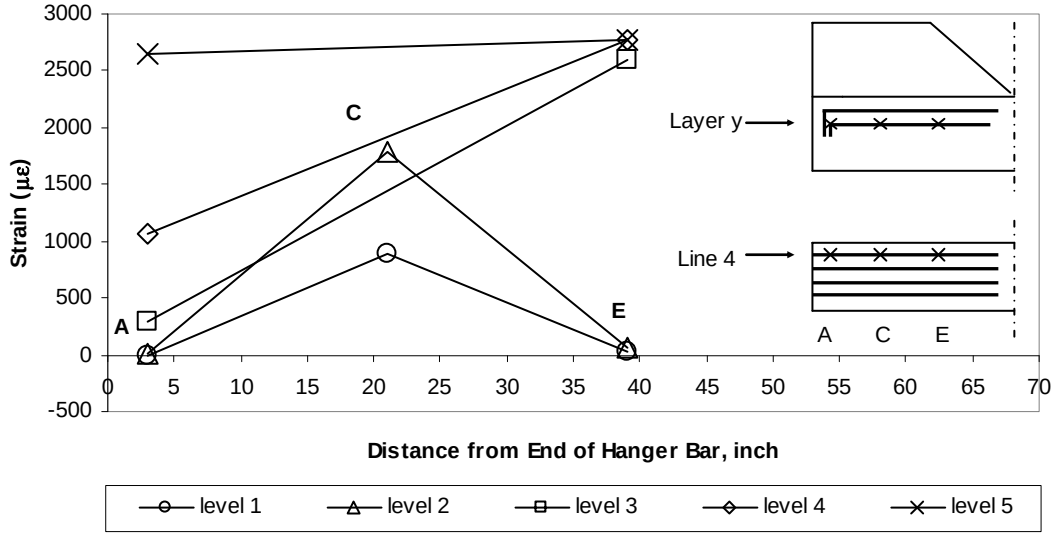

Figure A4- 18- Horizontal Strain Profiles, Layer y, Line 4, Unit 4B

10.1.3 Vertical Reinforcement Strain Profiles

Figures A4-19 to A4-26 show the vertical strain profiles of the U shape reinforcing bars of the shear keys. Figures A4-19, A4-20, A4-23, and A4-24 show a very high strain in the vertical bars nearest the toe of the shear key. However the strain gages far from the toe of the shear key had a very low strain which is indicating that the crack started from the toe of the shear key and grew diagonally to the toe of the stem wall. The strain profiles along "y" direction show the agreement with the crack pattern observed in Test Unit 4A and 4B.

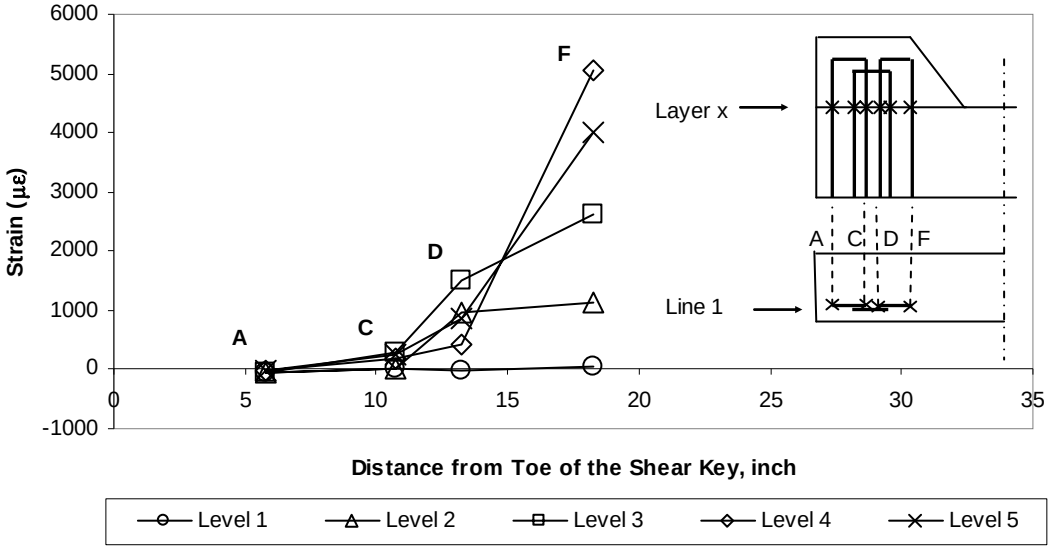

Figure A4- 19- Vertical Strain Profiles, Layer x, Line 1, Unit 4A

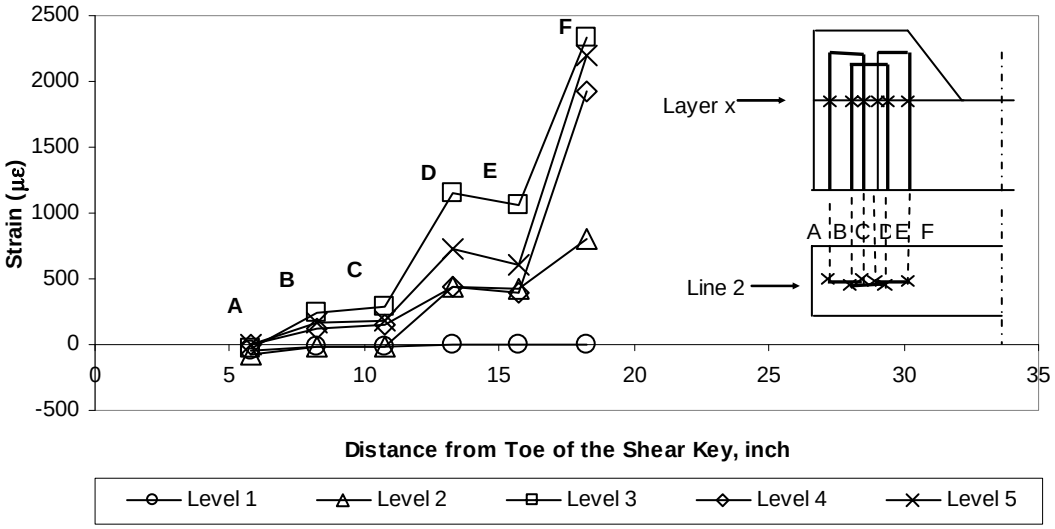

Figure A4- 20- Vertical Strain Profiles, Layer x, Line 2, Unit 4A

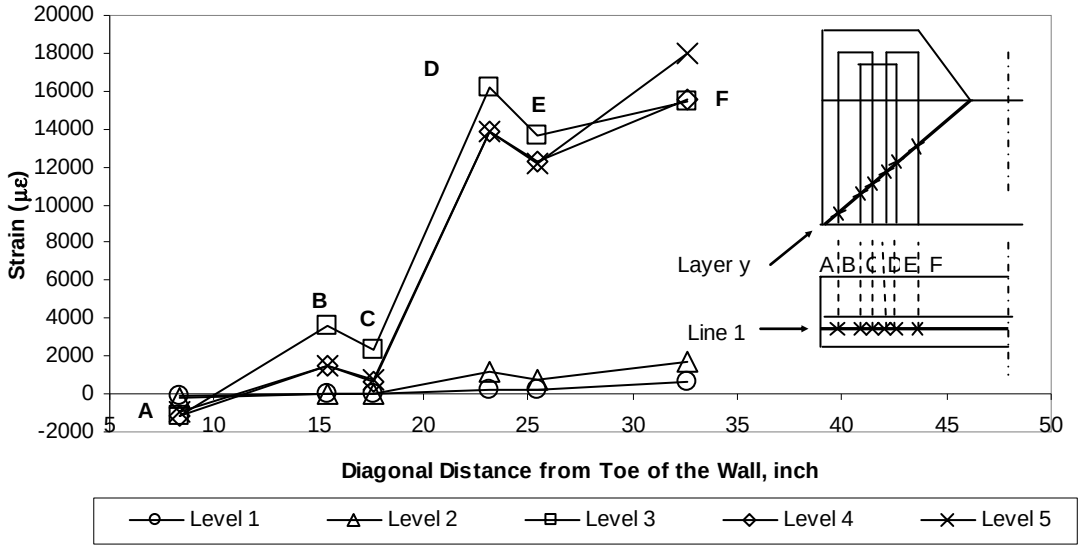

Figure A4- 21- Vertical Strain Profiles, Layer y, Line 1, Unit 4A

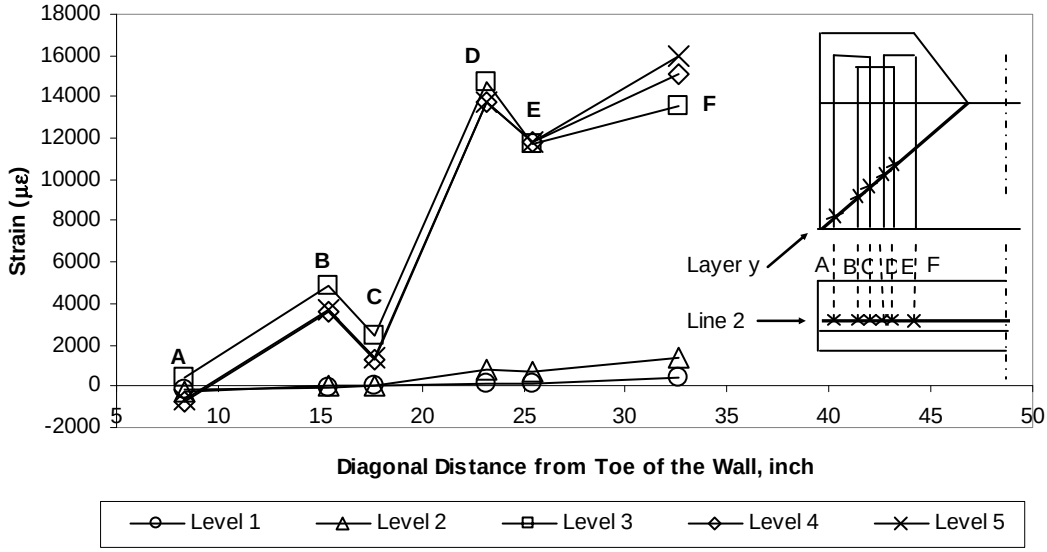

Figure A4- 22- Vertical Strain Profiles, Layer y, Line 2, Unit 4A

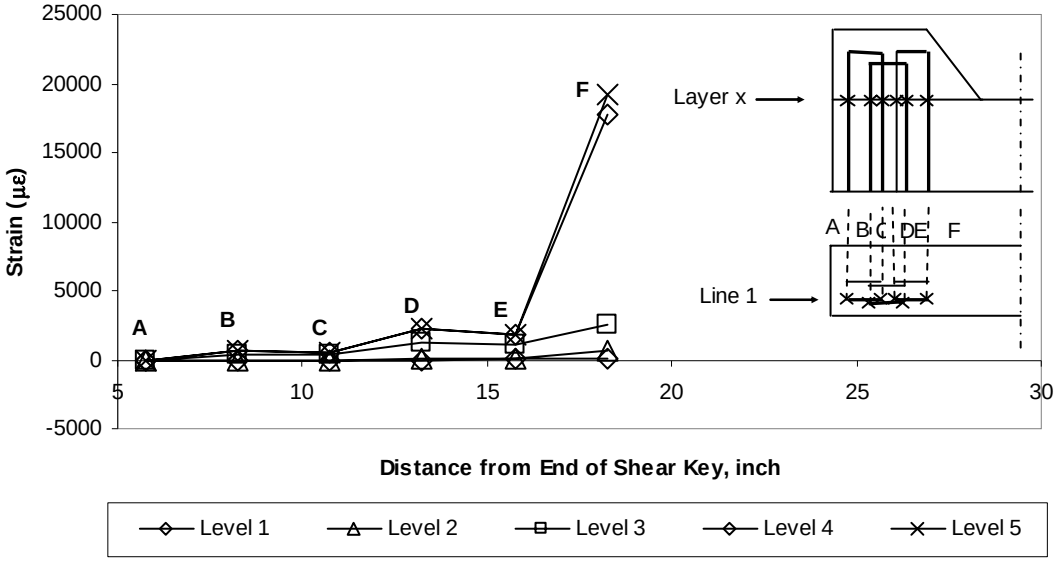

Figure A4- 23- Vertical Strain Profiles, Layer x, Line 1, Unit 4B

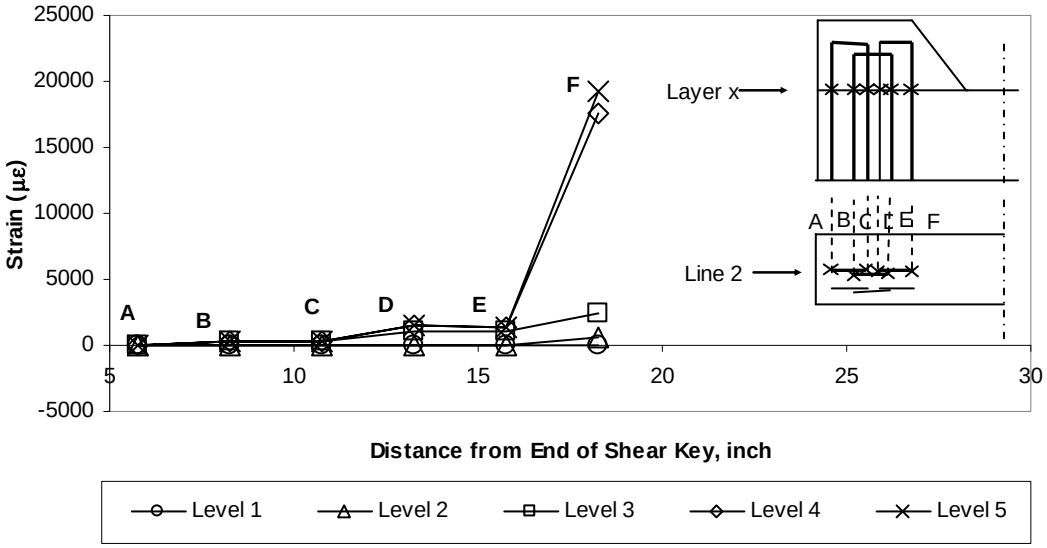

Figure A4- 24- Vertical Strain Profiles, Layer x, Line 2, Unit 4B

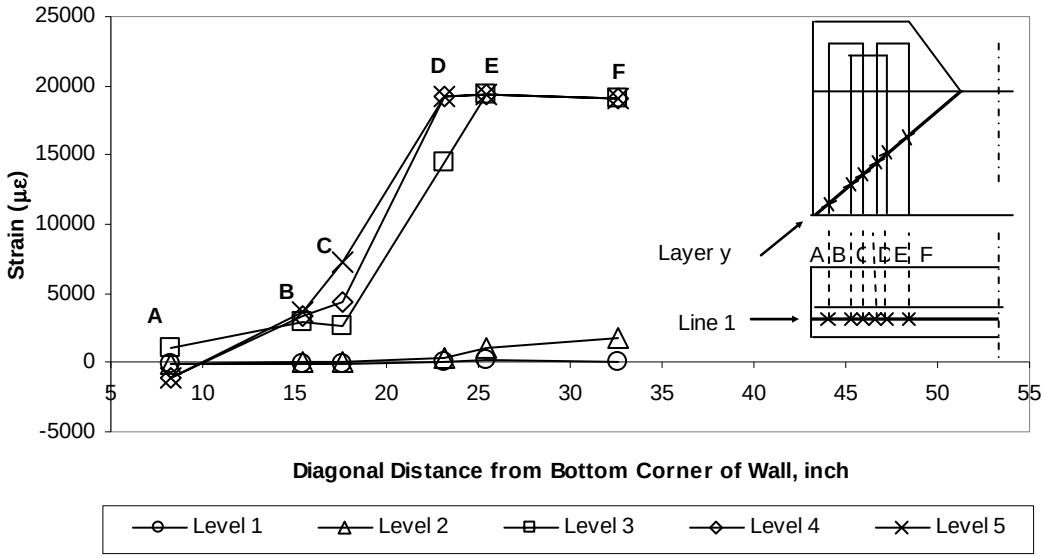

Figure A4- 25- Vertical Strain Profiles, Layer y, Line 1, Unit 4B

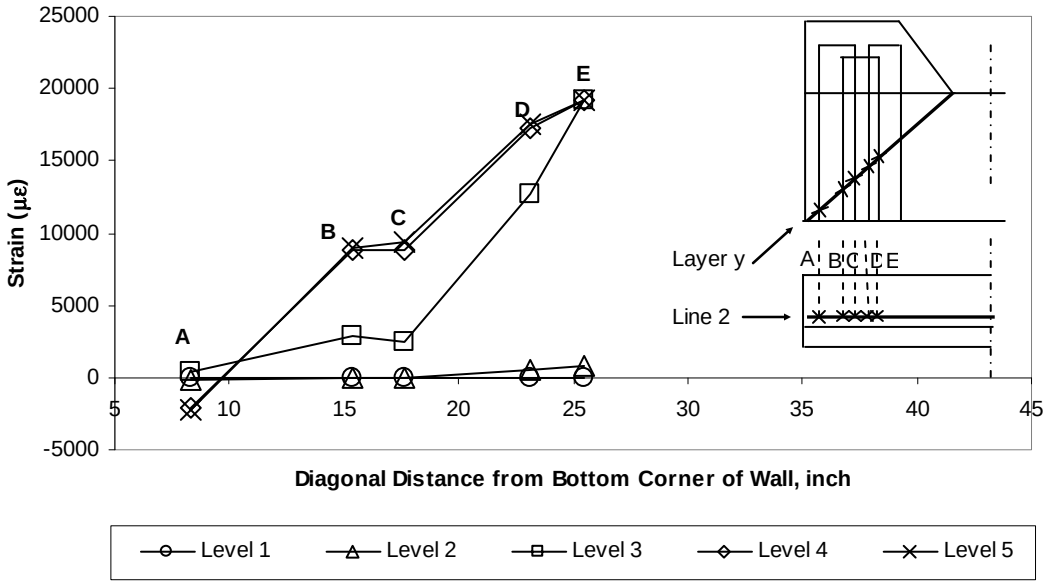

Figure A4- 26- Vertical Strain Profiles, Layer y, Line 2, Unit 4B

10.1.4 Shear friction capacity model proposed by Mattock

Mattock proposed model (Mattock, 1974) includes a cohesion term in shear friction evaluation. From a physical point of view, his model corresponds to a crack model where the crack is characterized by a general roughness and a local roughness. The local shearing off of a roughness surface is considered in cohesion term of his model which is given by:

$$v_s = 400 + 0.8(\rho_v f_y + \sigma_n) \quad \text{(psi)} \qquad \textbf{(A4. 13)}$$

where σ_n is the externally applied compressive stress perpendicular to the crack. The calculated capacity of exterior shear key Test Units 4A and 4B, using Mattock model is summarized in Table A4- 4. For this experimental units, b=16.75 in. (425.5 mm) and d= 24 in. (610 mm). It can be noticed that the concrete strength is not included in Mattock model. It has been shown that in reality the transmission of forces across a crack takes place at areas between aggregate particles (Walraven *et al*., 1987). Therefore strength of concrete should play an important role in developing shear capacity. Walraven *et al*. (1987) proposed a model considering the concrete strength which is presented in the following section.

Test Unit	A_s in^2. (mm^2)	ρ_v	f_y ksi (MPa)	$V = \frac{v_s}{bd}$ kips (KN)
4A	4.4 (2,839)	.011	61.1 (421.3)	375.87 (1,672)
4B	2.64 (1,703)	.007	61.1 (421.3)	289.84 (1,289)

Table A4- 4: Capacity Evaluation of Exterior Shear key Test Units 4A and 4B with Mattock Equation

10.1.5 Capacity Evaluation of Exterior Shear Key with Shear Friction Capacity Model Proposed by Walraven *et al*. (1987)

Walraven *et al*. (1987)'s proposed shear friction equations to determine the shear capacity of reinforced concrete were used to reevaluate the capacity of exterior shear keys. This model takes into consideration the influence of concrete strength as a basic parameter. The proposed equation is given by:

$$v_{u,th} = C_3(0.007\rho_v f_y)^{C_4} \quad \text{(psi)} \qquad \textbf{(A4. 14)}$$

where for psi units:

$$C_3 = 15.686 f_{cc}'^{\,0.406}$$
$$C_4 = 0.0353 f_{cc}'^{\,0.30} \qquad \textbf{(A4. 15)}$$

where f_{cc}' is the concrete compressive strength of 5.9 in. (150 mm) cubes. f_{cc}' can be assumed as a $\frac{f_c'}{0.85}$. The calculated capacity of exterior shear key Test Units 4A and 4B are summarized in Table A4- 5 (b=16.75 in. (425.5 mm) and d=24 in. (610 mm)).

Test Unit	A_s in^2. (mm^2)	ρ_v	f_y ksi (MPa)	f'_c psi (MPa)	f'_{cc} psi (MPa)	C_3	C_4	$V = \frac{0.82 v_s}{bd}$ kips (kN)
4A	4.4 (2,839)	.011	61.1 (421.3)	5780 (39.8)	6800 (46.5)	564.3	0.498	410. 44 (1,825.7)
4B	2.64 (1,703)	.007	61.1 (421.3)	5780 (39.8)	6800 (46.5)	564.3	0.498	311.22 (1,384.4)

Table A4- 5: Capacity Evaluation of Exterior Shear key Test Units 4A and 4B with Walraven *et al*.(1987)'s Equations

10.1.6 Capacity Evaluation of Exterior Shear Key with Caltrans Sliding Shear Friction Model

According to Caltrans Bridge Design Specifications (Caltrans, 1993a) the shear key capacity shall be computed by:

$$V = \mu(A_{vf} f_{yf} + A_{vs} f_{ys}) \qquad \textbf{(A4. 16)}$$

where μ is the coefficient of friction and shall be taken as 1.4λ for concrete placed monolithically such as in Test Unit 4A. As indicated in Caltrans Design Specifications (Caltrans, 1993a) the coefficient of friction, μ, is considered as 1.0λ at the interface between two concretes cast at different times, such as in Test Unit 4B. λ shall be taken as 1.0 for normal-weight concrete. A_{vf} and f_{yf} are the area and the yield strength of the vertical shear reinforcement

crossing the shear key-abutment stem wall interface, respectively. In Eq (A4. 16) A_{vs} and f_{ys} are, respectively, the area and the yield strength of the vertical reinforcement on the sides of the abutment back and wing walls crossing the shear key-abutment stem wall interface. Table A4- 6 summarized the calculation to evaluate the capacity of the exterior shear key Test Unit 4A and 4B. The capacity of the exterior shear key specimens was considered with and without the side Reinforcement steel which are for temperature control.

Test Series	Test Unit	Vertical Steel Area Crossing Interface of Shear Key & Wall		Vertical Steel Area of the Side Reinforcement Crossing the Interface of Shear Key & Wall		V_S Steel Contribution to Shear Key Capacity kips (KN) Eq. (1.3)	
		No. of Bars	A_{vf} in^2. (mm^2)	No. of Bars	$A_{vf\ (add)}$ in^2. (mm^2)	Including $A_{vf\ (add)}$	Without $A_{vf\ (add)}$
IV	4A	24#3	2.64 (1,703)	16#3	1.76 (1,135)	375.8 (1,672)	225.5 (1,003)
	4B	24#3	2.64 (1,703)	—	—	161.3 (717.5)	161.3 (717.5)

Table A4- 6: Capacity Evaluation of Exterior Shear key Test Units 4A and 4B with Caltrans Sliding Shear Friction Equation

10.2 Evaluation of the Capacity of the Test Series V

After observed failure in test series IV, test series V was designed with substantially different amount and configuration of steel reinforcement. In following, the capacity of exterior shear key was evaluated using three different models.

10.2.1 Strut-and-Tie Model:

Strut-and-tie model is considered as a very appropriate basis for the design of reinforced concrete loaded in shear by researchers and practitioners. Since the exterior shear key should act as fuse element by shear sliding under later seismic load during the earthquake, it was proposed to use this analogy. The design criteria in designing of sacrificial shear keys are (1) to have shear

sliding failure at the shear key-abutment stem wall interface, (2) to determine amount of vertical shear key reinforcement and horizontal steel ties close to surface of the stem wall. The developed model which illustrates the path of transferred load is shown in Figures A4-27 and A4-28.

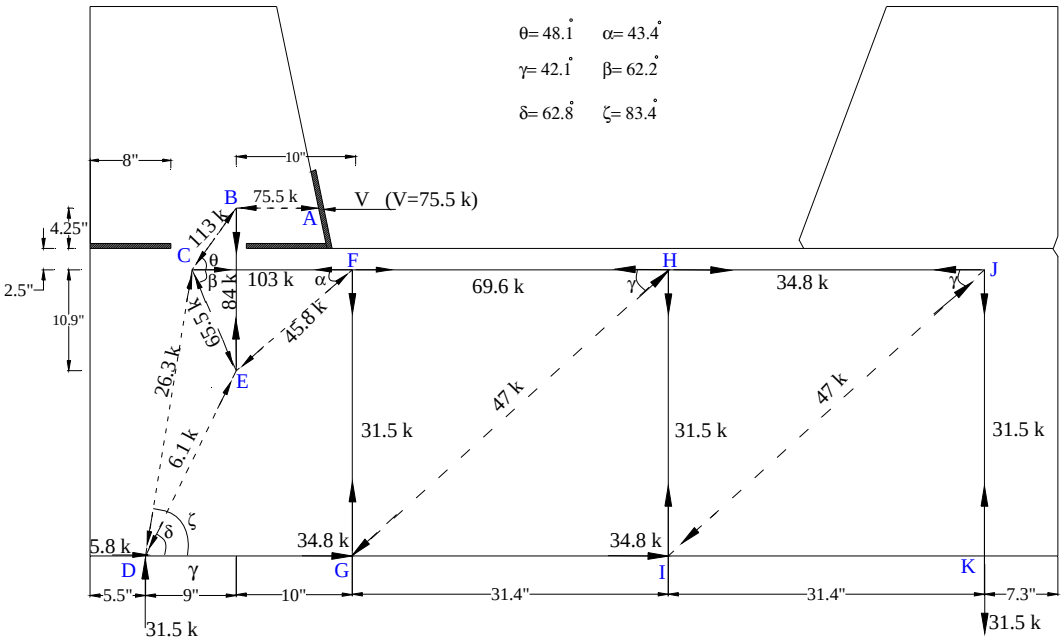

Figure A4- 27- Strut-and-Tie Model for Exterior Shear Key Unit 5A

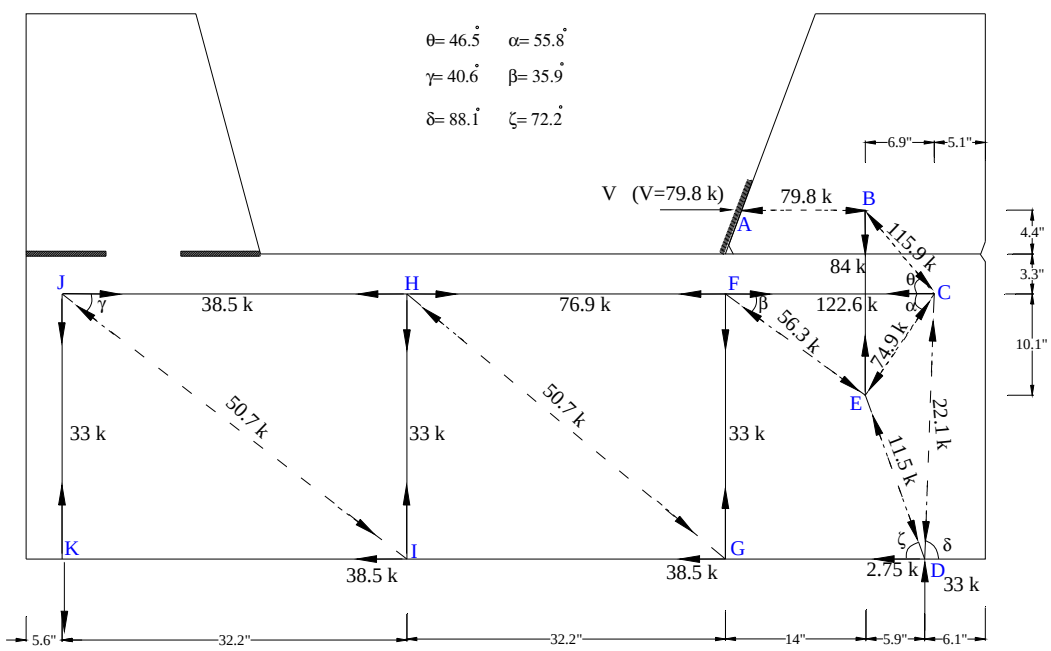

Figure A4- 28- Strut-and-Tie Model for Exterior Shear Key Unit 5B

Solid Lines represent struts, the compression members of a strut-and-tie model and dot lines are the tension members of a strut-and-tie model. The capacity of shear key Unit 5A and 5B was calculated as 75.5 kips and 79.8 kips, respectively. After solving for the truss members, reinforcing steel was selected to provide the necessary tie capacity. Fourteen #4 headed bars were used horizontally close to the top surface of the abutment stem wall. In Test Unit 5A, the foam with an 8”x8” hole at center was used at interface of the shear key and the wall. There was a rough construction joint between the shear key and the wall at the location of the hole and a smooth construction joint between the foam and the wall. All shear key vertical reinforcing bars are lumped at one location close to the side of the hole, which is closer to the inclined face of the shear key. In Test Unit 5B, there was a smooth construction joint between the shear key and the wall. A bond breaker is applied at interface to create a weak plane of failure. All shear key vertical reinforcing bars are lumped at one location near the centerline of the shear key. Four #4 bars were used as the shear key vertical reinforcement.

Table A4-7 shows the observed load and displacement of test series V at five damage levels as described in section 10.1.1. The failure mode in series V was shear sliding, the equations described in section 10.1.1 for prediction the load and displacement for each level cannot be applied.

	Test Unit 5A		Test Units 5B	
	Load kips(KN)	Displacement in.(mm)	Load kips(KN)	Displacement in.(mm)
LEVEL I	9.20(40.9)	0.004(0.1)	9.6(40.9)	0.002(0.05)
LEVEL II	130.3(579.5)	0.14(3.5)	37.2(165.6)	0.32(8.2)
LEVEL III	123.7(550.4)	1.50(38.2)	75.1(333.9)	1.40(35.6)
LEVEL IV	35.9(159.5)	1.70(42.8)	29.3(130.3)	1.60(40.4)
LEVEL V	35.4(157.6)	1.80(45.4)	32.1(142.8)	1.70(44.3)

Table A4- 7: Calculated Load and Displacement of Test Series V at Each Damage Level

10.2.2 Horizontal Reinforcement Strain Profiles

Figures A4-29 to A4-56 show the horizontal strain profiles in the two layers of horizontal reinforcement (headed bars) close to the top surface of the abutment stem wall in Unit 5A and

Unit 5B. The strain profiles in these figures had a good agreement with the crack pattern in test 5A and 5B, which indicates shear sliding occurred initiated from the toe of the shear key.

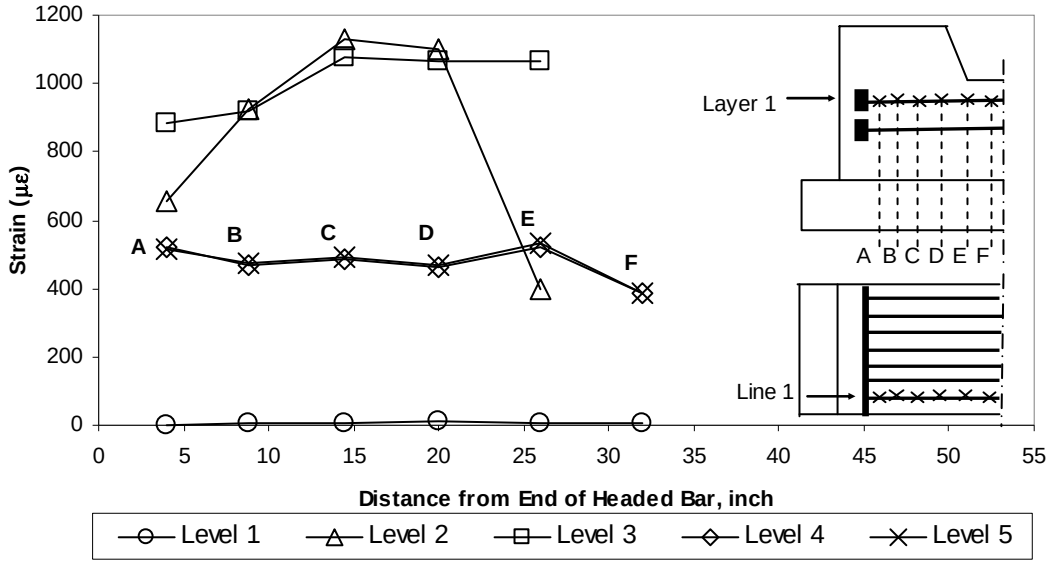

Figure A4- 29- Horizontal Strain Profiles, Layer 1, Line 1, Unit 5A

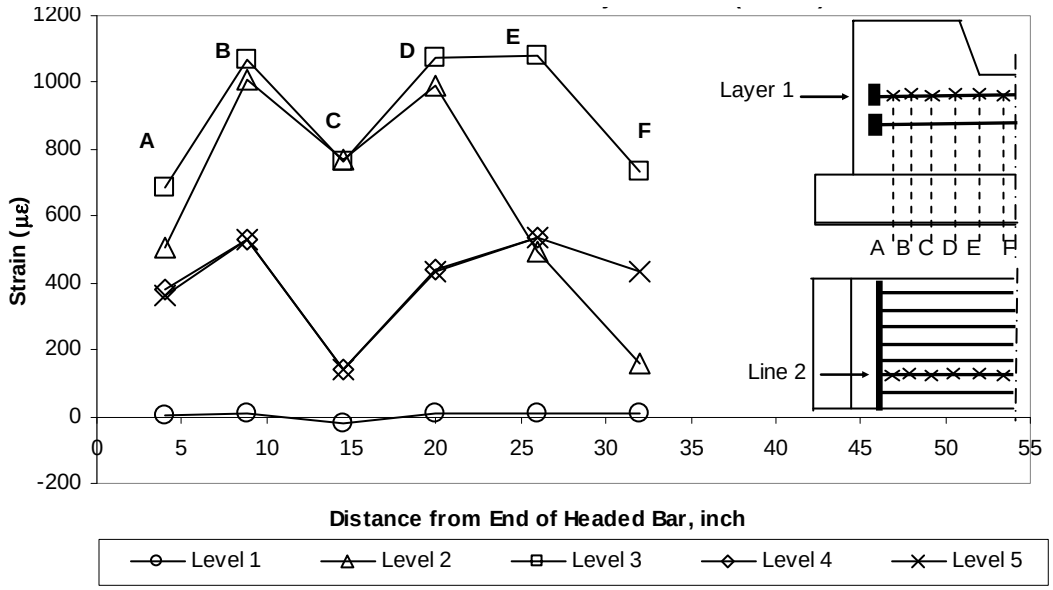

Figure A4- 30- Horizontal Strain Profiles, Layer 1, Line 2, Unit 5A

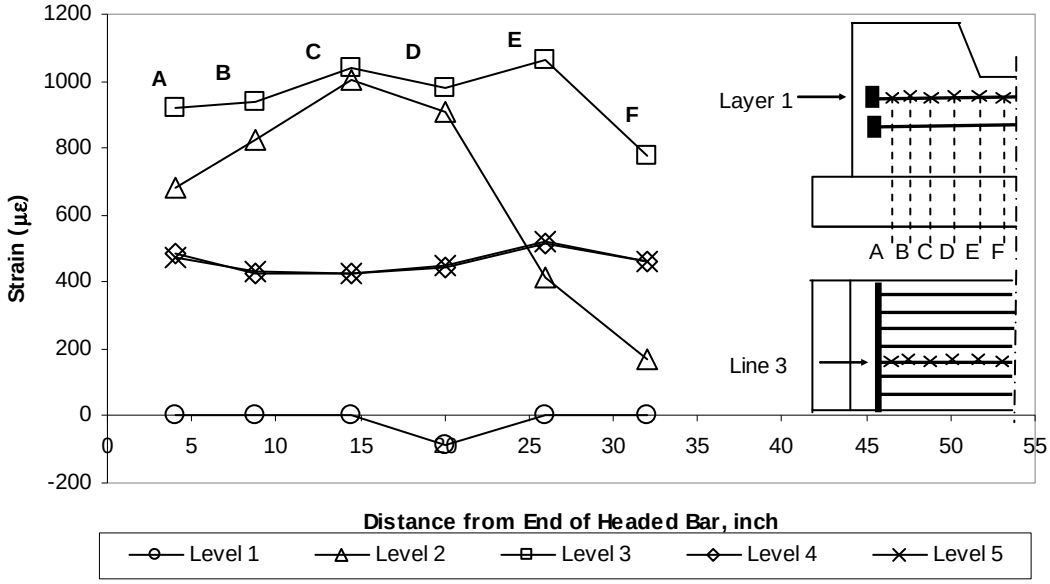

Figure A4- 31- Horizontal Strain Profiles, Layer 1, Line 3, Unit 5A

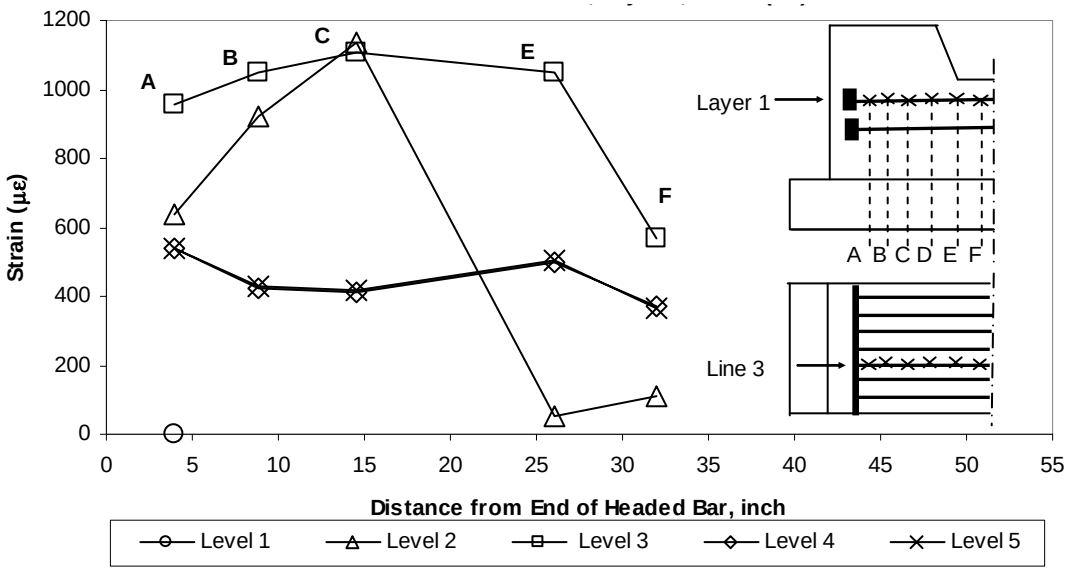

Figure A4- 32- Horizontal Strain Profiles, Layer 1, Line 4, Unit 5A

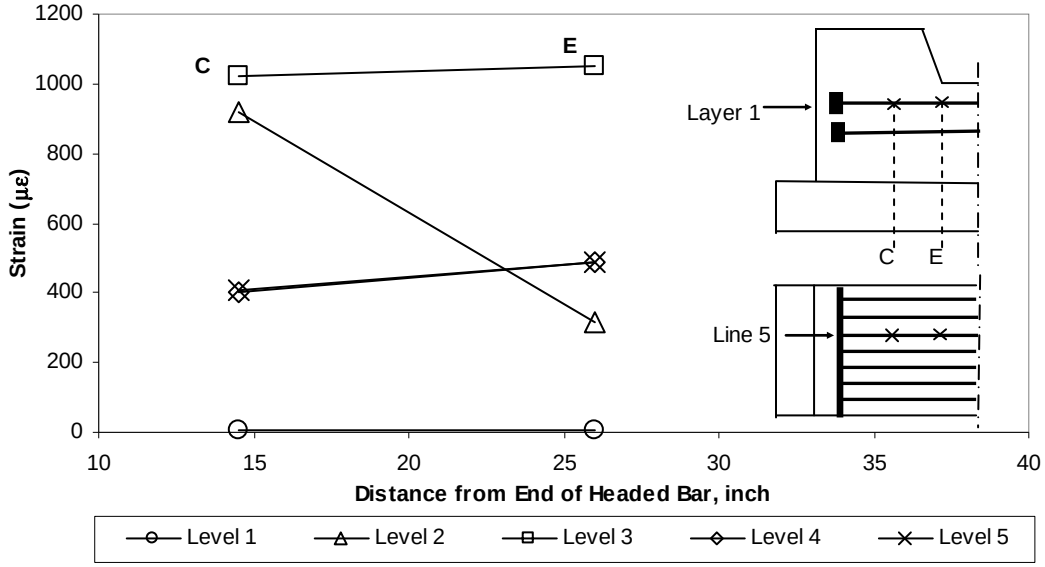

Figure A4- 33- Horizontal Strain Profiles, Layer 1, Line 5, Unit 5A

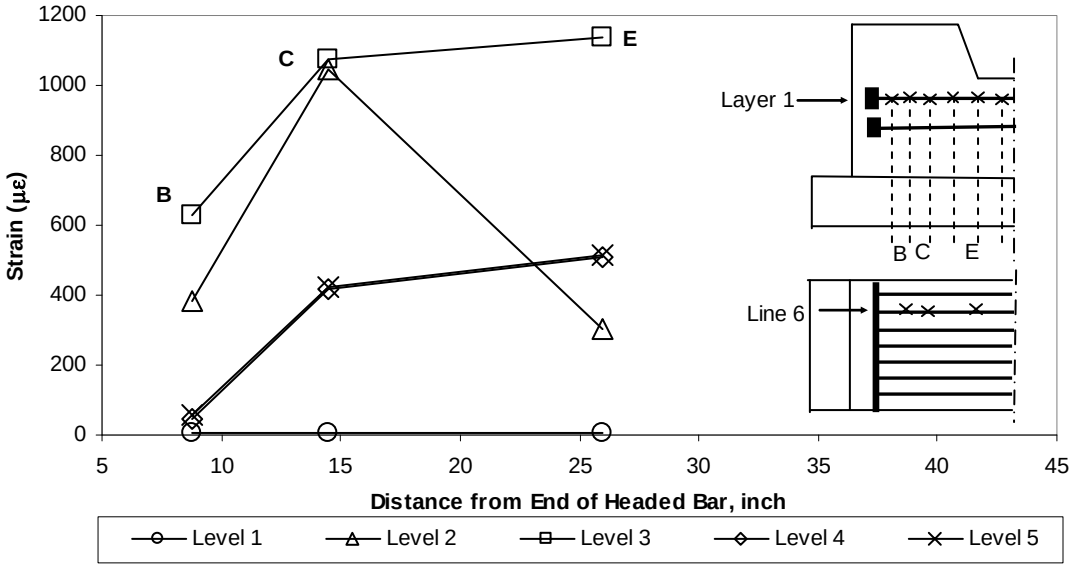

Figure A4- 34- Horizontal Strain Profiles, Layer 1, Line 6, Unit 5A

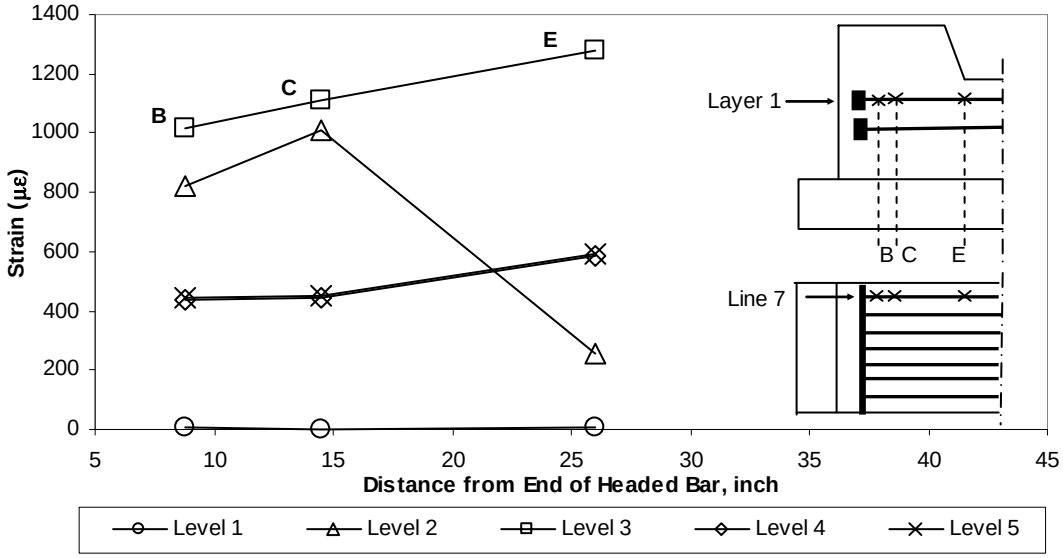

Figure A4- 35- Horizontal Strain Profiles, Layer 1, Line 7, Unit 5A

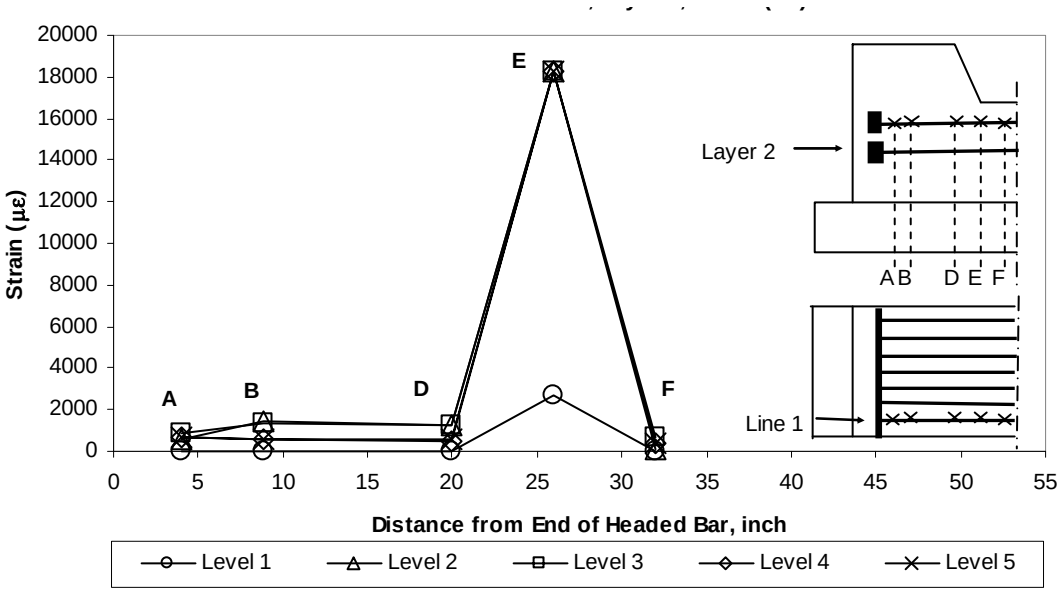

Figure A4- 36- Horizontal Strain Profiles, Layer 2, Line 1, Unit 5A

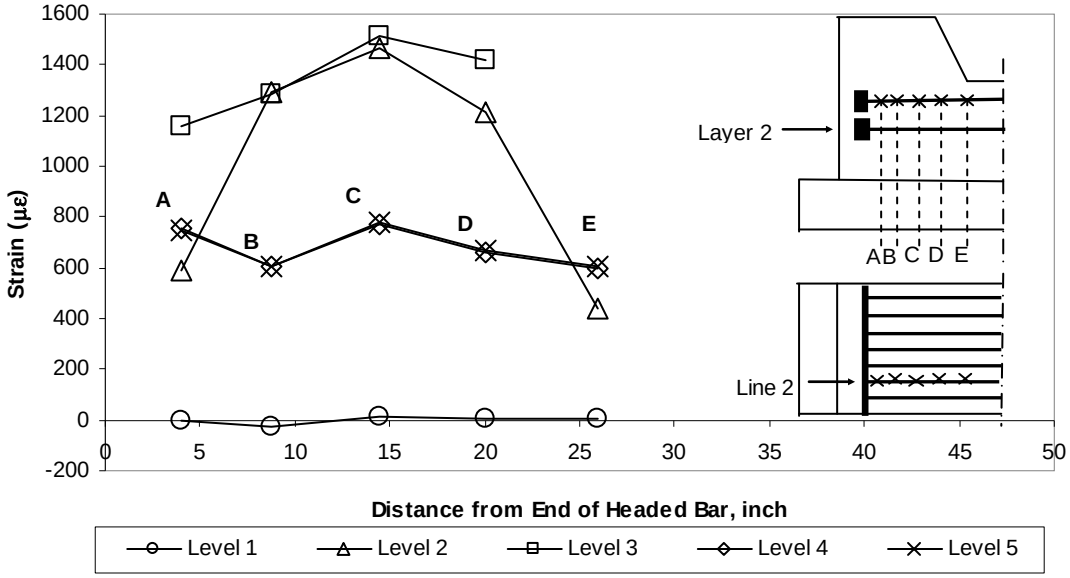

Figure A4- 37- Horizontal Strain Profiles, Layer 2, Line 2, Unit 5A

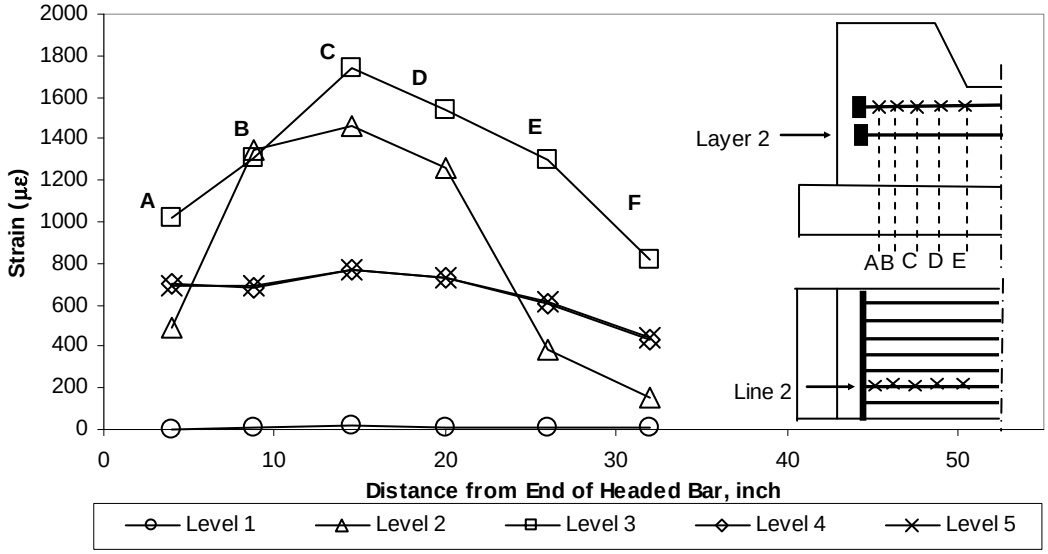

Figure A4- 38- Horizontal Strain Profiles, Layer 2, Line 3, Unit 5A

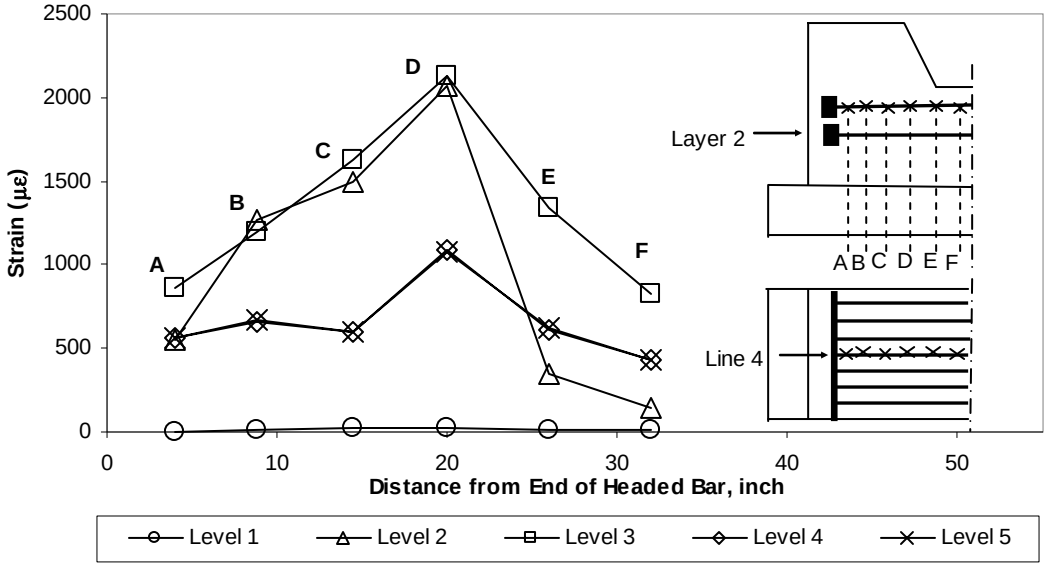

Figure A4- 39- Horizontal Strain Profiles, Layer 2, Line 4, Unit 5A

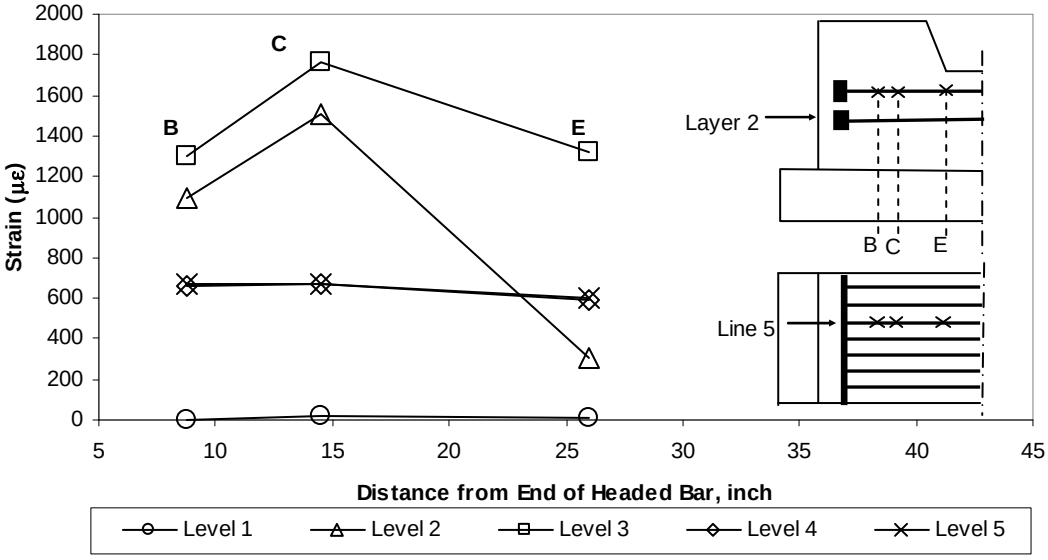

Figure A4- 40- Horizontal Strain Profiles, Layer 2, Line 5, Unit 5A

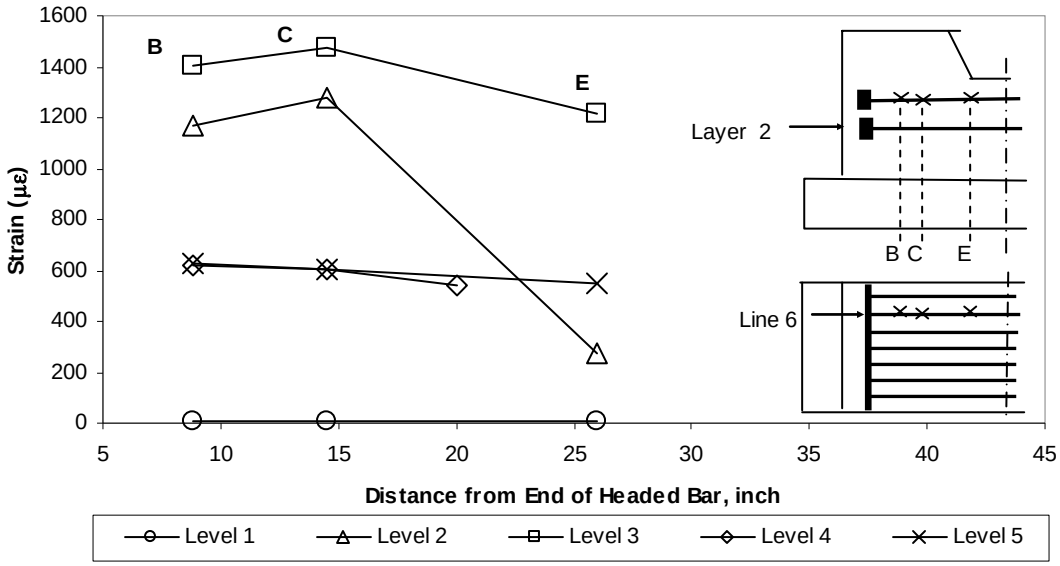

Figure A4- 41- Horizontal Strain Profiles, Layer 2, Line 6, Unit 5A

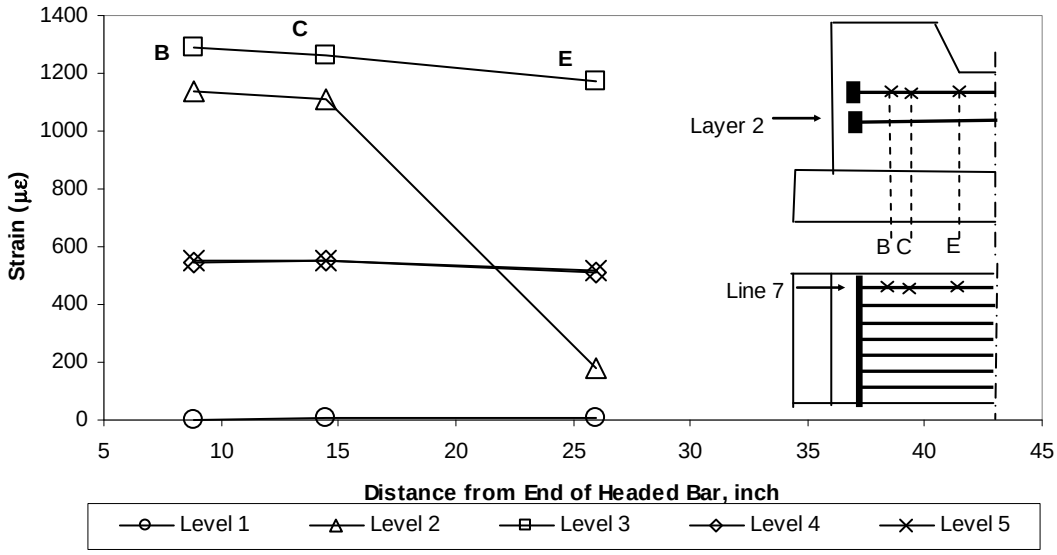

Figure A4- 42- Horizontal Strain Profiles, Layer 2, Line 7, Unit 5A

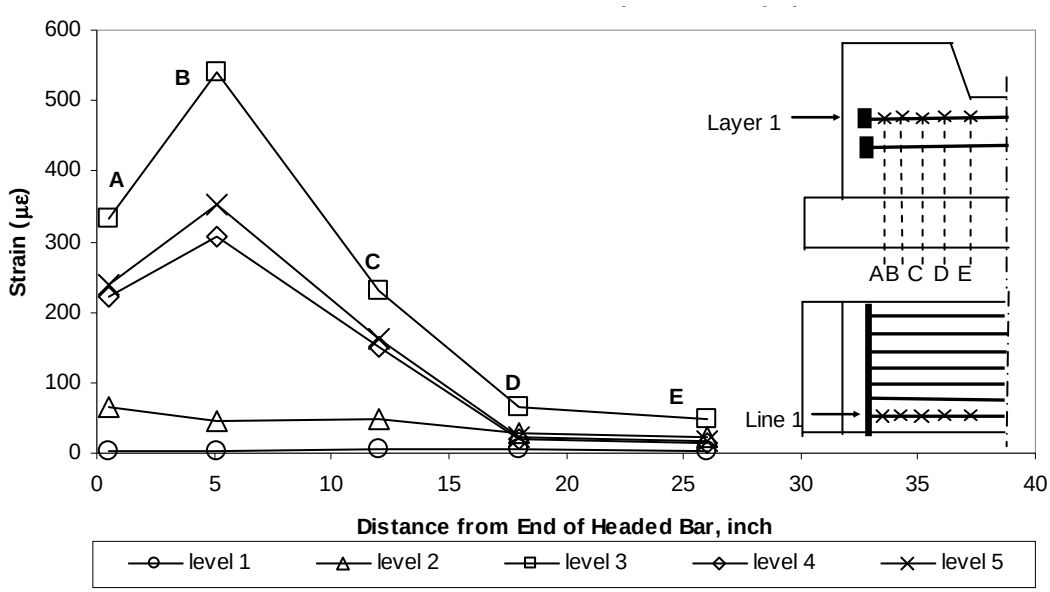

Figure A4- 43- Horizontal Strain Profiles, Layer 1, Line 1, Unit 5B

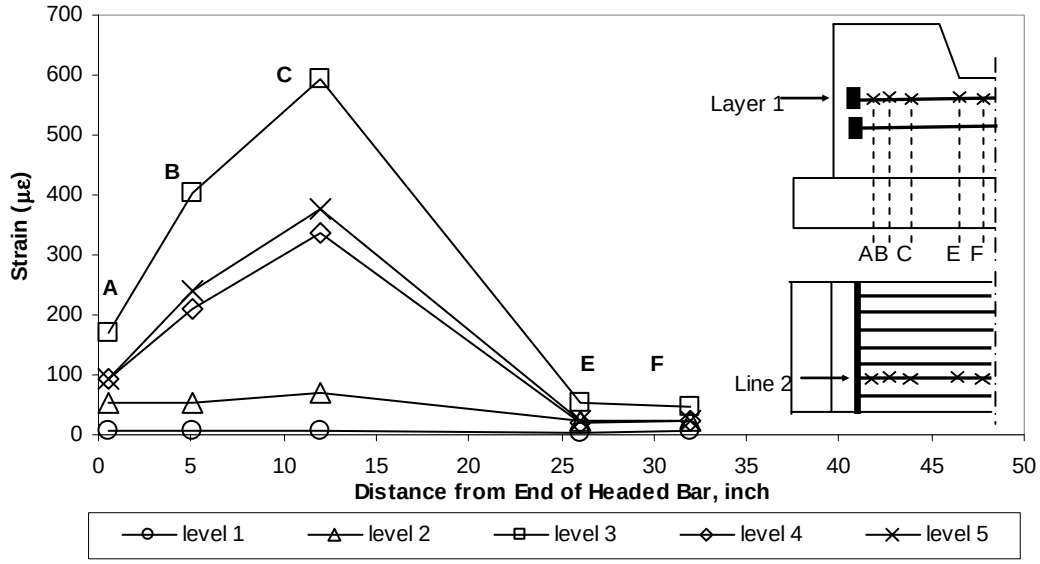

Figure A4- 44- Horizontal Strain Profiles, Layer 1, Line 2, Unit 5B

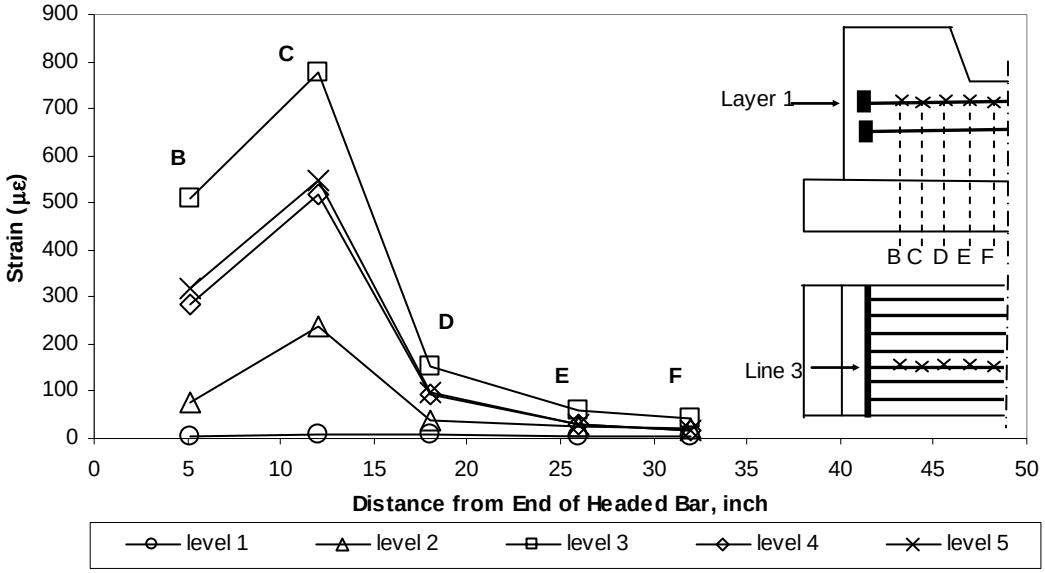

Figure A4- 45- Horizontal Strain Profiles, Layer 1, Line 3, Unit 5B

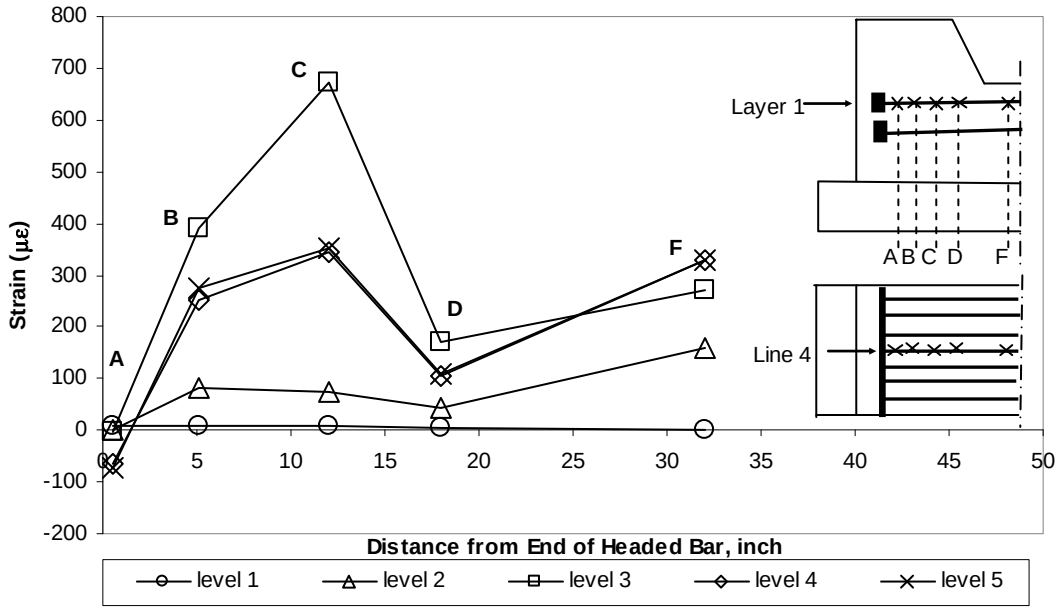

Figure A4- 46- Horizontal Strain Profiles, Layer 1, Line 4, Unit 5B

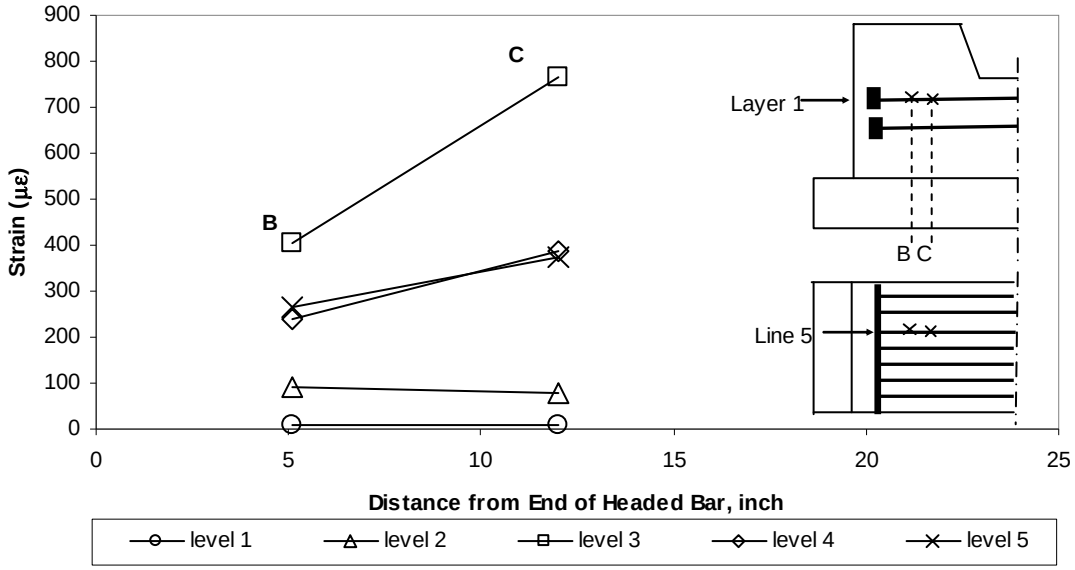

Figure A4- 47- Horizontal Strain Profiles, Layer 1, Line 5, Unit 5B

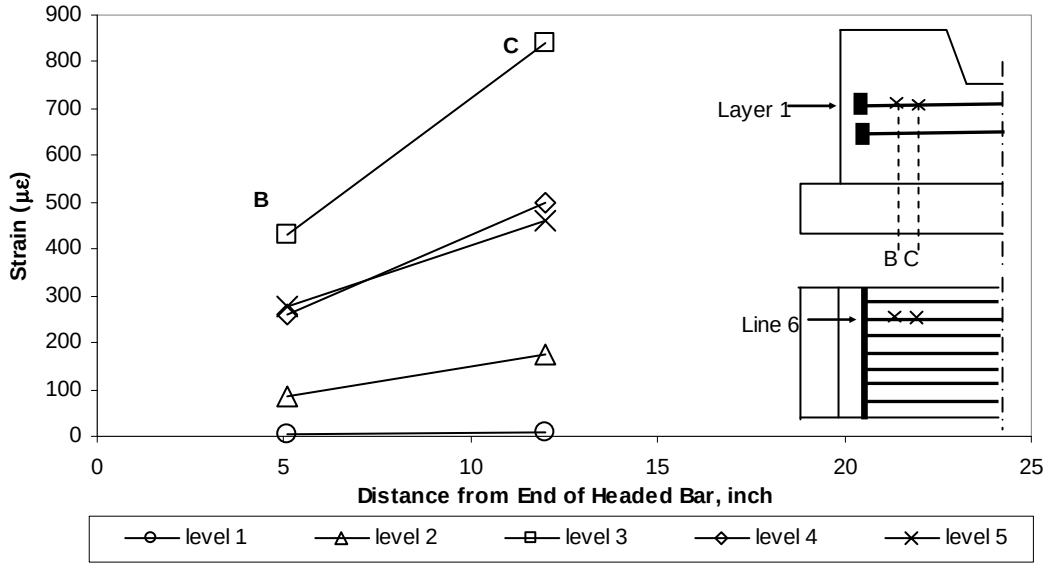

Figure A4- 48- Horizontal Strain Profiles, Layer 1, Line 6, Unit 5B

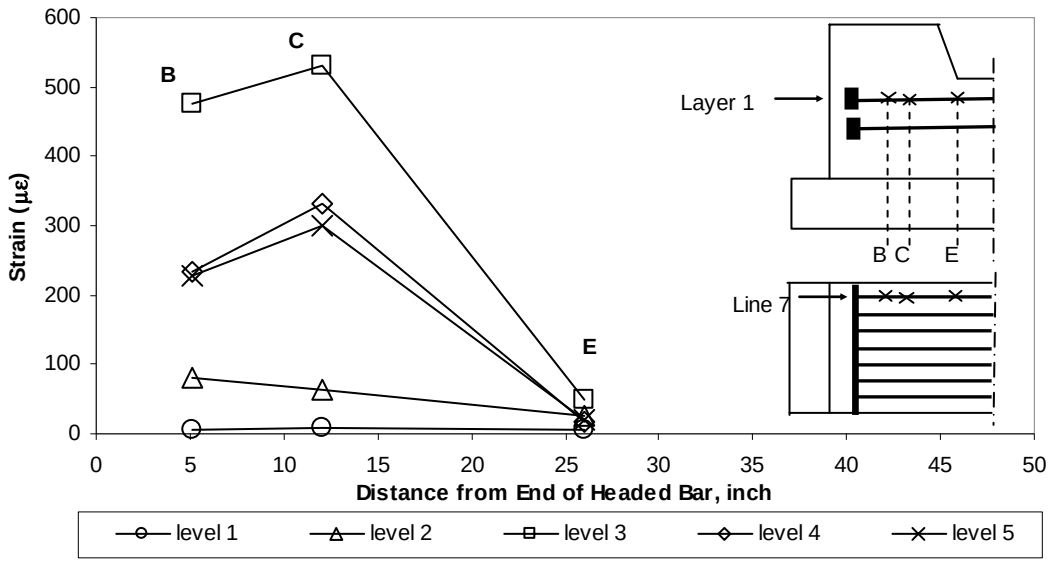

Figure A4- 49- Horizontal Strain Profiles, Layer 1, Line 7, Unit 5B

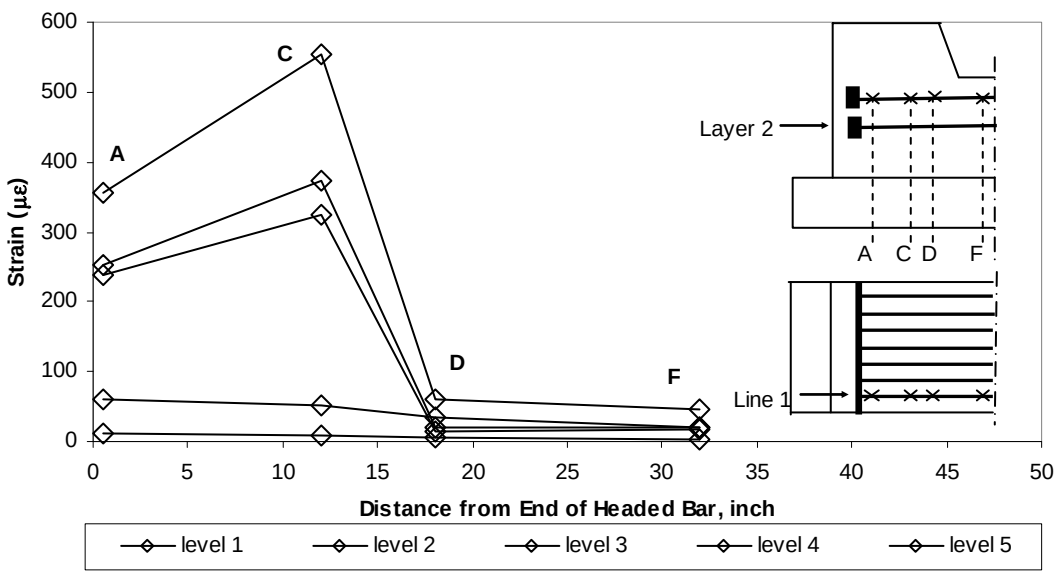

Figure A4- 50- Horizontal Strain Profiles, Layer 2, Line 1, Unit 5B

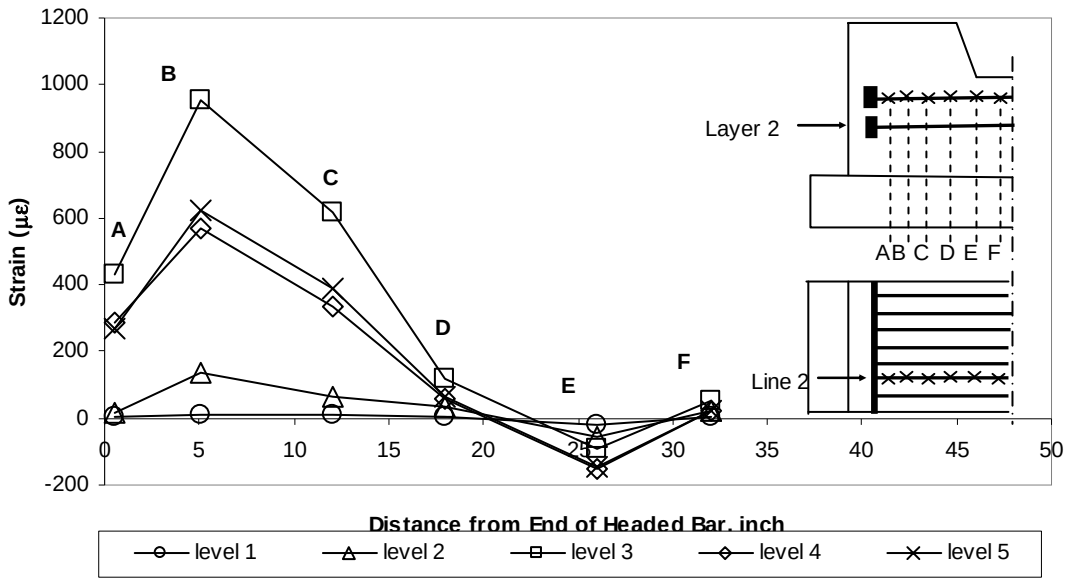

Figure A4- 51- Horizontal Strain Profiles, Layer 2, Line 2, Unit 5B

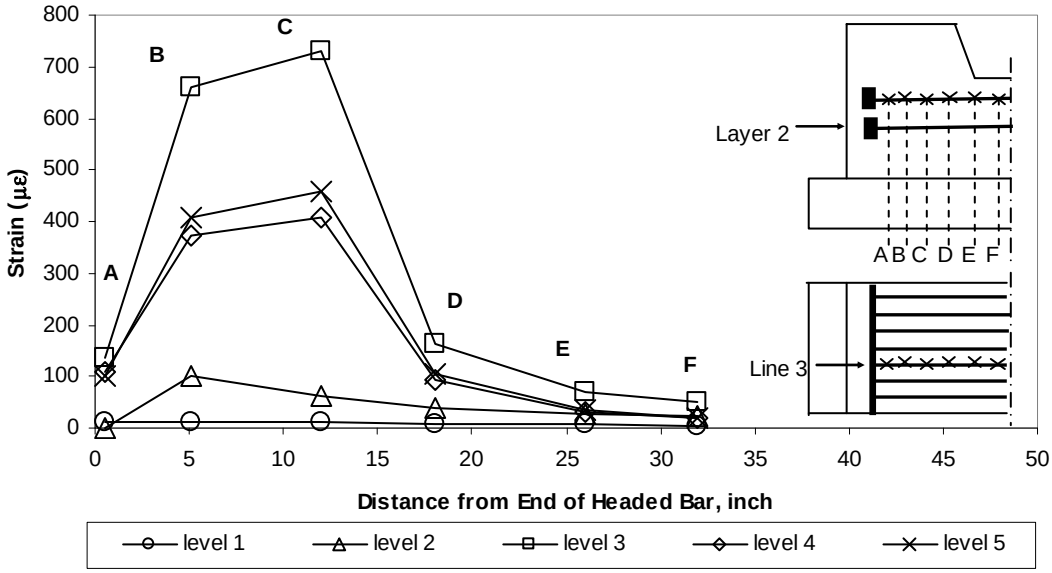

Figure A4- 52- Horizontal Strain Profiles, Layer 2, Line 3, Unit 5B

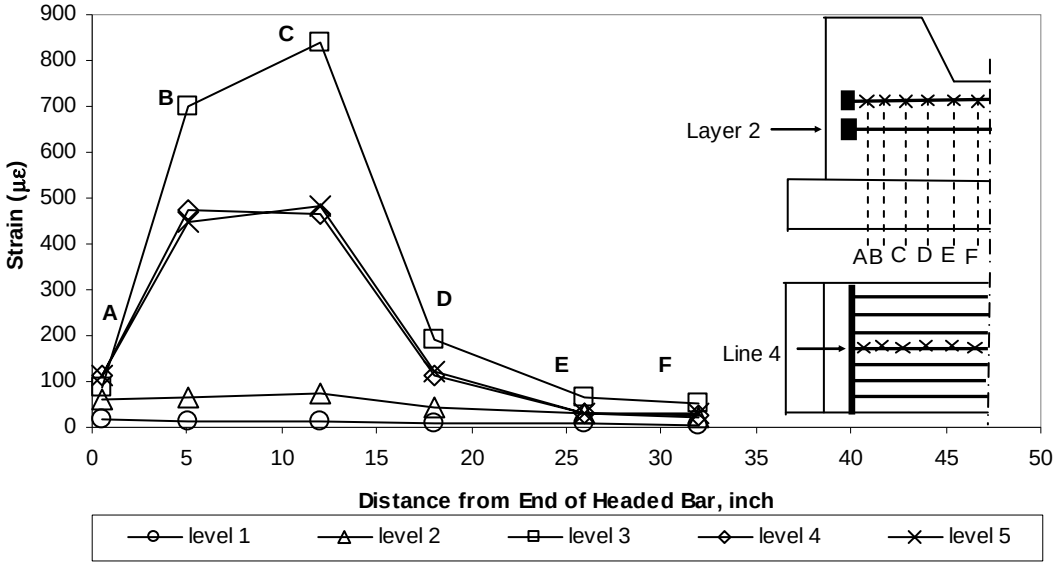

Figure A4- 53- Horizontal Strain Profiles, Layer 2, Line 4, Unit 5B

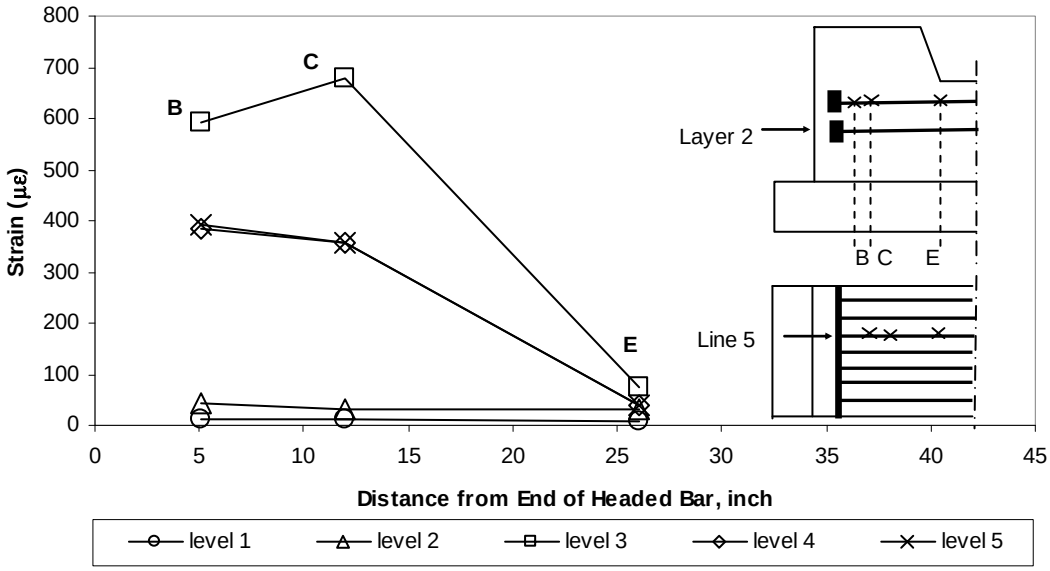

Figure A4- 54- Horizontal Strain Profiles, Layer 2, Line 5, Unit 5B

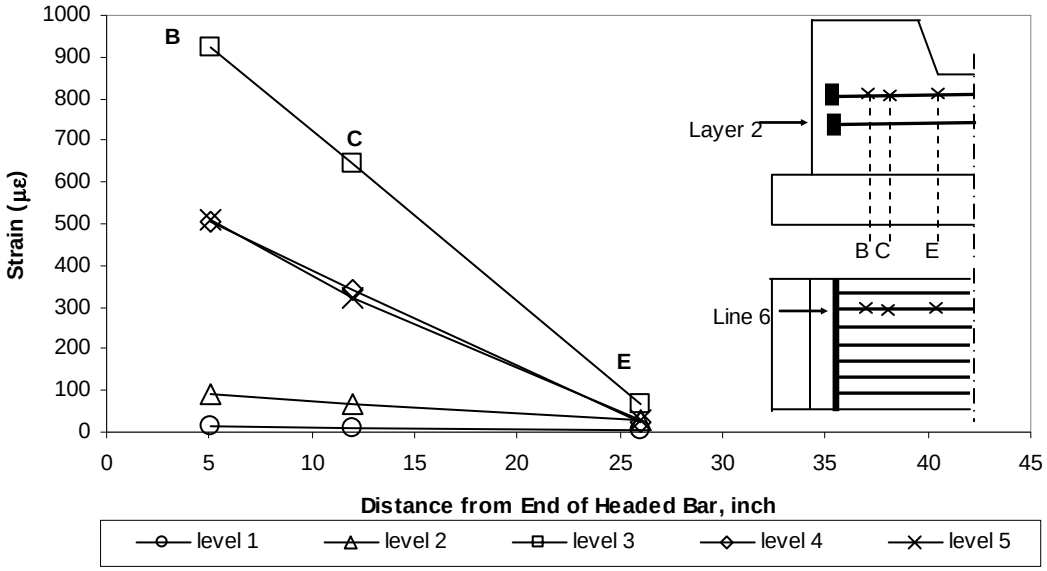

Figure A4- 55- Horizontal Strain Profiles, Layer 2, Line 6, Unit 5B

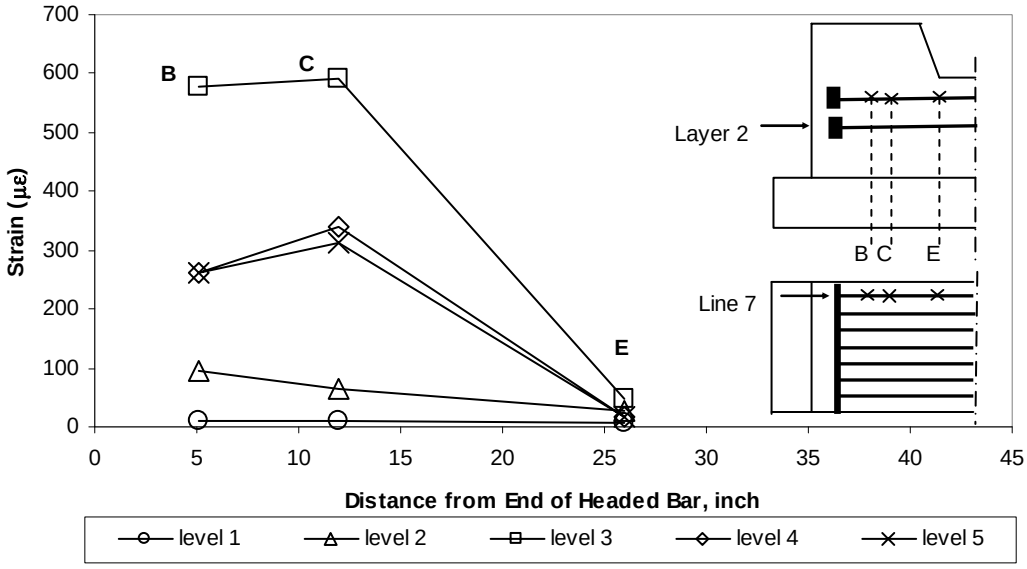

Figure A4- 56- Horizontal Strain Profiles, Layer 2, Line 7, Unit 5B

10.2.3 Vertical Reinforcement Strain Profiles

Figures A4-57 to A4-64 show the vertical profiles of the "L" shape vertical reinforcing bars of the shear keys Test Units 5A and 5B. A very high strain in gages located at the interface of shear key-stem wall is indicating that the crack started from the toe of the shear key and grew horizontally through the interface of the shear key-stem wall.

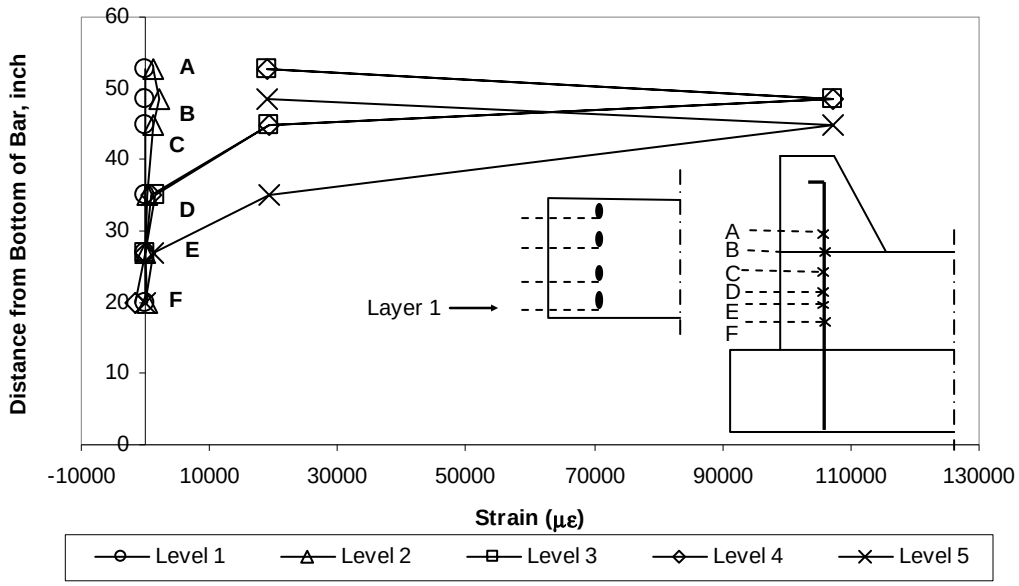

Figure A4- 57- Vertical Strain Profiles, Layer 1, Unit 5A

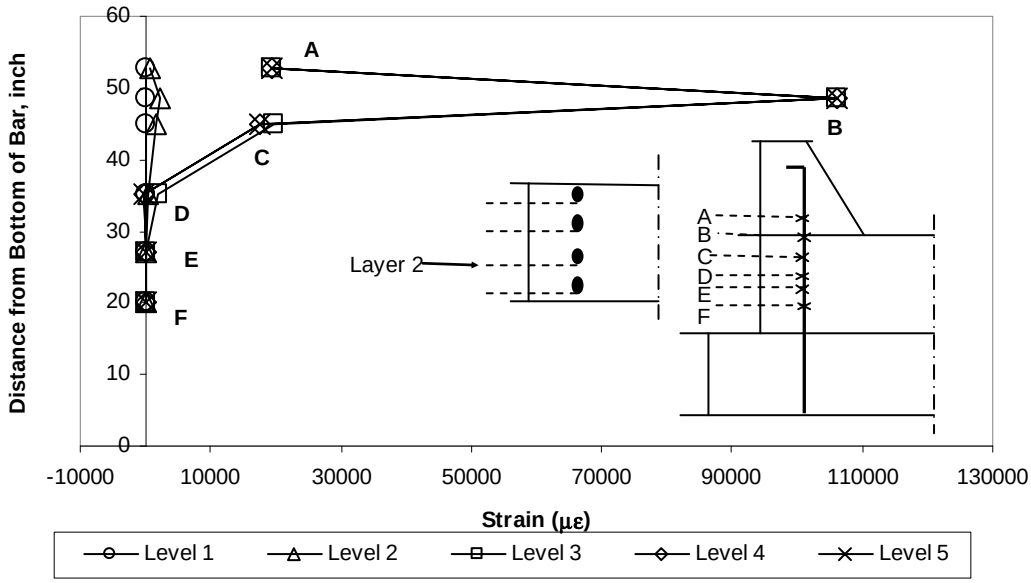

Figure A4- 58- Vertical Strain Profiles, Layer 2, Unit 5A

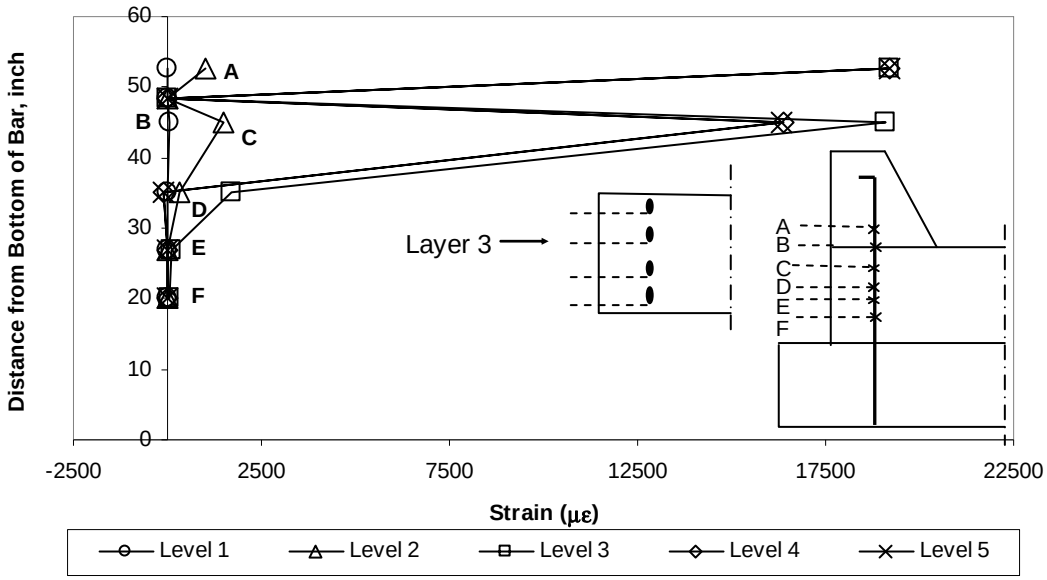

Figure A4- 59- Vertical Strain Profiles, Layer 3, Unit 5A

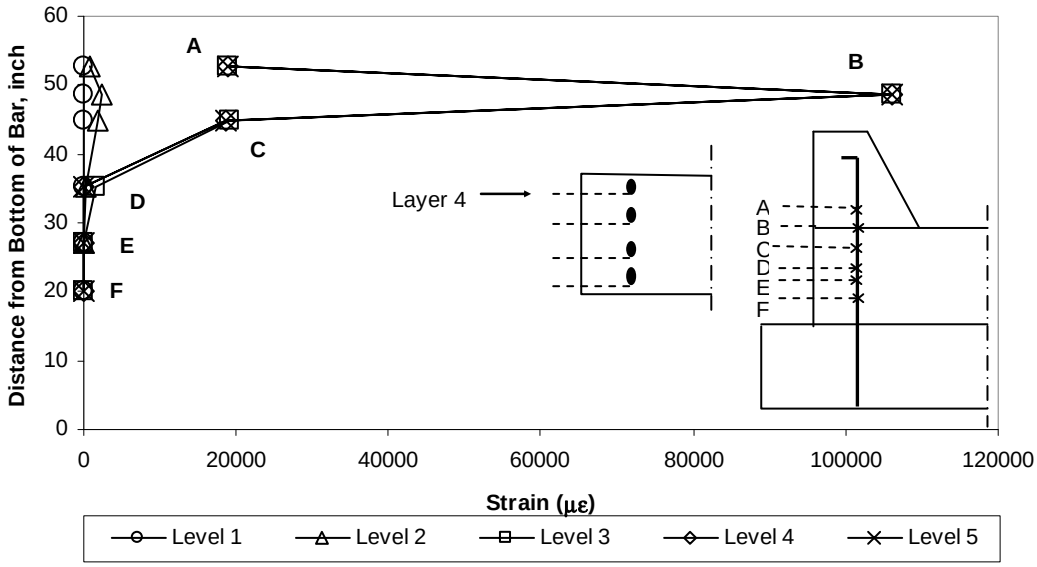

Figure A4- 60- Vertical Strain Profiles, Layer 4, Unit 5A

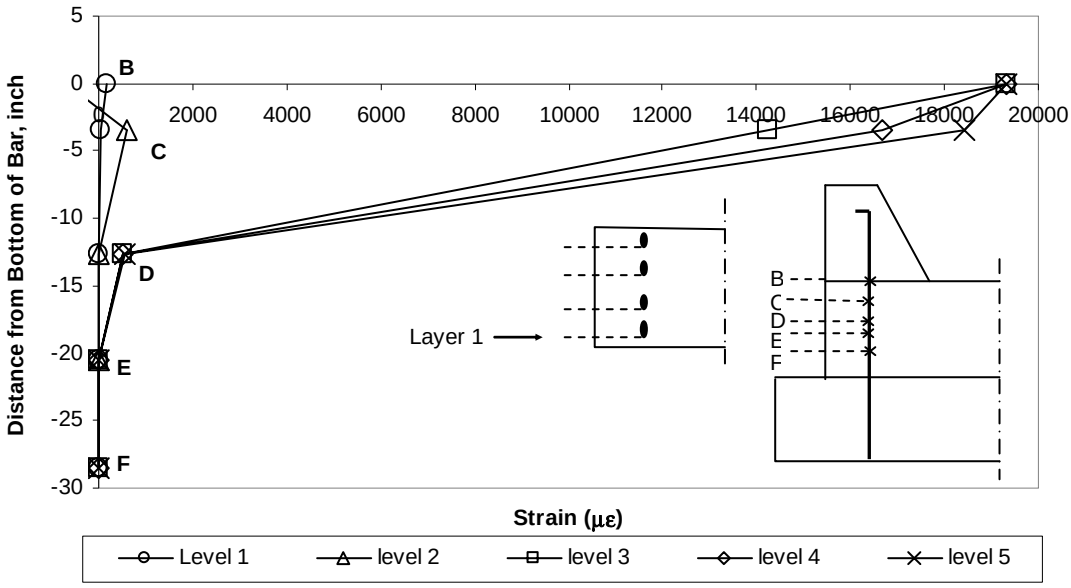

Figure A4- 61- Vertical Strain Profiles, Layer 1, Unit 5B

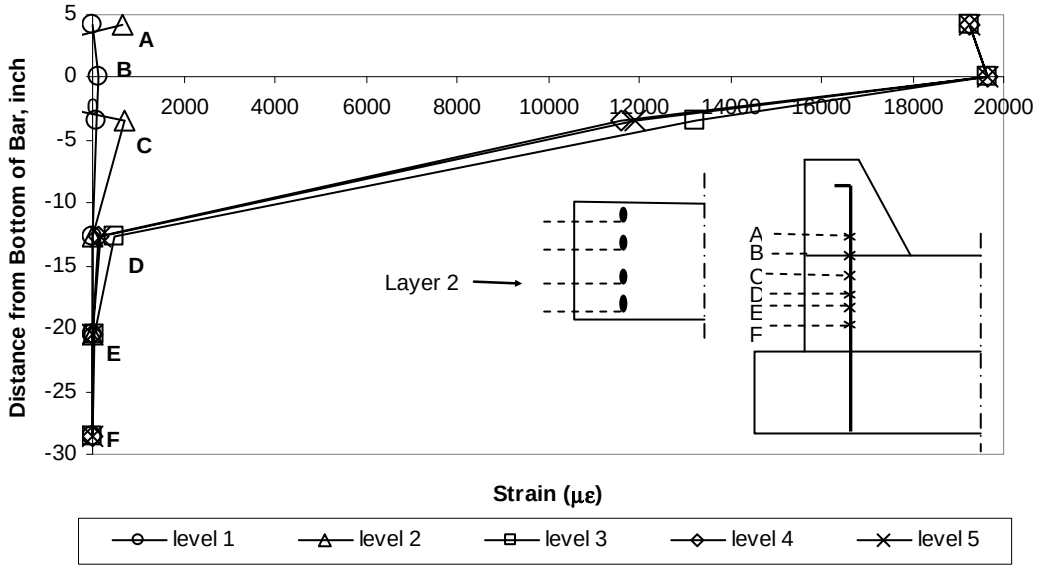

Figure A4- 62- Vertical Strain Profiles, Layer 2, Unit 5B

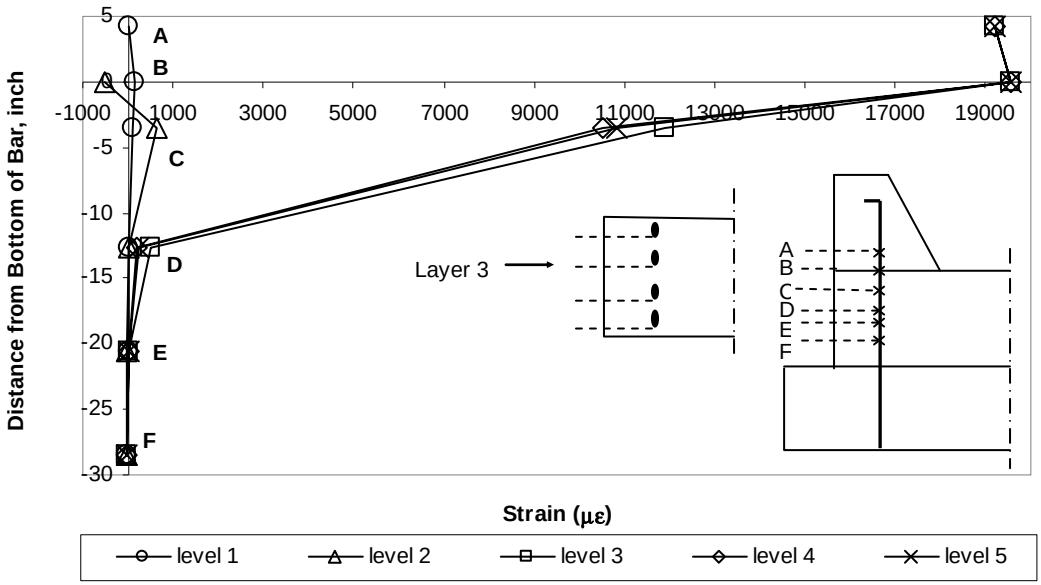

Figure A4- 63- Vertical Strain Profiles, Layer 3, Unit 5B

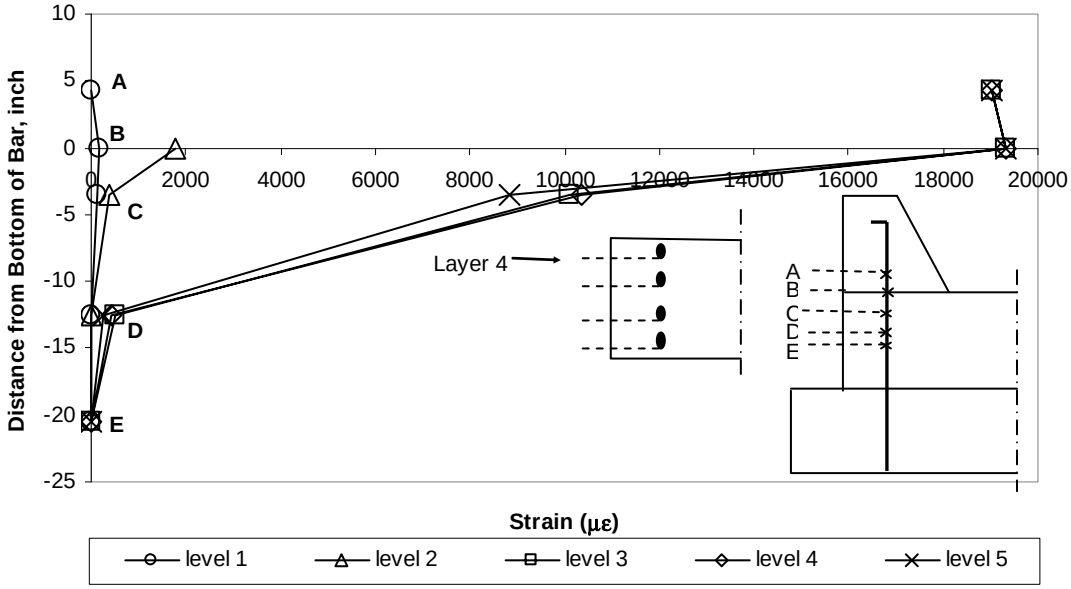

Figure A4- 64- Vertical Strain Profiles, Layer 4, Unit 5B

10.2.4 Shear friction capacity model proposed by Mattock, *1974*

This model is used to calculate the shear capacity of test units 5A and 5B. According to section 10.1.4 (Eq. (A4.13)), the shear capacity of the Test Unit 5A and 5B are calculated and shown in Table A4-8.

Test Unit	A_s in^2. (mm^2)	ρ_v	f_y ksi (MPa)	$V = \frac{v_s}{bd}$ kips (KN)
5A	0.8 (516)	0.002	63 (434.4)	40.9 (182)
5B	0.8 (516)	0.002	63 (434.4)	40.9 (182)

Table A4- 8: Capacity Evaluation of Exterior Shear key Test Units 5A and 5B with Mattock Equation

Test Unit 5A had the shear key-stem wall interface with rough and smooth surface area. However, the Mattock equation, Eq. (A4.13), does not take into account the situations with different surface conditions. In his proposed model, the coefficient of friction is assumed equal to one for the area with general roughness. In Test Unit 5B, the effect of smooth concrete surface on contact area was disregarded.

10.2.5 Capacity Evaluation of Exterior Shear Key with Shear Friction Capacity Model Proposed by Walraven *et al*. (1987)

Walraven *et al*. (1987)'s proposed shear friction equations to determine the shear capacity of reinforced concrete were used to reevaluate the capacity of exterior shear keys Series V. As mentioned in previous section, this model also does not consider the different concrete contact surface area. In his model the contact surface area of concrete was assumed to be rough. The calculated shear capacity of test specimen, using Eq. (A4.14) and Eq. (A4.15), is given in Table A4-9.

Test Unit	A_s in^2. (mm^2)	ρ_v	f_y ksi (MPa)	f'_c psi (MPa)	f'_{cc} psi (MPa)	C_3	C_4	$V = 0.82 v_s bd$ kips (KN)
5A	0.8 (516)	0.0125	63 (434.4)	4870 (33.6)	5729 (39.5)	526.4	0.47	198.7 (884)
5B	0.8 (516)	0.002	63 (434.4)	4870 (33.6)	5729 (39.5)	526.4	0.47	192.1 (855)

Table A4- 9: Capacity Evaluation of Exterior Shear key Test Units 5A and 5B with Walraven *et al. (*1987)'s Equations

11 Appendix A-5

11.1 Geometry and Reinforcement Details of Test Series IV

All test specimens were designed at a 2/5-scale with respect to a prototype abutment design provided by Caltrans. Figure A5-1 illustrates the elevation view of the test setup of Test Series IV. The simulated lateral load was applied to test units, by means of two servo-controlled. A hold-down frame was used to prevent any upward movement of the loading arm.

The foundation was post-tensioned to the strong floor by using ten tie-down bars in two rows on the sides of the shear key specimens. One central tie-down bar, at top of the stem wall was post-tensioned to the strong floor to simulate the vertical load corresponding to the weight of the bridge superstructure. The post-tensioned force at each bar was 150 kips (667 KN). In Test Unit 4-A, the shear key was built monolithically with the abutment stem wall, whereas the Test Unit 4-B was built with a rough construction joint between the shear key and the wall.

Reinforcement Layout:

Caltrans provided the main part of these specimens' design. The reinforcement amount and distribution were scaled down to %40 to match a regularly used in abutment design, provided by Caltrans. Based on that design, eight #4 hanger bars were used horizontally in two rows close to the top surface of the abutment stem wall. In test series IV, the U shape shear reinforcement consisted of 4 rows each of 6-#3 bars which were extended to the foundation block. The horizontal and vertical reinforcement on the sides of the shear key and abutment wall were placed at 4.75 in. (121 mm) spacing with #3 bars. The vertical side reinforcement in Test Unit 4B stopped below the shear key-abutment stem wall interface. Figure A5-1 to A5-3 show the schematic of the specimen reinforcement details at different cross sections.

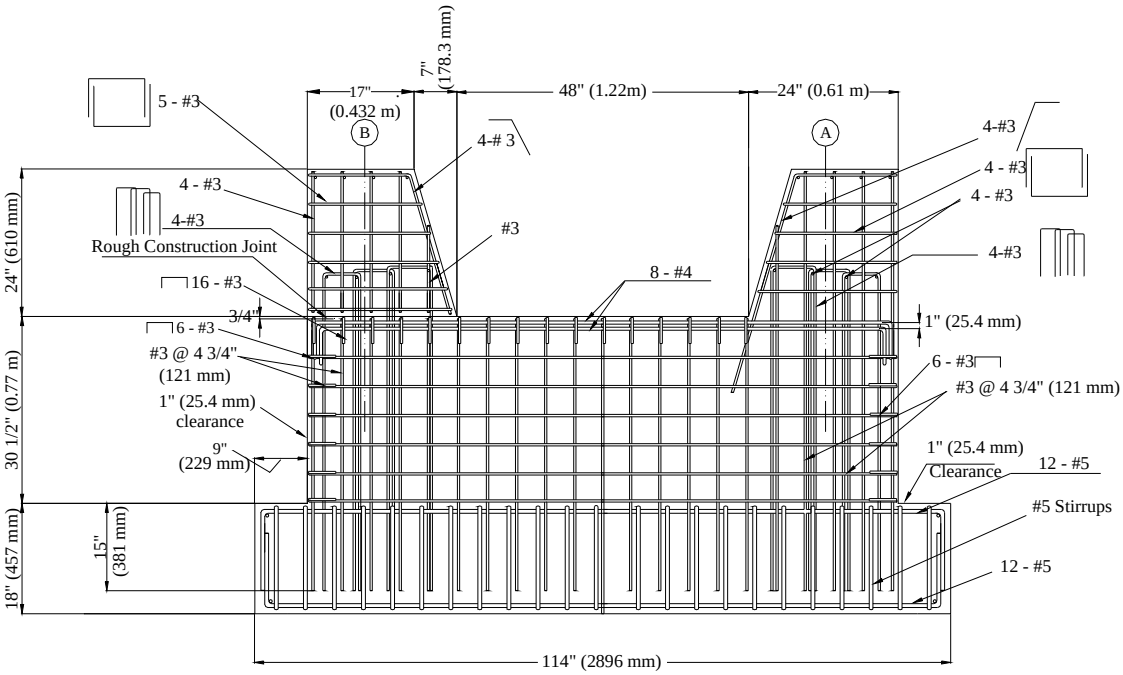

Figure A5- 1- Elevation View of the Reinforcement Layout-Test Series IV

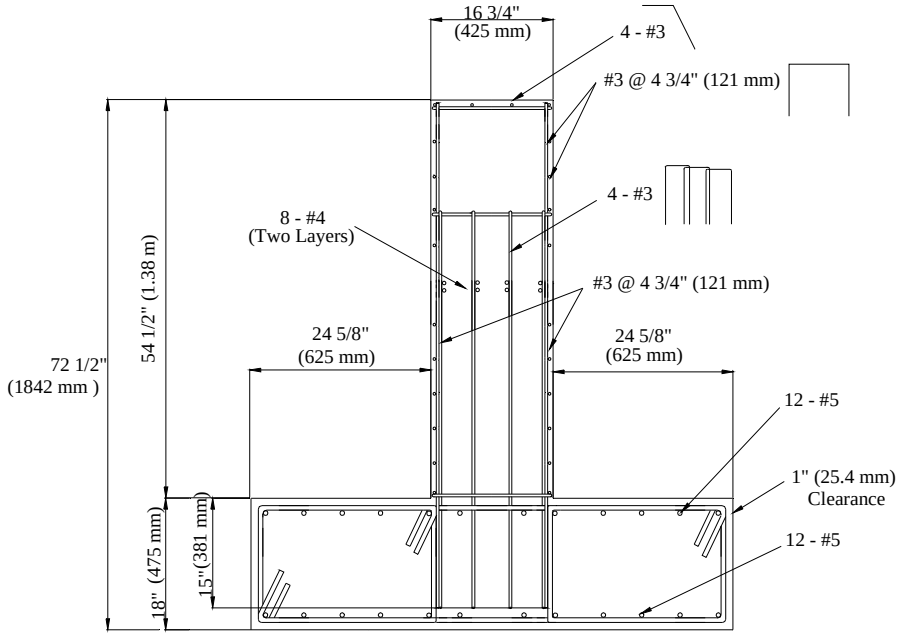

Figure A5- 2- Reinforcement Layout (Section A-A)-Test Series IV

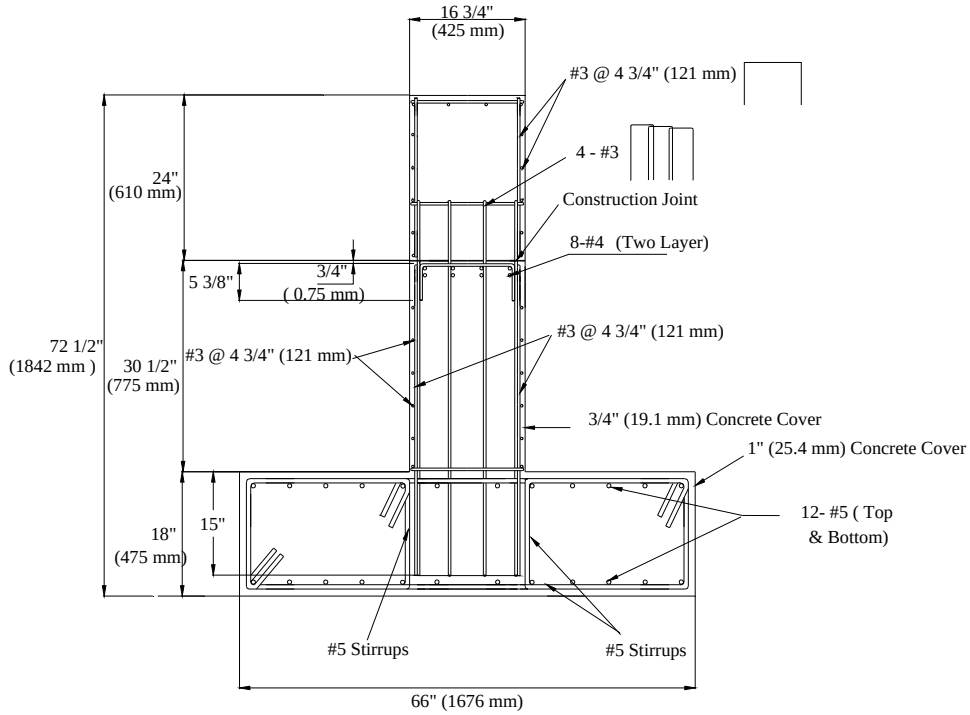

Figure A5- 3- Reinforcement Layout (Section B-B)-Test Series IV

11.2 Geometry and Reinforcement Details of Test Series V

In all previous shear key test units, except test series III, significant damage of the abutment stem wall could not be prevented. However it was shown in test series III, increasing the amount of tension tie reinforcement in the abutment stem wall can control damage of the abutment stem wall. The shear key in Test Unit 5A was separated from the abutment stem wall by foam, except for a central interface area of 8in. x 8in. (203mm x 203mm). In both test Units 5A and 5B, the abutment stem wall surface had smooth finish. Concrete surface of the abutment wall surface at the location of the hole had a rough finish. The 0.5” (12.7 mm) thick foam with an 8 in. (203 mm) square central hole was placed at the center of shear key-abutment interface area in Test Unit 5A. The smooth shear key- abutment stem wall interface was painted by a bond breaking material before casting the shear key on top it in Test Unit 5B to create a weak plane of failure.

Reinforcement Layout:

Based on strut-and-tie model, fourteen #4 headed bars were used horizontally close to the top surface of the abutment stem wall. The headed bars provide mechanical anchorage at ends of the

bars, which makes it possible for the bars to develop their full yield strength close to the welded ends. All shear key vertical reinforcing bars are lumped at one location close to the side of the hole that is closer to the inclined face of the shear key in Test Unit 5A while all shear key vertical reinforcing bars are lumped at one location near the centerline of the shear key in Test Unit 5B.Figure A5-4 illustrates the elevation view of the test setup of Test Series V. Figure A5-4 to A5-7 show the schematic of the specimen reinforcement details at different cross sections.

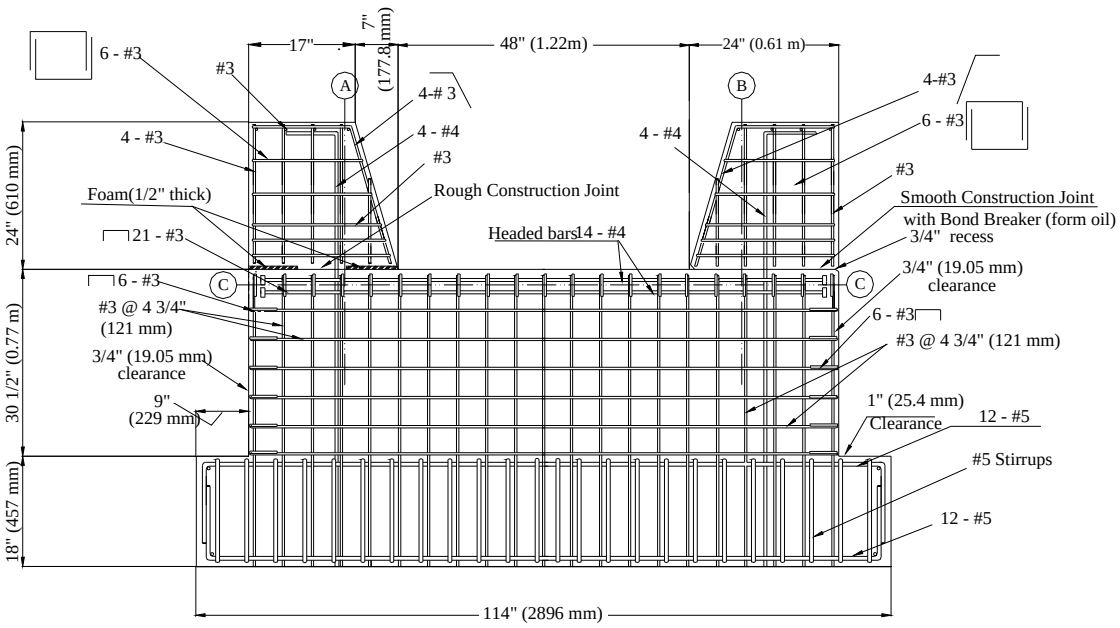

Figure A5- 4- Elevation View of the Reinforcement Layout-Test Series V

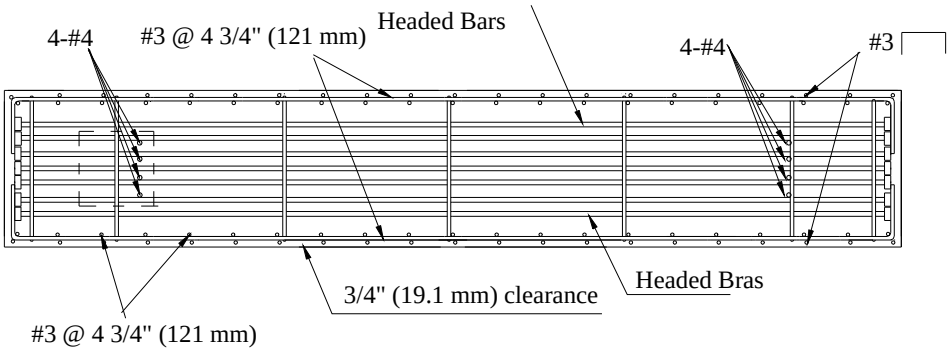

Figure A5- 5- Reinforcement Layout (Section C-C)-Test Series V

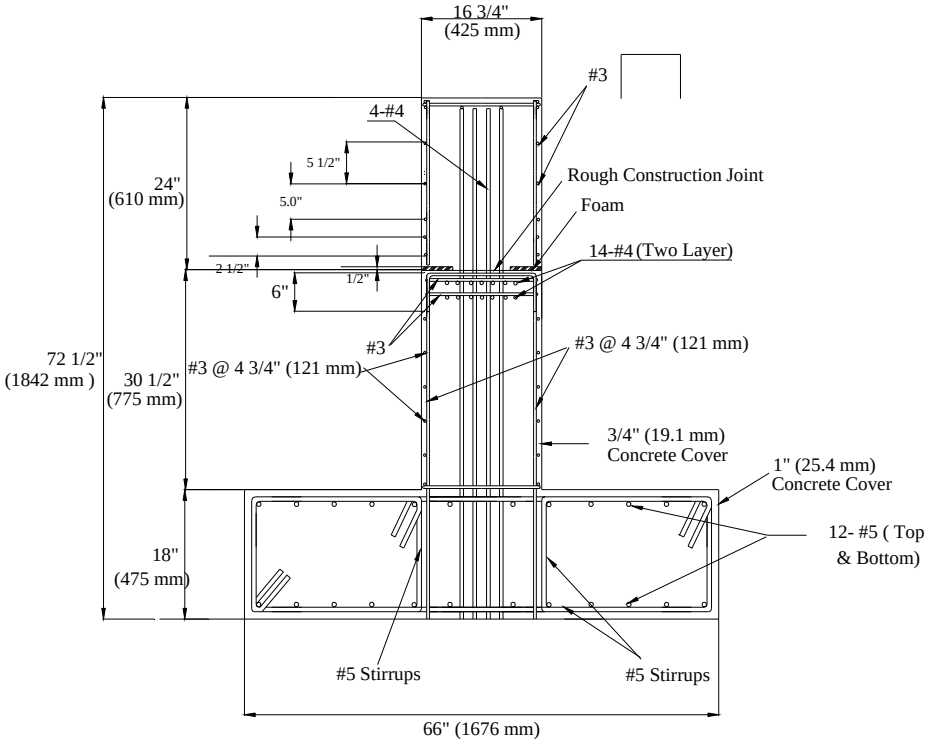

Figure A5- 6- Reinforcement Layout (Section A-A)-Test Series V

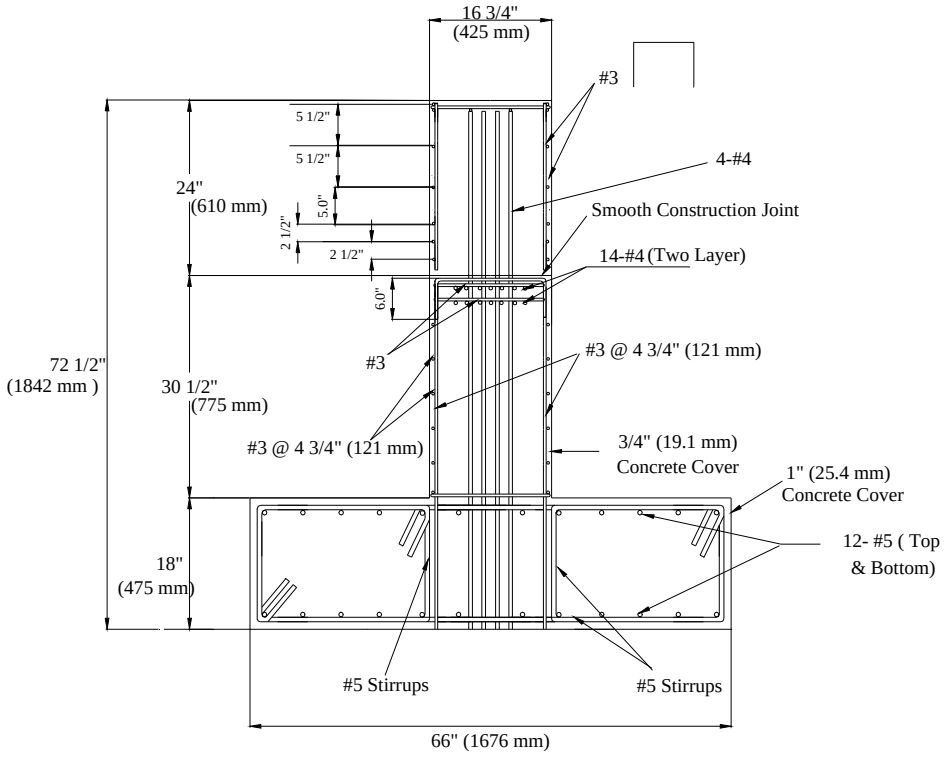

Figure A5- 7- Reinforcement Layout (Section B-B)-Test Series V

11.3 Instrumentation

External Instrumentation:

Linear potentiometers and inclinometer were attached to the test units to record displacement and rotation of the exterior shear key specimens. Displacement transducers were placed at location of expected large displacement or undesirable movement of the test units. These locations were along the centerline of the key at top and the interface level. Figures A5-8 and A5-9 show the potentiometers on test series IV and V, respectively.

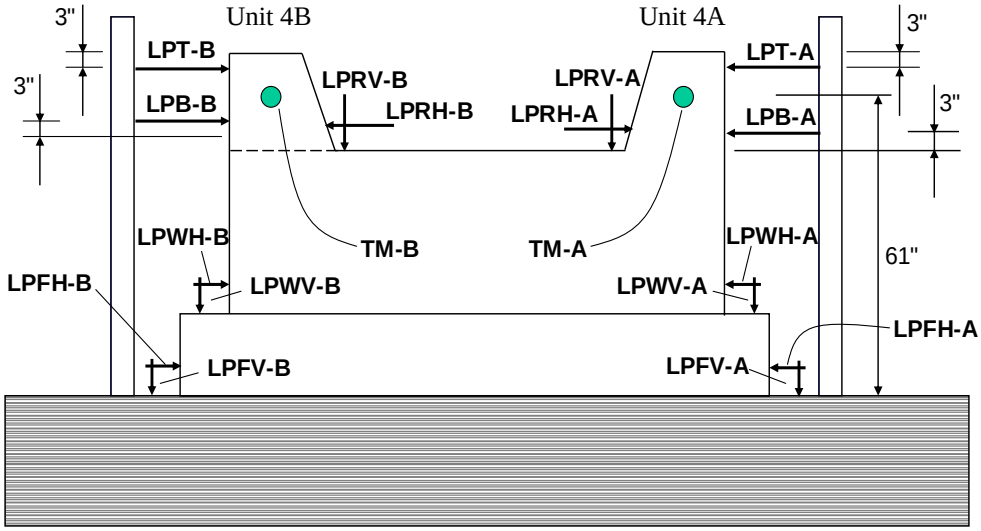

Figure A5- 8- Labels of Displacement Transducers- Test Series IV

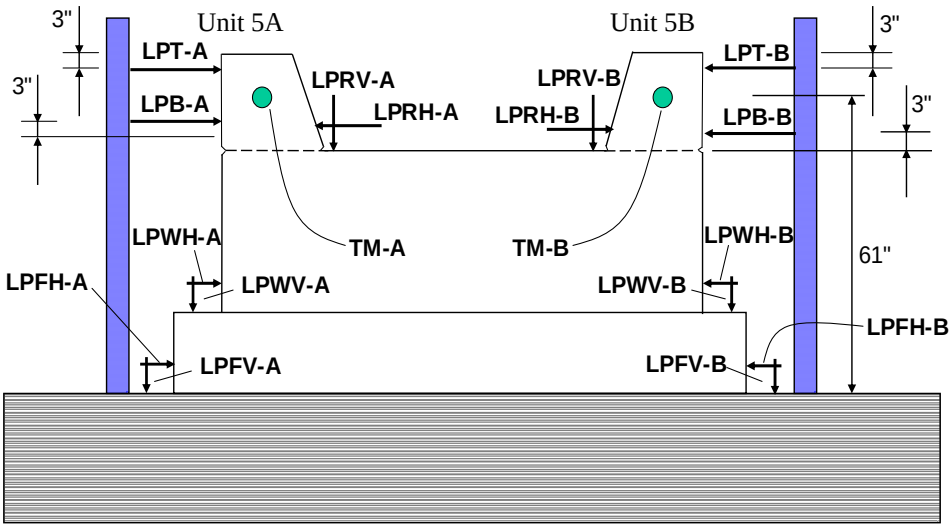

Figure A5- 9- Labels of Displacement Transducers- Test Series V

Internal Instrumentation:

Test units were instrumented with electrical resistance strain gauges. Most of the strain gauges were mounted on the reinforcing steel of the test units close to the shear key-stem wall interface and along the expected diagonal crack. The major locations of strain gauges for series IV and V are shown in Figures A5-10 to A5-16.

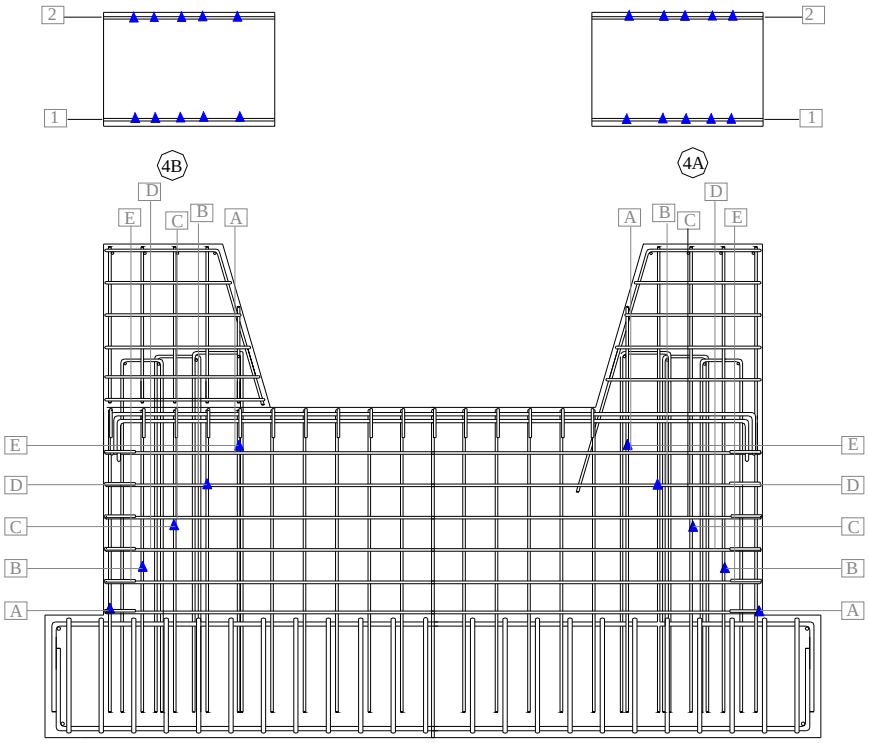

Figure A5- 10- Labels of Strain Gages on U Shape Vertical Bars, in Diagonal Direction- Test Series IV

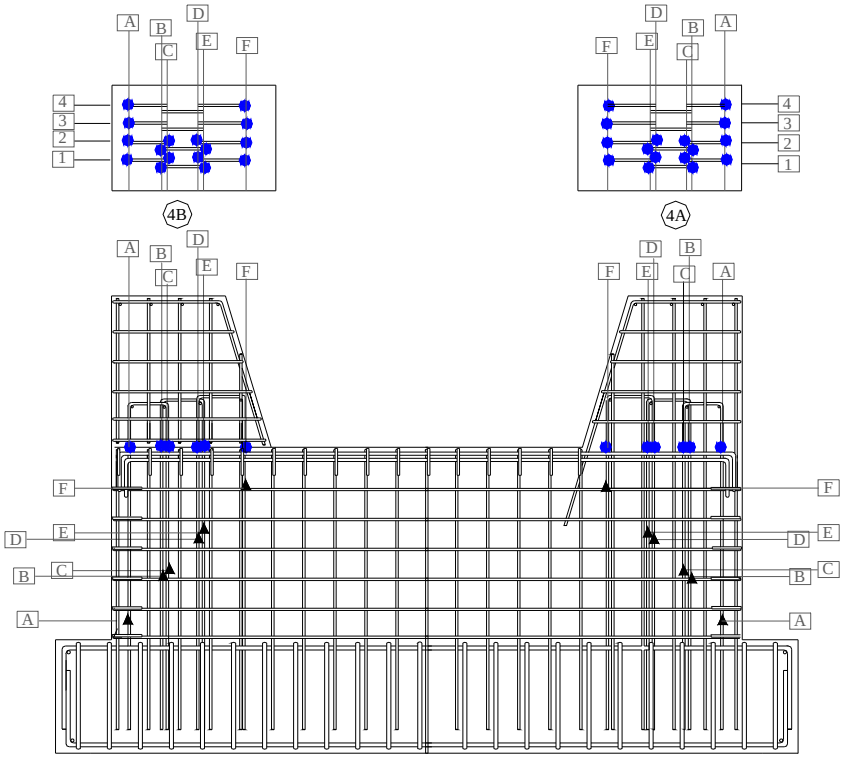

Figure A5- 11- Labels of Strain Gages on U Shape Vertical Bars, in Horizontal direction- Test Series IV

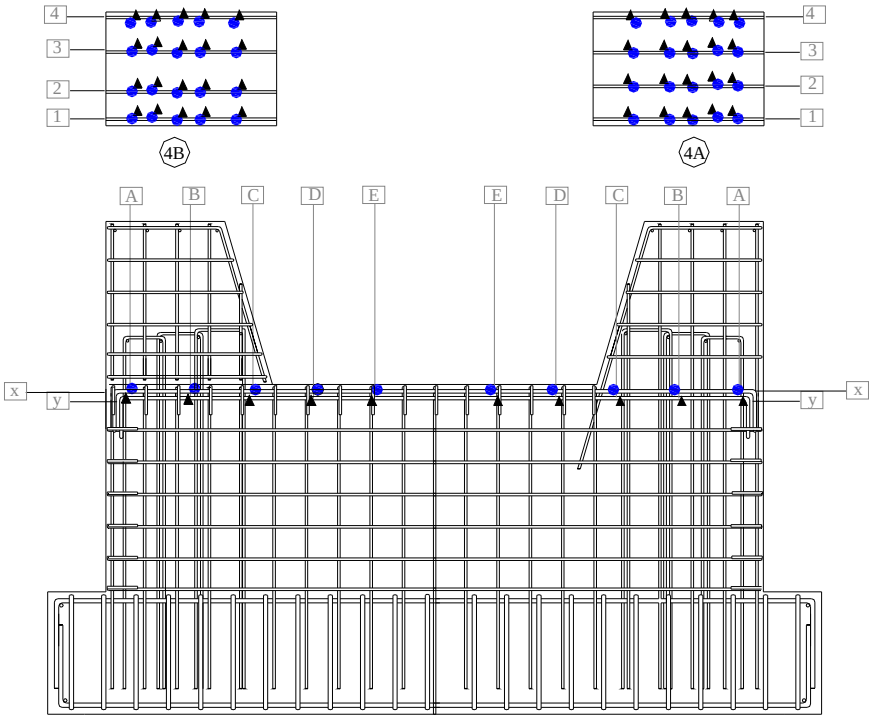

Figure A5- 12- Labels of Strain Gages on Horizontal Hanger Bars- Test Series IV

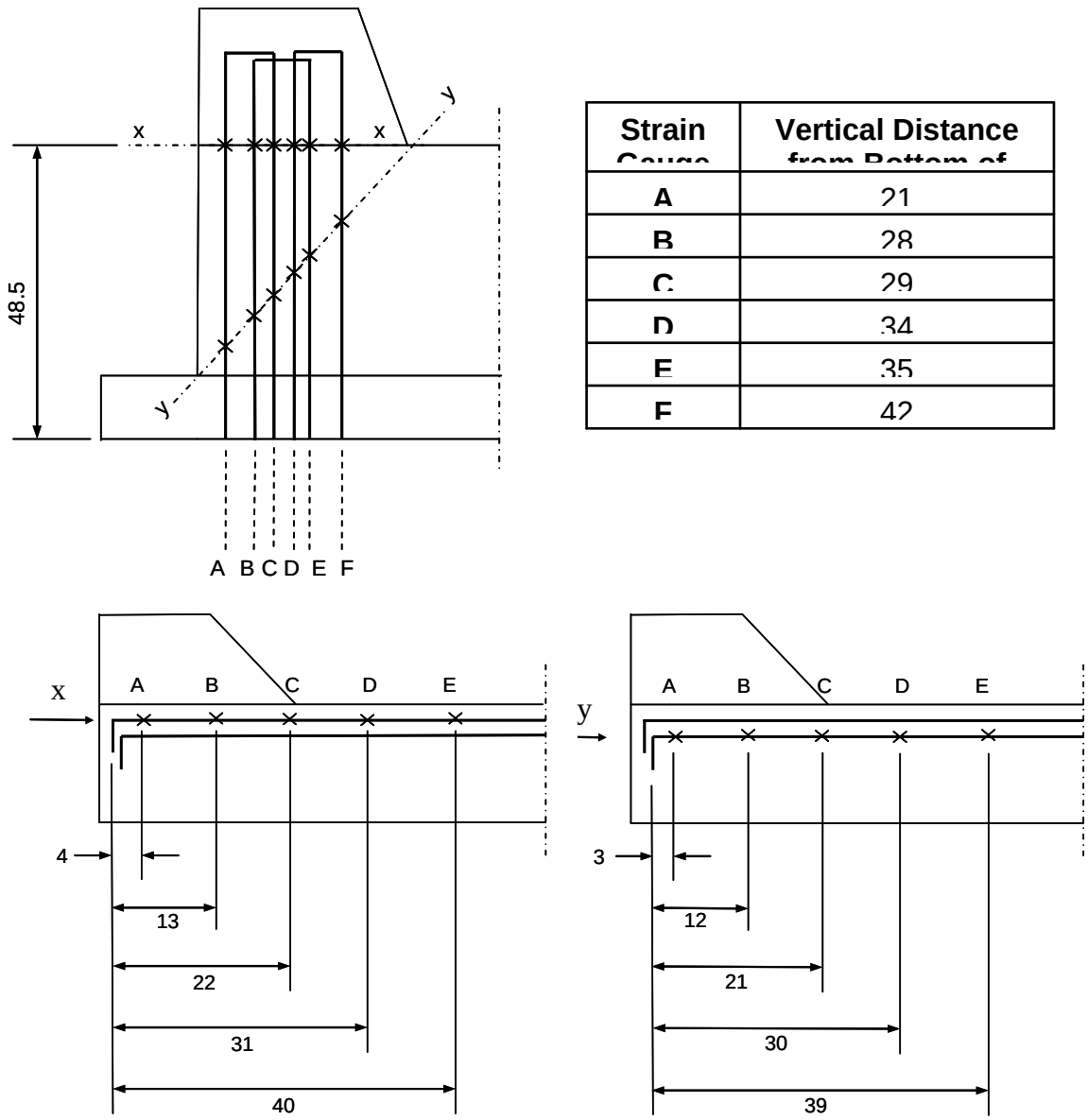

Strain Gauge	Vertical Distance from Bottom of
A	21
B	28
C	29
D	34
E	35
F	42

Figure A5- 13- Location of Strain Gages on Horizontal and Vertical Bars- Test Series IV

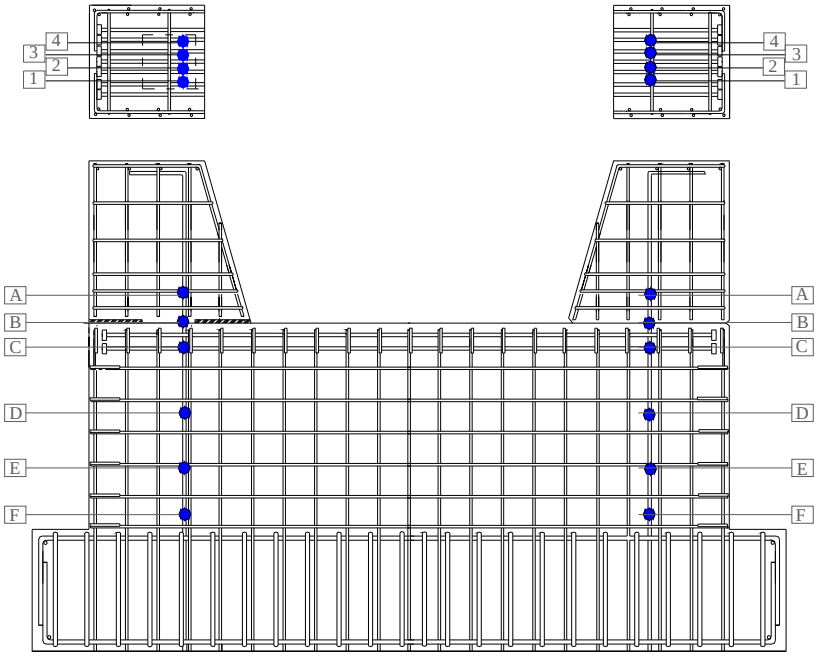

Figure A5- 14- Labels of Strain Gages on Vertical Shear Key Reinforcement- Test Series V

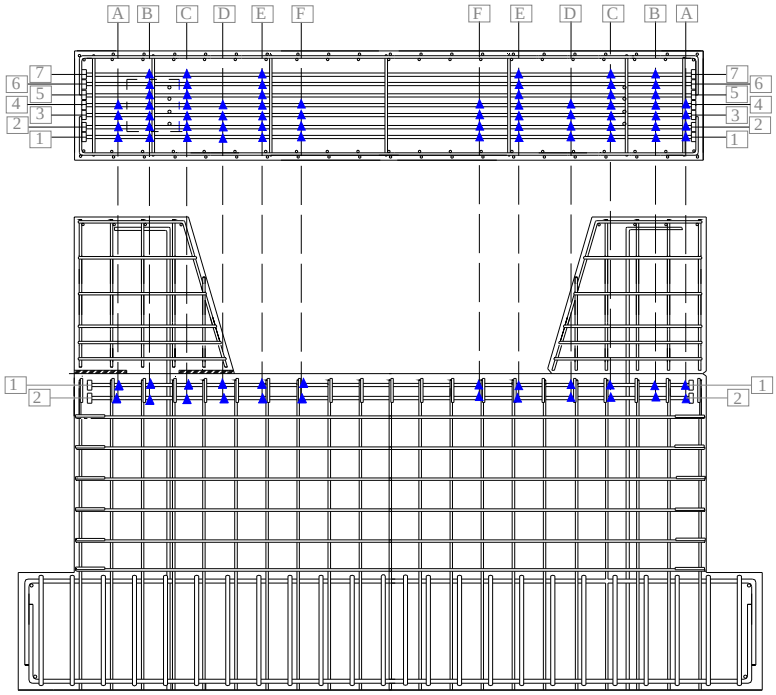

Figure A5- 15- Labels of Strain Gages on Horizontal Headed Bars- Test Series V

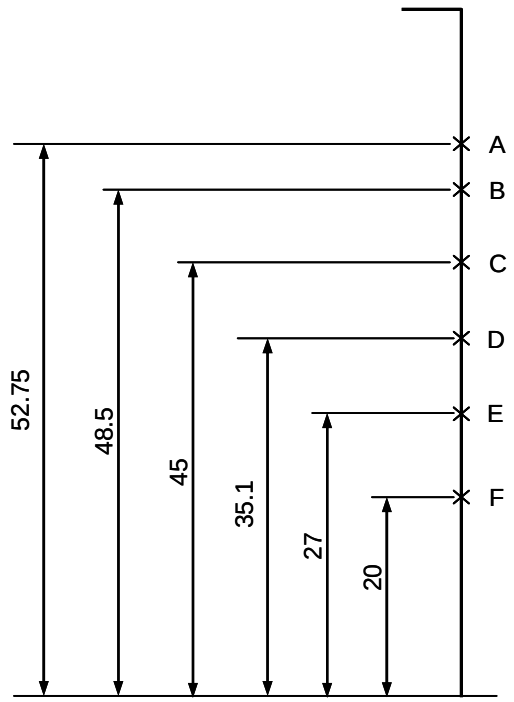

a: 5A-5B Vertical Shear Key Bars

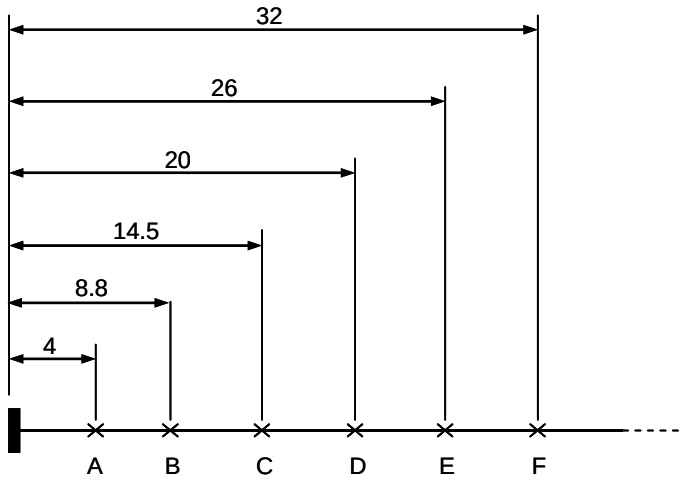

b: 5A-5B Horizontal Headed Bars

Figure A5- 16- Location of Strain Gages on Horizontal and Vertical Bars- Test Series V

12 REFERENCES

American Concrete Institute (ACI). (2005). Building Code Requirements for Structural Concrete (ACI 318-05) and Commentary (ACI 318R-05), Farmington Hills, MI.

Caltrans, *Bridge Design Specifications*, 1993a.

Caltrans, *Bridge Memo to Designers Manual*, Section 5, 1993b.

Crisafulli, F. J., Restrepo, J. I., Park, R. (2002). "Seismic design of lightly reinforced precast concrete rectangular wall panels." *PCI Journal*, 47(4), July-August, 104-121.

Mattock, A. H. (1974). "Shear transfer in concrete having reinforcement at an angle to the shear plane." *Shear in Reinforced Concrete, ACI Special Publication 42*, 17-42.

Megally, S.H., Silva, P. F., and Seible, F., *Seismic Response of Sacrificial Shear Keys in Bridge Abutments*, Structural Systems Research Report SSRP-2001/23, Department of Structural Engineering, University of California San Diego, La Jolla, CA, May 2001, 198 pp.

Priestley, M.J.N. and Seible, F., Calvi, G.M., *Seismic Design and Retrofit of Bridges.* John Wiley & Sons, New York 1996.

Walraven, J. C., Frénay, J., Pruijssers, A. (1987). "Influence of concrete strength and load history on the shear friction capacity of concrete members." *PCI Journal*, January-February, 66-83.